Generalised Radio Resource Sharing Framework for Heterogeneous Radio Networks

Raouf Abozariba

A thesis submitted in fulfilment of the requirement of Staffordshire University for the degree of Doctor of Philosophy

December 2017

Dedication

This dissertation is dedicated to the memory of my brother Ghaly.

Acknowledgments

I would like to acknowledge many people who helped me during the course of this work. First and foremost, I am heartily thankful to my supervisor, Prof. Mohammad Patwary, whose guidance and support from the initial to the final stage ensured the success of this work. I sincerely thank him for giving me the opportunity to be part of his research group and for his persistent support. Further, I owe my deepest gratitude to Dr. Abdel-Hamid Soliman and Prof. Mohamed Abdel-Maguid for their tremendous efforts and their invaluable assistance throughout the work done in this thesis. I gratefully acknowledge Dr Md Asaduzzaman for his constant encouragement, his constructive suggestions, and helpful comments on my thesis work. I have immensely benefited from his knowledge.

I am greatly thankful to my colleagues and friends from Staffordshire University: Hussain Al-Ezee, Anas Amjad, Hesham Gaber, Siva Karteek and Muhammad Kamran Naeem. I was very fortunate to have met up, discussed, and worked with them during my Ph.D journey.

Words fail me to express my appreciation to my family for their support and encouragement in every aspect of my life. Without their love and care, I would not have been able to complete this degree.

Finally I thank the examiners for their time and patience in reviewing this thesis.

Raouf Abozariba
Birmingham, February 2018

Abstract

Recent years have seen a significant interest in quantitative measurements of licensed and unlicensed spectrum use. Several research groups, companies and regulatory bodies have conducted studies of varying times and locations with the aim to capture the overall utilisation rate of spectrum. The studies have shown that large amount of allocated spectrum are under-utilised, and create the so called "*spectrum holes*", resulting in a waste of valuable frequency resources. In order to satisfy the requirements of increased demands of spectrum resources and to improve spectrum utilisation, dynamic spectrum sharing (DSS) is proposed in the literature along with cognitive radio networks (CRNs). DSS and CRNs have been studied from many perspectives, for example spectrum sensing to identify the idle channels has been under the microscope to improve detection probability. As well as spectrum sensing, the DSS performance analysis remains an important topic moving towards better spectrum utilisation to meet the exponential growth of traffic demand. In this dissertation we have studied both techniques to achieve different objectives such as enhancing the probability of detection and spectrum utilisation.

In order to improve spectrum sensing decisions we have proposed a cooperative spectrum sensing scheme which takes the propagation conditions into consideration. The proposed location aware scheme shows an improved performance over conventional hard combination scheme, highlighting the requirements of location awareness in cognitive radio networks (CRNs).

Due to the exponentially growing wireless applications and services, traffic demand is increasing rapidly. To cope with such growth wireless network operators seek radio resource cooperation strategies for their users with the highest possible grade of service (GoS). However, it is difficult to fathom the potential benefits of such cooperation, thus we propose a set of analytical models for DSS to analyse the blocking probability gain and degradation for operators. The thesis focuses on examining the performance gains that DSS can entail, in different scenarios. A number of dynamic spectrum sharing scenarios are proposed. The proposed models focus on measuring the blocking probability of secondary network operators as a trade-off with a marginal increase of the blocking probability of a primary network in return of monetary rewards. We derived the global balance equation and an explicit expression of the blocking probability for each model. The robustness of the proposed analytical models is evaluated under different scenarios by considering varying traffic intensities, different network sizes and adding reserved resources (or pooled capacity). The results show that the blocking probabilities can be reduced significantly with the proposed analytical DSS models in comparison to the existing local spectrum access schemes.

In addition to the sharing models, we further assume that the secondary operator aims to borrow spectrum bandwidths from primary operators when more spectrum resources available for borrowing than the actual demand considering a *merchant mode*. Two optimisation models are proposed using stochastic optimisation models in which the

secondary operator (i) spends the minimum amount of money to achieve the target GoS assuming an unrestricted budget or (ii) gains the maximum amount of profit to achieve the target GoS assuming restricted budget. Results obtained from each model are then compared with results derived from algorithms in which spectrum borrowings were random. Comparisons showed that the gain in the results obtained from our proposed stochastic optimisation model is significantly higher than heuristic counterparts. A post-optimisation performance analysis of the operators in the form of analysis of blocking probability in various scenarios is investigated to determine the probable performance gain and degradation of the secondary and primary operators respectively. We mathematically model the sharing agreement scenario and derive the closed form solution of blocking probabilities for each operator. Results show how the secondary and primary operators perform in terms of blocking probability under various offered loads and sharing capacity.

The simulation results demonstrate that at most trading windows, the proposed optimal algorithms outperforms their heuristic counterparts. When we consider 80 cells, the proposed profit maximisation algorithm results in 33.3% gain in net profit to the secondary operators as well as facilitating 2.35% more resources than the heuristic approach. In addition, the cost minimisation algorithm results in 46.34% gain over the heuristic algorithm when considering the same number of cells (80).

Keywords: Cognitive radio networks, cooperative spectrum sensing, Spectrum sharing, spectrum allocation, merchant mode.

Email: r.abozariba@ieee.org

List of Publications

J01 **Raouf Abozariba**, Mohammad Patwary, Abdel-Hamid Soliman and Mohamed Abdul-maguid , "On the Location-Aware Cooperative Spectrum Sensing in Urban Environments", The Jordanian Journal of Computers and Information Technology (JJCIT). [published]

J02 **Raouf Abozariba**, Md Asaduzzaman and Mohammad Patwary, "Radio Resource Sharing Framework for Cooperative Heterogeneous Networks with Dynamic Overflow Modelling", IEEE Transactions on Vehicular Technology. [Published]

J03 Md Asaduzzaman, **Raouf Abozariba** and Mohammad Patwary, "Dynamic Spectrum Sharing Optimization and Post-optimization Analysis with Multiple Operators in Cellular Networks", Transactions on Wireless Communications. [In Press]

C01 **Raouf Abozariba**, Mohammad Patwary, Abdel-Hamid Soliman and Mohamed Abdul-maguid , "Location-Aware Cooperative Spectrum Sensing within Cognitive Radio Networks", IEEE Jordan Conference on applied Electrical Engineering and Computing Technologies. [Published]

C02 Md Asaduzzaman **Raouf Abozariba** and Mohammad Patwary, "Spectrum Sharing Optimization in Cellular Networks under Target Performance and Budget Restriction", 2017 IEEE 85th Vehicular Technology Conference. [Published]

C03 Mohammad Patwary, **Raouf Abozariba** and Md Asaduzzaman, "Multi-Operator Spectrum Sharing Models under Different Cooperation Schemes for Next Generation Cellular Networks", 2017 IEEE 86th Vehicular Technology Conference. [Published]

C04 **Raouf Abozariba**, Anas Amjad, and Mohammad N. Patwary, "Optimized Resource Sharing for Federated Cloud Services with Desired Performance and Limited OpEx", 2017 IEEE Global Communications Conference. [Accepted]

Contents

Abstract **iv**

List of Figures **xi**

List of Tables **xv**

Abbreviations **xvii**

1 Introduction **1**
1.1 Background and motivation 1
1.2 Aim and objectives 3
1.3 Contribution to knowledge 6
1.4 Thesis outline 7

2 State of the Art in Spectrum Sensing and Spectrum Sharing **11**
2.1 Introduction 11
2.2 Spectrum sensing 14
2.3 Attenuation problem 17
2.4 Cooperative Spectrum Sensing 18
2.5 Radio resource sharing for cooperative networks 19
2.6 Radio resource sharing for cooperative networks (Multi-operators) . 22
2.7 Radio resource sharing framework for cooperative networks (Multi-operators) with optimisation and post-optimisation analysis 24

3 Location-aware Cooperative Spectrum Sensing **27**
3.1 Introduction 27
3.2 System model and assumptions 29
3.3 Location-aware cooperative spectrum sensing 33
3.3.1 Urban Propagation 33
3.3.2 Proposed Scheme 34
3.3.3 Trust Value 35

3.3.4 Elimination . . . 37
3.3.5 Proposed Fusion Rule . . . 37
3.4 Analysis and results . . . 44
3.5 Summary . . . 47

4 Radio resource sharing for cooperative networks 49
4.1 Introduction . . . 49
4.2 System model and assumptions . . . 50
4.3 Formulation of Agreements . . . 54
4.4 Proposed dynamic resource sharing algorithm . . . 57
4.4.1 Non-Sharing Model . . . 58
4.4.2 Sharing Model 1 (Uni-directional overflow) . . . 60
4.4.3 Sharing Model 2 (Bi-directional overflow) . . . 64
4.4.4 Sharing Model 3 (Bi-directional overflow with reserved capacity) . . . 66
4.5 Analysis and results . . . 69
4.5.1 Performance comparison between the Non-Sharing Model and Model 1 . . . 71
4.5.2 Performance comparison between the Non-Sharing Model, Model 1 and Model 2 . . . 75
4.5.3 Performance comparison between the Non-Sharing Model and Model 3 . . . 75
4.5.4 Evaluation of models under homogeneous traffic intensity . . . 79
4.5.5 Evaluation of models under heterogeneous traffic intensity . . . 81
4.5.6 Evaluation of Model 1 and Model 2 with reference to simulated blocking probabilities . . . 83
4.6 Summary . . . 84

5 Dynamic spectrum sharing (Multi-operator) 85
5.1 Introduction . . . 85
5.2 System model . . . 86
5.3 Dynamic spectrum sharing models . . . 87
5.3.1 Model A: Uni-Directional cooperation . . . 87
5.3.2 Model B: Bi-Directional cooperation . . . 91
5.3.3 Model C: Bi-Directional cooperation with pooled resources . . . 92
5.3.4 Bi-Directional cooperation with multi-primary operators and pooled capacity . . . 94
5.3.5 Marginal probability distribution and spectrum utilisation . . . 96
5.4 Analysis and results . . . 97
5.4.1 Effect of traffic intensity at the secondary operator on blocking probability . . . 97
5.4.2 Effect of traffic intensity at the secondary operators on blocking probability . . . 97

5.4.3 Effect of the number of available channels on blocking probability . . . 99
5.4.4 Evaluation of spectrum utilisation . . . 101
5.5 Summary . . . 102

6 Dynamic spectrum sharing optimisation and post-optimisation analysis 105
6.1 Introduction . . . 105
6.2 Dynamic spectrum management model . . . 107
6.2.1 Spectrum trading . . . 108
6.2.2 Service type and channel characteristics . . . 109
6.2.3 Spectrum request processing . . . 110
6.3 Problem formulation . . . 112
6.3.1 Modelling assumptions . . . 112
6.3.2 Notations used in Problem 1 and Problem 2: . . . 113
6.3.3 Spectrum allocation by minimising borrowing cost . . . 114
6.3.4 Spectrum allocation using the heuristic algorithm . . . 119
6.3.5 Expected profit maximisation under a restricted budget . . . 122
6.3.6 Spectrum allocation using the heuristic algorithm under budget constraint . . . 126
6.3.7 Spectrum demand-supply strategy . . . 128
6.3.8 Performance analysis under resource sharing between the SNO and PNOs . . . 129
6.3.8.1 Case 1: SNO is sharing with three PNOs . . . 130
6.3.8.2 Case 2: SNO is sharing with two PNOs . . . 134
6.3.8.3 Case 3: SNO is sharing with one PNO . . . 136
6.4 Analysis and results . . . 137
6.4.1 Cost analysis under target performance (Problem 1) . . . 137
6.4.2 Expected profit under budget constraints analysis (Problem 2) . . . 142
6.4.3 Expected profit under budget constraints with multiple types of services (Problem 2) . . . 145
6.4.4 Impact on the performance of the operators . . . 146
6.5 Summary . . . 148

7 Conclusions and Future Work 151
7.1 Conclusions . . . 151
7.2 Future work . . . 153

A Performance analysis under resource sharing between S SNOs and N PNOs 155

References **161**

List of Figures

1.1 Spectrum hole concept 2
1.2 Framework for heterogeneous radio networks 7
1.3 An illustration of the contents of the thesis chapters 9

2.1 Hidden Terminal Problem 19

3.1 Cognitive cycle 29
3.2 System Model 30
3.3 Proposed location aware scheme 34
3.4 Signal strength from empirical propagation predictions 36
3.5 Probability of detection comparison of the proposed location-aware scheme and conventional hard combining scheme for different SNR when the false alarm probability constraint is 0.1 and 0.2 45
3.6 ROC comparison of the proposed location-aware scheme and conventional hard combining scheme under Gaussian channel when the number of cooperative users = 30 for different trust values 46
3.7 ROC of proposed location-aware scheme with different number of cognitive radio users under Gaussian channel and 35% of secondary users are located in highly shadowed areas 46

4.1 System Model: Coexisting Network Operators in a DSA 52
4.2 Non-Sharing network with two operators 59
4.3 A two-operator network with uni-directional overflow (Model 1) . . 60
4.4 A two-operator network with bi-directional overflow (Model 2) . . . 64
4.5 A two-operators network with bi-directional overflow and reserved resources (Model 3) 66
4.6 The flowchart for the proposed overflow models 70
4.7 Comparison of the blocking probability for the Non-Sharing Model with Model 1 with $c_1 = c_2 = 10$ for (A) $\lambda_1 = 0 : 30$, $\lambda_2 = 10$ and (B) $\lambda_1 = 10$, $\lambda_2 = 0 : 30$ 72
4.8 Gain and degradation performance trade-off between Operator 1 and 2 for the Non-sharing and Uni-directional model 73
4.9 Comparison of the blocking probability for the Non-Sharing Model with Model 1 with $\lambda_1 = \lambda_2 = 10$ for (A) $c_1 = 5 : 25$, $c_2 = 10$ and (B) $c_1 = 10$, $c_2 = 1 : 25$ 74

4.10 Comparison of the blocking probability for the Non-Sharing Model with Model 1 and Model 2 with $c_1 = c_2 = 10$ for (A) $\lambda_1 = 0:30$, $\lambda_2 = 10$ and (B) $\lambda_1 = 10$, $\lambda_2 = 10$ 74
4.11 Comparison of the blocking probability for the Non-Sharing Model with Model 1 and Model 2 with $\lambda_1 = \lambda_2 = 10$ for (A) $c_1 = 1:25$, $c_2 = 10$ and (B) $c_1 = 10$, $c_2 = 1:25$ 76
4.12 Comparison of the blocking probability for the Non-Sharing Model ($c_1 = c_2 = 10$) with Model 3 ($c_1 = 10, c_2 = 5$, reserved capacity $= 5$) for (A) $\lambda_1 = 0:30$, $\lambda_2 = 10$ and (B) $\lambda_1 = 10, \lambda_2 = 0:30$ 77
4.13 Comparison of the blocking probability for the Non-Sharing Model with Model 3 for $\lambda_1 = \lambda_2 = 10$. See Table 4.3 for server configurations for (A) and (B). 78
4.14 Comparison of the blocking probability for Model 1 (A) and Model 2 (B) using analytical and numerical approaches. 83

5.1 Uni-Directional service operators sharing network 88
5.2 Bi-Directional service operators sharing network 90
5.3 Bi-Directional with pooled capacity service operators sharing network 92
5.4 Comparison of the blocking probability for the secondary operator using the proposed models with $\rho_0 = 1:10$, see Table 5.1 for full configuration details. 98
5.5 Blocking probability for Operator 1 and 2, see Table 5.1 for full configuration details. 99
5.6 Blocking probability for (a) Operator 1 and 2 and (b) Operator 3, see Table 5.1 for full configuration details. 100
5.7 Comparison of blocking probability for the secondary operator with the varying number of channels using the proposed models when $\rho_s = 5, \rho_1 = 3, \rho_2 = 4, \rho_3 = 5, c_{0,2,3} = 2, c_1 = 1:10, c_p = 1$. 100
5.8 Comparison of channel utilisation for the secondary operator using the proposed models with $\rho_0 = 1:10$. 102
5.9 Comparison of channel utilisation for the secondary operator using the proposed models with ρ_1, ρ_2 and $\rho_3 = 1:10$. 103

6.1 Network model for cellular network with N PNOs and S SNOs . . . 108
6.2 Cost of optimal and heuristic algorithms per cell 138
6.3 Cost of optimal and heuristic algorithms for varying number of cells. 139
6.4 Effect of varying target blocking probability on cost for optimal and heuristic algorithms. 141
6.5 Effect of borrowing on bandwidth acquisition for the optimal and heuristic algorithms. 142
6.6 Profit using the optimal and heuristic algorithms per cell. 143
6.7 Profit using the optimal and heuristic algorithms for varying number of cells. 143

6.8 Expected profit of the SNO for spectrum borrowing with target blocking probability = 0 to 0.8 and budget = 0 to 250. 144
6.9 Bandwidth acquisition of the SNO for spectrum borrowing by the optimal and heuristic algorithms. 145
6.10 Effect of spectrum borrowing on profit with budget = 50 (top) and budget= 500 (bottom). 146
6.11 Blocking probability for each operator when configuration details are according to Table 6.2 147
6.12 Blocking probability for each operator when configuration details are according to Table 6.2. 148

A.1 Network model for cellular network with N PNOs and S SNOs . . . 155

List of Tables

3.1 Notations Used 31
3.2 Sensing Procedure Comparison 47

4.1 Symbols Used for the Analytical Modelling 51
4.2 Number of servers considered in Figure 4.12a and Figure 4.12b . . . 77
4.3 Number of servers considered in Figure 4.13a and Figure 4.13b . . . 78
4.4 Comparison of the blocking probabilities for the Non-Sharing Model with Model 1, Model 2 and Model 3 with homogeneous traffic intensity 80
4.5 Comparison of the blocking probability for the Non-Sharing Model, Model 1, Model 2 and Model 3 with heterogeneous traffic intensity . 82

5.1 Configurations used in Figure 5.4, 5.5 and 5.6 99
5.2 Configurations used in Figure 5.8 102

6.1 Simulation parameters. 138
6.2 Configurations used in Figure 6.11 and 6.12. 147

Abbreviations

3G	**3**rd **G**eneration
4G	**4**th **G**eneration
AR	**A**ugmented **R**eality
AOA	**A**ngle of **A**rrival
ASA	**A**uthorised **S**pectrum **A**ccess
AWGN	**A**dditive **W**hite **G**aussian **N**oise
CAC	**C**all **A**dmission **C**ontrol
CCR	**C**ooperative **C**ognitive **R**adio
CDBS	**C**onsolidated **D**atabase **S**ystem
CDMA	**C**ode **D**ivision **M**ultiple **A**ccess
CRN	**C**ognitive **R**adio **N**etwork
CSS	**C**ooperative **S**pectrum **S**ensing
DSA	**D**ynamic **S**pectrum **A**ccess
DSA	**D**ynamic **S**pectrum **S**haring
DVB	**D**igital **V**ideo **B**roadcasting
EGC	**E**qual **G**ain **C**ombining
FCC	**F**ederal **C**ommunications **C**ommission
GHz	**G**igahertz
GoS	**G**rade of **S**ervice
GPS	**G**lobal **P**ositioning **S**ystem
GSM	**G**lobal **S**ystem for **M**obile **C**ommunications
HLR	**H**ome **L**ocation **R**egister

LOS	**L**ine of **S**ight
LLR	**L**og **L**ikelihood **R**atio
LTE	**L**ong **T**erm **E**volution
MNO	**M**obile **N**etwork **O**perator
MHz	**M**egahertz
NLOS	**N**on **L**ine of **S**ight
NP	**N**eyman **P**earson
OFDMA	**O**rthogonal **F**requency **D**ivision **M**ultiple **A**ccess
PBS	**P**rimary **B**ase **S**tation
PCS	**P**ersonal **C**ommunications **S**ervice
PU	**P**rimary **U**ser
QADP	**Q**uality **A**ware **D**ynamic **P**ricing
RSS	**R**eceived **S**ignal **S**trength
ROC	**R**eceiver **O**perating **C**haracteristic
SBS	**S**econdary **B**ase **S**tation
SNO	**S**econdary **N**etwork **O**perator
PNO	**P**rimary **N**etwork **O**perator
SNR	**S**ignal to **N**oise **R**atio
SU	**S**econdary **U**ser
TDMA	**T**ime **D**ivision **M**ultiple **A**ccess
TOA	**T**ime of **A**rrival
TV	**T**elevision
UMTS	**U**niversal **M**obile **T**elecommunications **S**ystem
WCDMA	**W**ideband **C**ode **D**ivision **M**ultiple **A**ccess

Chapter 1

Introduction

1.1 Background and motivation

Due to the rapid growth of wireless communication technologies and the widespread use of mobile devices, unprecedented demand for spectrum has been witnessed. However, today's wireless networks are allocated by a fixed spectrum assignment policy. For operators to increase their allocated spectrum, they need to go through a very complex and time consuming process. In addition, increasing spectrum holdings come at high costs to the operators. Also, many regulatory bodies as well as governmental agencies are involved in spectrum releases, which make the process of gaining additional spectrum resources not efficient. Therefore, static spectrum allocation is considered as an obstruction to the continued growth of wireless services. In addition, recent years have seen a significant interest in quantitative measurements of licensed and unlicensed spectrum use. Several research groups, companies and regulatory bodies have conducted studies of varying times and locations with the aim to capture the overall utilisation rate of spectrum. These studies have given a significant amount of insight on spectrum use [1, 2]. Most of these studies have shown that a large amount of allocated spectrum is under-utilised, and creates what is called "*spectrum holes*" (in time and

frequency domain), resulting in a waste of valuable frequency resources, see Figure 1.1 [3, 4, 5, 6, 7]. Subsequently, users experience high blocking probabilities due to the poor utilisation of frequency resources by their respective operators.

In order to satisfy the requirements of increased demands of wireless applications and to improve spectrum utilisation, dynamic spectrum sharing (DSS), along with other technologies, such as spectrum aggregations (or carrier aggregation), are proposed in the literature to solve these current spectrum inefficiency problems [8, 4].

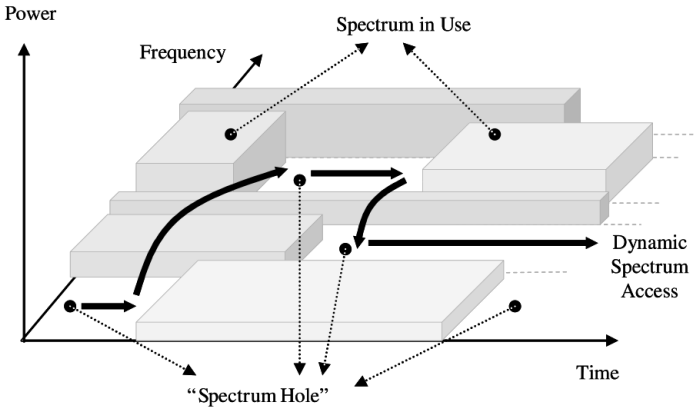

FIGURE 1.1: Spectrum hole concept

DSS allows unlicensed operators (secondary operators) to dynamically access the licensed bands from licensed spectrum holders (primary operators) based on negotiated trade deals or on an opportunistic basis [9]. DSS has a diverse importance in telecommunications industry. For example, public safety, emergency and military applications are all areas where DSS can be used to improve spectrum availability. Furthermore, applications of 4G cellular networks such as real-time multimedia, augmented reality (AR), novel application scenarios, vehicle-to-vehicle communications, machine-to-machine communications, rapidly deployable mesh networks of devices/machines etc., are all relevant applications for DSS concept deployment.

Resource allocation of DSS is broadly categorised by the roles of primary operators, namely, the passive and active primary network models. The passive model

assumes that a primary network is unaware of the operations of secondary networks (secondary networks perform spectrum sensing to determine idle spectrum), and it does not require any modification for the primary network systems. In contrast, in the active model, spectrum sensing is not required by secondary networks because it is assumed that there exists a level of cooperation between network operators, where information about the frequency allocation and occupancy characteristics of the channels, and other parameters, can be exchanged to ensure low interference to the primary networks. In addition, DSS allows the networks that are engaged in the active mode to benefit economically by leasing their respective unused spectrum resources to each other. However, the passive model is considered to have a higher complexity than the active model due to added tasks such as spectrum sensing and control overhead. In this thesis we investigate these problems individually and we propose sensing, analysis and stochastic optimisation models.

1.2 Aim and objectives

The aim of the investigation is to improve the overall spectrum utilisation of networks and the objectives are to improve spectrum sensing performance, reduce blocking probability to subscribers, minimise the acquisition-cost of secondary network operators while meeting a given grade of service and maximise the profit of the secondary network operator subject to a budget limit. Below is an itemisation of the various research objectives.

- In order to cope with increasing demand of wireless services and applications and to improve the spectrum utilisation, dynamic spectrum sharing (DSS) is required. For a given operator with many spectrum resources from other operators in the same geographical location boundaries, it is hard to detect vacant channels with high accuracy. To achieve better probability of detection (and low probability of false alarm), cooperative spectrum sensing can be exploited to collect sensing

data from multiple secondary users and to provide effective and reliable sensing. While the use of cooperative spectrum sensing contributes to higher probability of detection and lower probability of false alarm, it is not always possible in urban environments due to high terrain, building structure etc. More importantly, it is known that inaccurate spectrum sensing, can result in interference to the primary operators and thus, in order to improve the accuracy of sensing, the effect of noise uncertainty, fading, and shadowing needs to be considered. While cooperative spectrum sensing is a well-studied problem in the literature and many spectrum sensing algorithms have been proposed for secondary networks, cooperative spectrum sensing considering location awareness has not been thoroughly investigated in the literature. Therefore, one objective in this thesis is to investigate the impact of location aware spectrum sensing in urban environment and to improve the detection probability by designing an efficient cooperative spectrum sensing (CSS) algorithm.

- In spectrum sharing environments, as the level of interaction between operators (e.g., sharing of information, resources, etc.) and number of operators increase, the complexity of the system analysis also increases and spectrum allocation has to deal with demands from a mix of types of services of these networks [10]. For example, considering TDMA and OFDM based services increases the allocation complexity further. As the complexity increases it becomes difficult to realise the benefit of spectrum sharing. There are many works which can be found in the literature on the usage of DSS to support radio access within heterogeneous networks [11, 12, 13, 14, 15]. However, none of the works discussed the overflow between coexistent network operators when different models of resource sharing are considered. Although intensive research has been carried out on resource sharing, only a few studies addressed the blocking probability gain and degradation when considering overflow in such coexisting networks [16, 17, 18, 19]. In this thesis detailed comparisons between various possible models for DSS are presented. Moreover, a number of analytical models have been derived specifically to allow

for more general analysis which is crucial for the new emerging DSS applications and future generation of cellular networks. The purpose of this investigation was to gain a better understanding of the possible short term benefits of the DSS.

- Operators aim to provide a stable grade of service (GoS)[1] to their end users with their limited statically allocated spectrum. However, in high demand periods, operators would require additional spectrum. A solution to increase the spectrum by means of sharing has been addressed in the research domain [21, 22, 23]. Spectrum sharing between operators often results in a significant improvement of GoS, although it would incur additional costs to the operators [24]. Since network operators often operate with a limited budget, the borrowing decisions of a network operator would be affected. Consequently, the operators would need to make dynamic, on-demand and correct choices of borrowing additional bandwidths from other operators in order to minimise cost or improve the profitability of the system. Given a market scenario with several operators, rules and conditions of spectrum access, spectrum requirement and their prices, and other parameters, our main objective is to optimise the resource sharing under a target GoS and budget restriction. We propose two models: the first is to optimise the amount of savings that secondary operator could achieve when they engage in spectrum trading with primary operators (incumbent holders of spectrum licenses) to gain a certain threshold of GoS. Second and more complicated is to optimise the profit of secondary operator under budget restrictions.

- Due to the mutual spectrum sharing agreement between the operators, the targeted GoS cannot be always guaranteed. Therefore, a post-optimisation analysis is needed to calculate the actual GoS in terms of blocking probability. Hence, another objective of this study is to provide a post-optimisation analysis where the leased spectrum bandwidth can be claimed back by the primary operator according to the operators' internal demand.

[1]The grade of service is generally defined by the level of blocking probability, where higher blocking probability means lower grade of service [20].

1.3 Contribution to knowledge

Major contributions of this thesis are summarised as follows:

- In order to optimise the spectrum sensing for cooperative cognitive radio, we propose a scheme that adopts the location awareness into cooperative spectrum sensing with cognitive radio networks. We argue that sensing performance to identify the spectrum vacant channels can be improved if local decisions from secondary users are processed according to their location in the coverage area in reference to the source signal. The proposed location aware scheme shows an improved performance over conventional hard combination scheme, highlighting the requirements of location awareness in CRNs. The analytical results obtained show that the proposed spectrum sensing scheme performs well in highly dense area. We also derive the optimum fusion rule of incoming decisions (the decisions which are coming from the secondary users) for spectrum sensing while taking location reliability into consideration. (Chapter 3)

- Considering spectrum sharing, six dynamic models are proposed. We show that a non-sharing model leads to poor performance in terms of blocking probability as performance measure; whereas there are possibilities of under-utilised spectrum within neighbouring network operators. In addition, we show that overflow modelling to access under-utilised frequency bands by using additional spectrum from adjacent operators within a given geographical region can be beneficial to the network, even if it comes with certain regulatory and operational limits. A network with dynamic and real time overflow capabilities can improve the performance of the network even for limited overflow access such as in the uni-directional overflow model. A performance comparison method was derived to evaluate the proposed models by evaluating the spectrum utilisation of the formed agreements. (Chapter 4 and 5)

- By adding trading and pricing functionalities to the sharing models, a novel purchase approach for dynamic spectrum sharing (DSS) network is proposed in

the presence of multiple primary service operators. Two optimisation problems are introduced in *merchant mode* DSS. The robustness of the proposed algorithms is investigated in the presence of a large number of cells and various types of spectrum bandwidths and the proposed algorithms are compared with heuristic borrowing algorithms. Comparisons show a substantial gain over the heuristic borrowing algorithms, which uses iterative procedure to solve the optimisation problem. In addition, a post-optimisation analysis technique of the operators' performance (secondary and primary) in the form of blocking probability is derived, which gives the actual GoS of the operators. (Chapter 6)

Presented in Figure 1.2 is an outline summary of the framework which emerged from our research.

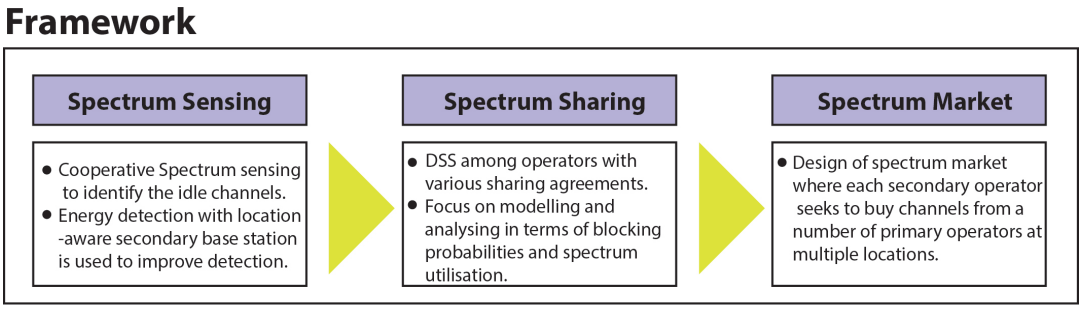

FIGURE 1.2: Framework for heterogeneous radio networks

1.4 Thesis outline

The rest of the thesis is organised as follows. Chapter 2, presents a comprehensive survey of the state-of-the-art in spectrum sensing and spectrum resource sharing. The main contributions of the thesis are discussed in details in Chapters 3, 4, 5 and 6. In Chapter 3, location aware spectrum sensing is proposed. While in Chapter 4, overflow modelling with two operators is discussed. In Chapter 5, we extend the work in Chapter 4 to model multi-operator network. In Chapter 6 we consider two optimisation problems in merchant mode spectrum sharing and we

present post-optimisation analysis at the end of the chapter. Finally, conclusions and future work are presented in Chapter 7.

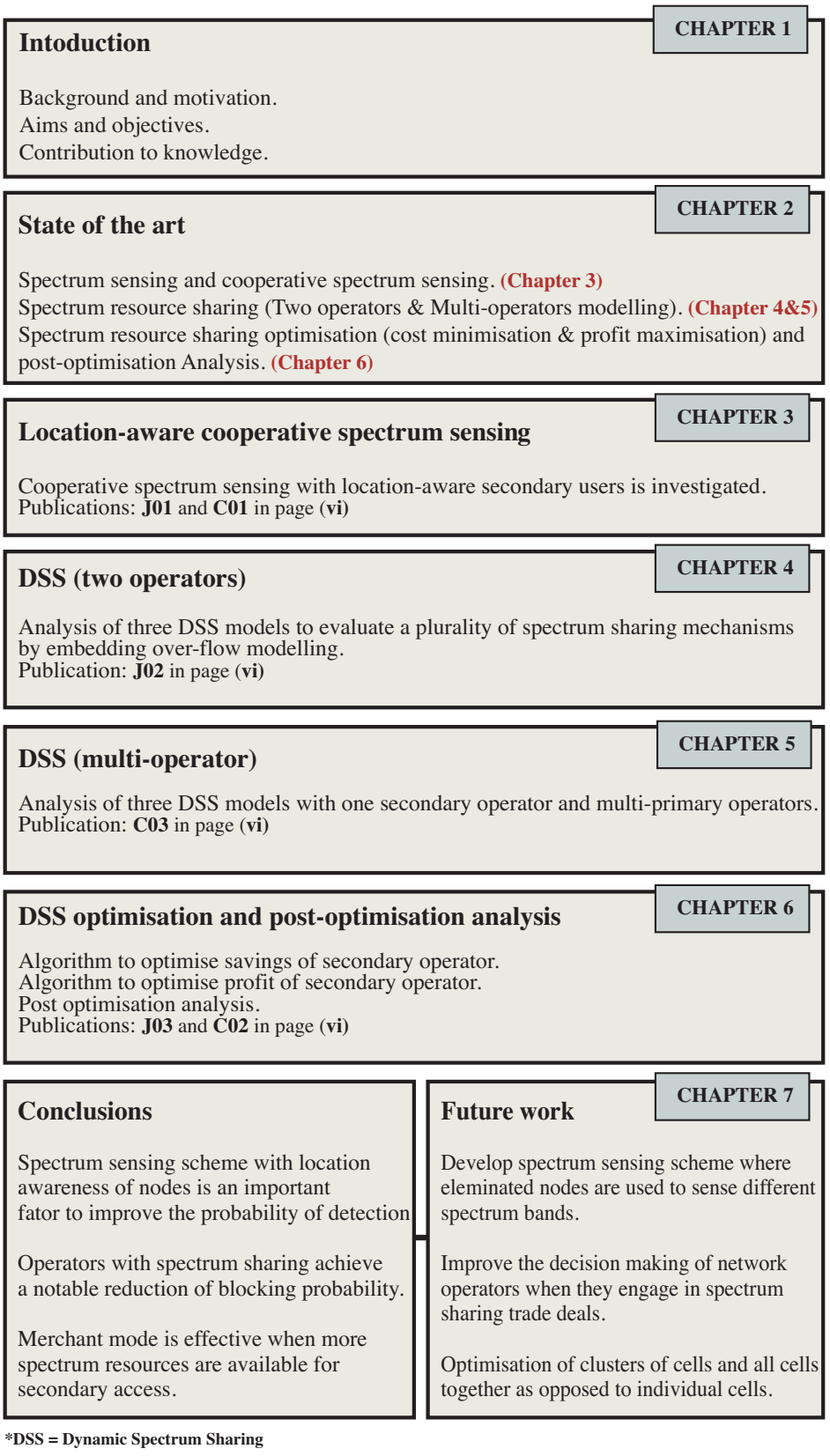

FIGURE 1.3: An illustration of the contents of the thesis chapters

Chapter 2

State of the Art in Spectrum Sensing and Spectrum Sharing

2.1 Introduction

The radio frequency spectrum is a natural resource, which covers the entire world and it is used for a wide variety of purposes. It is not only used for voice communications but also for communications of multimedia and data [25]. A large amount of spectrum below 60GHz has potential use for wireless telecommunications. The utility of the spectrum is obtained from its ability to be modulated to transport useful information [25]. Conventionally, spectrum is allocated in an exclusive manner. Exclusive licensing has many advantages including good interference management and baseline guarantee of Quality-of-Service (QoS) for users, which is necessary for creating an adequate investment and innovation environment. However, it also suffers from low flexibility and as a result low spectrum utilisation might occur in time and frequency domain. Since spectrum demand

increases significantly every year and most of the usable spectrum is already allocated (especially below 6 GHz) to various services[2], the operators are encouraged to improve the efficiency of allocated spectrum utilisation [26]. There are a number of current initiatives to improve the utilisation of spectrum. This section provides relevant background information on the recent approaches to increase the spectrum resources and improve the utilisation of existing bandwidths.

TV white space (TVWS) is one of the most promising solutions, which refers to the unused TV channels in the ultra-high frequency (UHF) spectrum. TVWS has shown that over 50% of locations in the UK are likely to have more than 150 MHz of TV spectrum and that even 90% of locations might have around 100 MHz of spectrum available [27]. The UK communication regulator, Office of Communications (Ofcom), has announced the licence exempt regulations for TVWS in December 2015 [28].

Light licensing is an approach developed when technology in millimeter-wave (mmWave) radio emerged. This mainly refers to frequency bands at 60 and 80 GHz, whose propagation properties enable operation of high data rate (e.g., in the magnitude of Gbps). Another distinguishing characteristic of mmWave signals is the directional transmission where large-scale directional antenna arrays can be used to provide substantial array gains, which help to compensate for the additional free space path loss caused by the ten-fold increase of the carrier frequency [29]. In the US, there is 7 GHz of unlicensed spectrum in the 60 GHz band, which is suitable for short-range links. Much of this overlaps with unlicensed 60 GHz spectrum in Europe and Japan, which opens the path for worldwide standardisation [30]. The spectrum in mmWave has attracted a lot of attention from the industry and research communities to measure and model mmWave channels and to evaluate its potential for future wireless systems [31, 29, 32].

[2]With the exception of new useful frequencies which have been identified and are either in the testing stages or waiting for governmental approval. An example of these frequencies are the 700 MHz band, 3.4 to 3.8GHz and 24.25 to 27.5GHz.

Enabling inter-operator spectrum sharing in a co-primary manner, is called co-primary spectrum sharing (CoPSS), where multiple operators jointly use a part of their licensed spectrum to enable an operator to cope with temporary peaks in capacity demand. Multi-operator spectrum sharing has been considered in many studies over the years. Most of the multi-operator spectrum sharing research has been done in macro cell networks [26, 33]. Inter-operator spectrum sharing has been treated as a game where operators participating in the game are players, each operator can either cooperate or compete to deal with the strategic interactions of one another for a game-theoretic problem [26].

Licensed shared access (LSA) has recently emerged in the literature [34, 35, 36]. LSA is a supervised shared access proposal based on an exclusive regime of spectrum sharing among spectrum holders, which have the right to commercially use a given wireless spectrum bandwidth. The LSA concept can offer a complementary approach to traditional exclusive licensing and license-exempt operations. It can be realised with reasonable modifications to the existing network infrastructure and regulatory framework with two new elements for managing the varying spectrum availability: the LSA Repository and LSA Controller [36].

In addition to the above mentioned approaches, dynamic spectrum sharing have been proposed to address spectrum scarcity and rapid growth in demand for spectrum resources. Regulators on the other hand are expected to provide greater flexibility for spectrum sharing among different operators and thus enabling optimised utilisation of allocated spectrum bandwidths within existing operators. New regulatory paradigms for spectrum authorisation are needed in addition to the classical exclusive assignments.

Resource allocation of dynamic spectrum access (DSA) is broadly categorised by the roles of primary networks, namely, the passive and active primary network models [37]. The passive model assumes that a primary network is unaware of the operations of secondary networks (secondary networks perform spectrum sensing

to determine idle spectrum), and it does not require any modification for the primary network systems. In contrast, in the active model, spectrum sensing is not required by secondary networks because it is assumed that a level of cooperation exists between network operators, where information about the frequency allocation and occupancy characteristics of the channels, and other parameters, can be exchanged to ensure low interference to the primary networks. In addition, DSS allows the networks that are engaged in the active mode to benefit economically by leasing their respective unused spectrum resources to each other. However, the passive model is considered to have a higher complexity than the active model due to added tasks such as spectrum sensing and control overhead. In this thesis we investigate these problems individually and we propose relevant analytical models for each problem. In the following, a summary is provided on the technical challenges and the relevant topics that need to be considered when introducing resource allocation of DSS.

2.2 Spectrum sensing

The term Cognitive Radio (CR) was first introduced by Mitola in the 1990s to take advantage of the under-utilised scarce wireless spectrum [38]. Cognitive radio technology is a key enabling technology for dynamic spectrum access [8]. Dynamic spectrum access provides high bandwidth to mobile users via heterogeneous wireless architectures [4]. In general, CR technology is proposed to solve the spectrum inefficiency problems. Typically, there are three main cognitive radio paradigms for sharing the spectrum: interweave, overlay and underlay. In the interweave paradigm, cognitive users opportunistically exploit the primary radio spectrum only when the primary signals are detected to be idle. In overlay paradigm, cognitive users help maintain and/or improve primary users' communication while utilising some spectrum resources for their own communication needs. The underlay paradigm, allows cognitive users to share the frequency bandwidth of the

primary network only if the resultant interference power level at the primary receiver is below given threshold. In terms of operation, the cognitive radio consists of three main stages: spectrum sensing, dynamic spectrum allocation and transmit power control. Spectrum sensing is considered as one of the most challenging tasks in CR technology [39, 40, 41, 42]. Users in a cognitive radio network can be allocated channels based on spectrum availability. This allocation also depends on internal and/or external policies. Transmit power control enables cognitive radio transmission to be controlled during and at the beginning of the transmission. This provide cognitive radio technology the ability to allow more users to share the spectrum and maintaining low interference to primary networks [3].

Spectrum sensing is considered as one of the most challenging tasks in cognitive radio technology [39, 40, 41, 42]. In the literature, various spectrum sensing methods and algorithms have been investigated, each having different operational requirements, advantages and disadvantages, such as matched filtering and energy detection. If the structure of the primary signal is known, the optimal detector in stationary Gaussian noise is a matched filter followed by a threshold test. This type of coherent detection may be a viable approach for early cognitive radio deployments where the secondary system is limited to operate within a few primary systems such as Television (TV) and Digital Video Broadcasting (DVB). However, if more primary bands are opened for opportunistic access, the implementation cost and complexity associated with this approach will increase [43]. A simpler alternative for the detection of a primary signal in Gaussian noise is to employ energy detection [44]. The latter has drawn more attention in recent years, mainly due to its low complexity [5, 42, 45, 46, 47, 48, 49, 50, 51]. Energy detection determines the existence or absence of primary users by comparing the received energy at a CR to a pre-defined threshold. The performance of the energy detection increases monotonically with the quality of the received signal [45, 52]. In [42], energy detection has been studied for low signal-to-noise ratio environment, while in [45], sequential energy detection was proposed to reduce sensing

time. The authors in [49] and [53] studied the performance of energy detection under different channel constraints such as additive white gaussian noise (AWGN) and fading channels.

Spectrum sensing based on energy detection is considered as the basis of spectrum sensing in this investigation due to its low complexity and also because it does not require prior knowledge of licensed users, however, it still requires a good estimation of the noise variance. The only requirement is to measure the power of the received signal and then compare it with a pre-defined threshold to make a local decision [54].

Careful selection of the threshold is one of the most influential parameters that defines the spectrum sensing reliability of the energy detection [55, 56]. Hence, thresholding is viewed as an optimisation problem within CR networks [42]. In [57], the double threshold technique was employed to improve the performance of spectrum sensing. Thresholding is also utilised to maximise the average transmission rate and throughput as shown in [58]. Selection of an appropriate threshold is still an open challenge in CCR approach due to the variable nature of the sensing environment, which varies from one application to another [59, 60, 61].

In spectrum sensing the performance is usually measured by two key factors: probability of detection and probability of false alarm. The former, is the probability that the detector correctly detects the signal when it is present in a given band. On the contrary, probability of false alarm is the probability that the detector incorrectly detects the presence of a signal though it is actually in temporary/permanent idle state. Probabilities are usually represented in a plot of the probability of detection versus the probability of false alarm which is commonly referred as receiver operating characteristics (ROC). In this thesis these two factors will be the basis to determine the reliability of the proposed scheme and the results will be compared with results of conventional spectrum sensing schemes.

2.3 Attenuation problem

One important issue in cognitive radio detection is the attenuation of target signals. The attenuation of the signal strength in cellular frequencies is caused by three factors, path loss, multi-path fading, and shadowing [62]. Here we define three attenuation factors:

- The path loss factor characterises the rate at which the signal strength decays as a distance from a transmitter increases. Path loss factor increase is observed when signal propagation is subject to reflection and deflection from surrounding objects, such as floors, walls and trees. There are many published models of path loss related to the frequency bands, which have described the various mechanisms that enable us to describe signal attenuation [63].

- Multi-path fading, also called fast fading, is the propagation phenomenon that results in radio signals reaching the receiving antenna by two or more paths. This is caused by reception of multiple copies of a transmitted signal through multi-path propagation. An amplitude distribution is often described by a Rician or Rayleigh distribution, depending on whether a dominant component among the multiple copies exists or not. Multi-path fading can influence the performance of the spectrum sensing at the SU [64]. Unlike path loss, multi-path fading can be tackled by cooperative sensing schemes. This is because only a subset of SUs may experience multi-path fading and shadowing at a given time and space [65, 66].

- Shadowing, often referred to as slow fading, represents a slow variation in a received signal strength, due to obstacles in propagation paths. This factor increases the signal detection uncertainty and reduces the diversity gain achievable through short-range cooperation [67, 68].

2.4 Cooperative Spectrum Sensing

The main challenge faced today by CR researchers is the ability to detect and utilise spectrum opportunities on a non-interference basis. Constructive and/or destructive interference can occur when signals travel along different paths to reach receivers, see Figure 2.1. This issue has prompted researchers to turn to Cooperative Cognitive Radio (CCR) networks, where all users collaborate in the spectrum sensing process. The advantage gained by using CCR networks lies at the achievable space diversity due to using multiple CRs [69, 70]. In this context, cooperation indicates that multiple users are responsible to sense one particular channel at defined time and location. Cooperative spectrum sensing has gained interest in many research papers such as the work in [71, 72, 73, 74, 75]. Different cooperative sensing strategies have been studied to achieve better reliability of detecting primary users. The sensing performance of a multiple primary user detector is discussed in [43]. Analytical formulae have been found for its false alarm probability and decision threshold. Numerical examples show significant performance gain over several detection algorithms in scenarios with realistic parameters.

Cooperative sensing is proposed in the literature as a solution to the problems that arise in spectrum sensing due to noise, fading, and shadowing [71]. However, the performance of Cooperative Spectrum Sensing (CSS) can be deceptive because it highly depends on the reliability of the global decision[3]. To address this challenge, various potential solutions were presented, as in [76, 43, 64].

Observations: Although it has been validated in many studies that cooperative sensing improves detection probability and false alarm [65, 64, 69], the majority of these studies do not consider the location of the CRs in reference to the source

[3]Global decision is a decision made by the fusion centre based on the observations of all the local decisions received by the base station to sense a targeted channel.

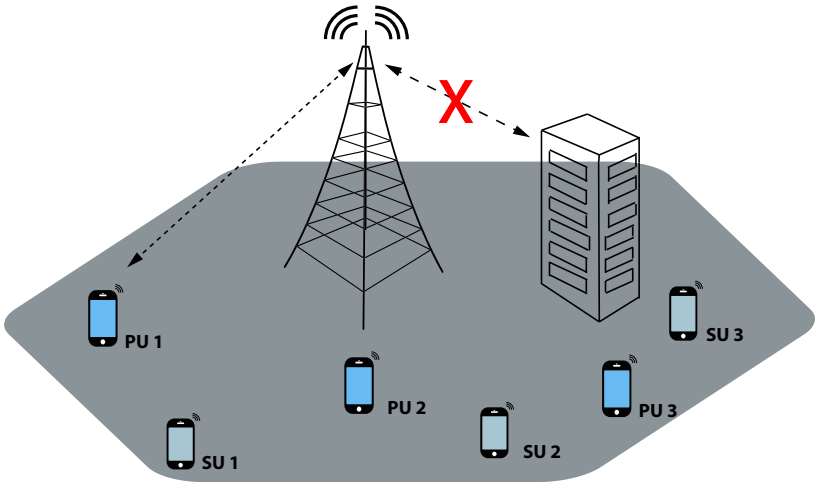

FIGURE 2.1: Hidden Terminal Problem

signal, which implies that all of the involved CRs' local decisions are taken into account with the same weight.

In this report we specifically address this issue and propose a new scheme to optimise spectrum sensing by considering location awareness. We show that the accuracy of spectrum sensing can be improved by avoiding secondary users' incorrect decision caused by refraction and diffraction. Furthermore, the proposed scheme takes advantage of spatial diversity raised due to the random distribution of secondary users within the coverage area.

2.5 Radio resource sharing for cooperative networks

There are many works which can be found in the literature on the usage of DSS to support radio access within heterogeneous networks [11, 12, 13, 14, 15]. In [11] the benefits of authorised spectrum access (ASA) are shown, considering different methods to optimise the resources, by simulating an LTE network where a mobile

network operator (MNO) is allowed to use the 2300 MHz band as an ASA licensee. The authors of [12] study a spectrum sharing problem in an unlicensed band where multiple systems coexist and interfere with each other. The more recent study [13] proposes a control-free dynamic spectrum access (DSA) algorithm for cognitive radio networks (CRNs).

Although intensive research has been carried out on resource sharing, only a few studies addressed the blocking probability gain when considering overflow in such coexisting networks [16, 17, 18, 19]. In [16], to comprehend statistical multiplexing and scheduling of non-trivial traffic sources in a framework for end-to-end analysis of multi-node networks, an intuitive approach to stochastic network calculus was obtained. The minimum blocking probabilities and maximum spectrum utilisations of three co-located systems with different bandwidth requirements were derived for one-channel band scenario in [17]. A channel packing scheme was then proposed for the multiple-channel band scenario to decrease the blocking probability and reduce the overall failure probability of the cognitive radio systems. In [18], call arrivals from primary users and secondary users in the opportunistic spectrum sharing system are modelled by a Markovian arrival process which captures correlation in the aggregate arrival process consisting of the two types of call arrivals. Stationary probability vector using matrix-analytic methods were also derived. A cognitive radio system based on scheduling technology was modelled in [19]. A hybrid priority dynamic policy, which indicates the primary user's preemptive priority and the secondary user's nonpreemptive priority, is developed to reduce spectrum switch overhead during the spectrum leasing process. A Markov chain analysis for spectrum access in licensed bands for cognitive radios is presented and forced termination probability, blocking probability and traffic throughput are derived in [77]. A channel reservation scheme for cognitive radio spectrum handoff was also proposed.

In [78], the authors focused on performance modelling for heterogeneous wireless networks based on a hierarchical overlay infrastructure. In particular, the new

traffic blocked in a network due to capacity limit can be overflowed to the networks with available capacity at the higher tiers. Such traffic overflow is considered a uni-directional overflow. While in [79], the authors considered a speed-sensitive call admission control (CAC) scheme to assign overflowed calls to appropriate tiers. If the new calls of fast-speed users in a low tier network are blocked due to capacity limits, the blocked new calls are overflowed to a high-tier network for possible service. If the blocked new calls are from slow-speed users in a high tier network, they are overflowed to a low-tier network. Blocked calls from fast-speed users are overflowed to the higher tier networks with larger coverage; blocked calls from slow-speed users are overflowed to the lower tier networks with smaller coverage. A bi-directional call overflows are supported in the hierarchical heterogeneous overlay systems. In [80], the load sharing scheme was considered, an incoming voice call is preferably distributed to the cell, and overflows to the WLAN only if there is not sufficient free bandwidth for a voice call in the cell. Dynamic transfer of ongoing voice calls in the WLAN to the cell via vertical handoff occurs whenever the cell has free bandwidth to accommodate more voice calls. Meta information of data calls that can be passed to the network layer is exploited. This scheme is also considered a bi-directional overflow model.

Five overflow policies were discussed in [81], the approach taken is to allow the new calls and handovers to compete on a first-come, first-served basis, to limit the number of times a new call may attempt to access a free channel compared with a handover. The authors developed an analytical method that treats overflow in a unified manner. The aim was to allow the approximate performance of overflow strategies that balance the need to maintain calls in progress with the desire to accept more new calls to be evaluated for large networks.

Observations: The models discussed in the literature are specific to hierarchical admission, type of service and mobility of users. We, on the other hand, present detailed comparisons between various possible models for DSA. In particular, we show that for a given operator the blocking probability does not always improve

and it depends on the level of interaction between operators. Moreover, our analytical models have been derived specifically to allow for a more general analysis which is crucial for the new emerging DSA applications (e.g. cognitive radio technology) and future generation of wireless telecommunications.

The spectrum allocation problem increases as we deal with heterogeneous networks. When we have this level of complexity, spectrum allocation has to deal with demands from a mix of types of services of these networks [10]. For example, considering TDMA and OFDM based services increases the allocation complexity further. To the best of our knowledge, none of the above works discussed the overflow between coexistent network operators when different models of resource sharing are considered. Although intensive research has been carried out on resource sharing, only a few studies addressed the blocking probability gain when considering overflow in such coexisting networks [16, 17, 18, 19].

2.6 Radio resource sharing for cooperative networks (Multi-operators)

The blocking probability evaluation is a popular tool to evaluate telecommunication networks/systems. It requires the description of the service arrival and departure process, which are stochastic in nature. Modelling of networks analysis is performed by the three-dimensional stochastic process where the arrival is random in both time and space. In cellular networks, the service is blocked from admission if required resources for given user are more than the available resource at the operator base station. Thus, the blocking probability of a service depends on the service arrival density and the number of channels available at the server [82].

In the recent years, a number of research papers focused on analysing systems' performance in terms of blocking probability and network wide spectrum utilisation.

Modelling of capacity management for cellular networks using Poisson process is presented in the literature. In [82], a multi-class service scenario is modelled using the multi-dimensional Markov Chain. The Markov chain is further approximated using the Erlang approximation method to evaluate the activity factor of a base station. The work in [83] presents the analytical expressions for blocking probability to evaluate the performance of the wireless network virtualisation under different sharing policies. The analytical results confirm that the framework is accurate and showing its suitability to serve as a tool to design an efficient policy for sharing the physical spectrum in the wireless network virtualisation. Blocking probability assessment, when both secondary user traffic and primary user traffic are present in the system have been investigated in [84]. The results obtained were validated through live mobile data of the primary user network. The authors in [85] present an analytical formulation of the dynamic spectrum allocation problem for handling multi-class services in two cellular radio systems using a complete sharing (CS) scheme. In [86], the multi-dimensional Markov process is used to obtain results on the blocking probabilities. In [87], the authors study the system performance using the two-dimensional Markov chain with handover and new calls based on the Erlang B systems. In [88], the authors studied co-operative resource sharing for wireless communication networks. In particular, the authors studied four models and present the analytical results of blocking probability for each model. With the limited level of cooperation or small number of operators in the network, it is easier to analyse the system performance and the closed form solutions can be obtained.

Observations: The majority of the analytical models presented above, do not provide a precise dynamic performance measure of cooperative operators' demand patterns. Although the pooled capacity issues were largely studied, their trade-off with respect to spectrum utilisation and blocking probability was not discussed in previous research.

In this thesis, in addition to the previous works, we consider the scenario emerging

from spectrum sharing where one secondary operator interacts with multi-primary operators according to certain mutual agreements. We analyse three types of multi-operator joint spectrum management schemes by considering a loss system. Analysis and modelling of the loss system are vital for the ubiquitous real-time multimedia (voice and video) communications where delay is not tolerable. The modelling and analysis of the loss systems are increasingly important due to the growing percentage of the multimedia traffic. Modelling of non real-time multimedia traffic by using the queue system is also important but beyond the scope of this thesis.

2.7 Radio resource sharing framework for cooperative networks (Multi-operators) with optimisation and post-optimisation analysis

In the literature, a great number of studies has appeared in recent years on the design of dynamic spectrum sharing within cellular networks [89, 90, 91, 92, 93, 88, 94]. Interests in this context include secondary leasing and pricing strategies among incumbent spectrum license holders, secondary operators and secondary users. These prior studies mainly focused on approaches using *auction mode* and game theory to implement the spectrum pricing and allocation schemes by taking into account the variation of the networks demands and constraints such as power, price and interference [89, 90, 91, 92, 93, 88, 95]. In [95], the authors proposed a multiple-dimension auctioning mechanism through a broker to facilitate an efficient secondary spectrum market. In [94] a knapsack based *auction mode* that dynamically allocates spectrum to the wireless service providers such that revenue and spectrum usage are maximised. A dynamic pricing strategy for the service providers is also proposed. Auction schemes where a central clearing

authority auctions spectrum to bidders, while explicitly accounting for communication constraints is proposed in [96]. The used techniques are related to the posterior matching scheme, which is used in systems with channel output feedback. While in [97], spectrum auctions in a dynamic setting where secondary users can change their valuations based on their experiences with the channel quality was studied. The authors in [91] investigate price-based resource allocation strategies for two-tier femtocell networks, in which a central macrocell is underlaid with distributed femtocells, all operating over the same frequency bandwidths. A Stackelberg game is formulated to study the joint utility maximisation of the macrocell and femtocells subject to a maximum tolerable interference power constraint at the macrocell base station. Price-based DSS has also been investigated from the business perspective [98, 99]. For example, in [100] an extensive business portfolio for heterogeneous networks is presented to analyse the benefits due to multi-operator cooperation for spectrum sharing. High resolution pricing models are developed to dynamically facilitate price adaptation to the system state. In [101], a quality-aware dynamic pricing algorithm (QADP) which maximises the overall network revenue while maintaining the stability of the network was studied.

Observations: The vast majority of the aforementioned studies consider competitive market scenarios and therefore auction and game theory have been discussed to develop DSS strategies. By using the same assumption, pricing in the context of DSS has mainly been considered from the spectrum owners perspective to maximise their revenues [98, 93, 102]. However, when the number of available bandwidths from multiple license owners is higher than SNO's demand, then *auction mode* is not always the best strategy. This is because the number of bidders might be too small and the best selling price cannot be achieved for the license owners by using *auction mode*. A more realistic and pragmatic model in this case

is a *merchant mode*[4], which to the best of the our knowledge, has not been investigated in the context of DSS. Moreover, spectrum borrowing when considering budget restrictions has not been addressed. Also, there is currently no published work, which attempted to study the admission cost minimisation in the *merchant mode* with target performance. Thus, the problems that we formulate and solve substantially differ from those available in the literature.

The analysis of blocking probability and dynamic aggregated channel assignment has been extensively considered in the context of cellular networks [77, 79]. However, there are significant differences between *auction mode* and the focus of our work. For example, in *auction mode* network operators are not assumed to claim back the leased spectrum within a single trading window during busy intervals [36]; whereas in our approach, the leased capacity is dynamic in size. To the best of our knowledge, our post-optimisation analysis is the first to study the blocking probability behaviour during a trading window with the presence of multiple operators. It also addresses the issue of primary operators' change in state during a single trading window.

[4] ***Merchant mode:*** The primary operators determine the spectrum price based on their current utilisation and demand. The price is then advertised on a "take-it or leave-it" basis and is assigned on a first come basis. No negotiation is conducted with the secondary operators [10].

Chapter 3

Location-aware Cooperative Spectrum Sensing

3.1 Introduction

High blocking probabilities are unavoidable for many users due to shortages of frequency resources caused by inefficient utilisation. Cognitive radio (CR) technology was introduced in the literature to solve these ongoing spectrum inefficiency problems. The term cognitive radio was first introduced by Mitola in the 1990s to take advantage of the under-utilised wireless spectrum [38, 1, 2]. Cognitive radio is a key enabling technology for dynamic spectrum access which provides higher bandwidth to mobile users via heterogeneous wireless architectures [8, 5, 6, 7].

There are three main cognitive radio paradigms for dynamic spectrum access: interweave, overlay and underlay. In the interweave paradigm, cognitive users opportunistically exploit the primary radio spectrum only when the primary signals are detected as idle. In the overlay paradigm, cognitive radio users (or secondary users) help maintain and/or improve primary users' (incumbent users) communication while utilising some spectrum resources for their own communication needs.

The underlay paradigm allows cognitive users to share the frequency bandwidth of the primary network only if the resultant interference power level at the primary receiver is below given threshold.

Cognitive radio is performed by a cycle which consists of three main stages: spectrum sensing, dynamic spectrum allocation and transmit power control, see Figure 3.1. Spectrum sensing is considered as one of the most challenging tasks in cognitive radio technology [39, 42]. In dynamic spectrum allocation, channels are allocated to users based on spectrum availability. This allocation also depends on internal and/or external policies between cooperative networks. Transmit power control enables cognitive radio transmission to be controlled at the beginning and during the transmission. This enables cognitive radio networks to serve more users, and to lower the interference to the spectrum owners [3].

In spectrum sensing the performance is usually measured by two key factors: probability of detection and probability of false alarm. The former, is a probability that the detector correctly detects the signal when it is present in a given band. On the contrary, probability of false alarm is a probability that the detector incorrectly detects the presence of a signal though it is actually in temporal/permanent idle state. Probabilities are usually represented in a plot of the probability of detection versus the probability of false alarm which is commonly referred as radio operating characteristics (ROC). These two factors will be the basis for determining the reliability of the proposed scheme and the results will be compared with the performance of conventional hard combining scheme.

The remainder of the Section is organised as follows. In Section 3.2 we define the system model and assumptions of the cooperative cognitive radio network that is used in our analysis. Section 3.3 gives a review of our proposed sensing method. Analytical results are discussed in Section 3.4 and finally, we give the summary and discussion in Section 3.5.

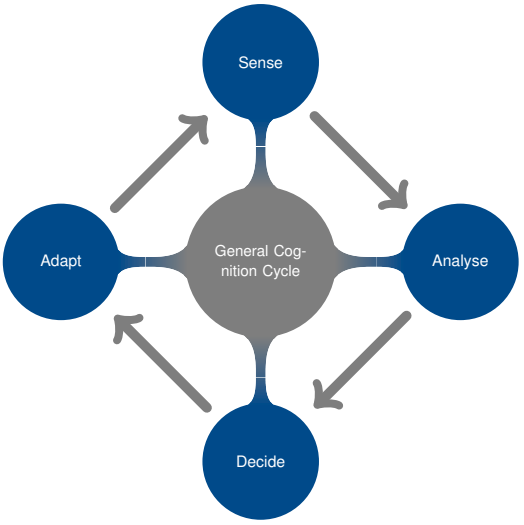

FIGURE 3.1: Cognitive cycle

3.2 System model and assumptions

In this section, we consider an infrastructure-based cooperative cognitive radio network which consists of one primary and one secondary network. A secondary base station (SBS) which also functions as a fusion centre is also part of the secondary network. The network includes M (where $m = 1, 2, \ldots, M$) secondary users (SUs) which are scattered in a given geographical area at the periphery of the coverage of the secondary base station. In Figure 3.2, secondary users observe the same hypotheses independently and transmit their measurements to the secondary base station through a dedicated control channel which is assumed to maintain communication between secondary users and their associated secondary base stations. Here, we assume the control channel is error free [103, 104, 105].

Similarly, the primary network consists of a primary base station (PBS) and primary users (PUs). Since we are interested in the downlink frequency channels of the primary network, secondary users only perform spectrum sensing to target downlink channels (from the base station to the user), which are transmitted by the primary base station. Secondary base station decides whether a primary signal exists or not which is a normal random process that depends on both the

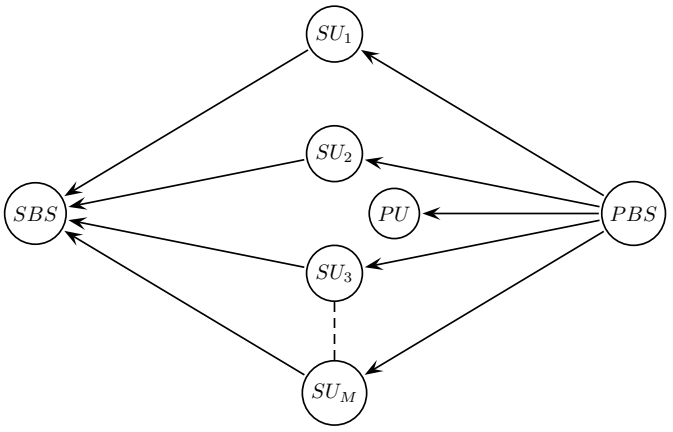

FIGURE 3.2: System Model

primary base station activities and the spectrum sensing accuracy of secondary users. Spectrum sensing at the secondary users is performed using energy detection which is commonly formulated as a Neyman-Pearson (NP) type binary hypothesis test problem. In such sensing technique, the received signal $r_i(t)$ at the ith SU receiver and at time t is given by [53, 106]

$$r_i(t) = \begin{cases} w_i(t) & \text{if channel is free} \quad H_0 \\ h\ s_i(t) + w_i(t) & \text{if channel is busy} \quad H_1, \end{cases} \tag{3.1}$$

where h is the channel gain, $s_i(t)$ is the signal that comes from a primary base station and is received at the ith SU and $w_i(t)$ is the additive white Gaussian noise (AWGN) with zero mean and unit power $\mathcal{N}(0, 1)$. Note that $s_i(t) = 0$ when there is no transmission by primary base station. The hypothesis models H_0 and H_1 as presented in equation (3.1) denote the absence and the presence of the primary signal, respectively. Notations used in this chapter are described in Table 3.1.

The performance's measurement of any cognitive radio system is determined by its probability of detection ($P_{d,i}$) and probability of false alarm ($P_{f,i}$). High ($P_{d,i}$) guarantees minimal interference to the primary networks, and low ($P_{f,i}$) guarantees throughput improvements for the secondary network. Both measurements are used

TABLE 3.1: Notations Used

Notations	Descriptions
$P_{f,i}$	Probability of false alarm at the ith SU
$P_{d,i}$	Probability of detection at the ith SU
H_0	Null hypothesis
H_1	Alternative hypothesis
λ	Decision threshold
σ_w^2	Noise power
$Q(.)$	Q function
γ	Average signal to noise ratio of the primary base station received by the secondary users
Y	Received energy for binary hypothesis
$r(t)$	Received energy
h	Channel gain
$s(t)$	Transmitted signal
$w(t)$	AWGN with zero mean and unit power
N	Sample Number
M	Number of secondary users
u_0	Global binary decision at the secondary base station
u_i	Binary decision at the ith SU
Q_d	Overall detection probability
Q_f	Overall false alarm probability
S_j	Set of all decisions at the secondary base station which are equal to j where $j \in (0, 1)$

as the basis to determine the performances of the proposed cooperative cognitive radionetwork. $P_{d,i}$ and $P_{f,i}$ can be estimated by [42]

$$P_{d,i} = \Pr\{Y > \lambda | H_1\} \tag{3.2}$$

and

$$P_{f,i} = \Pr\{Y > \lambda | H_0\}, \tag{3.3}$$

where Y is the received energy. The probability of detection in equation (3.2) refers to the probability of accepting H_1 when H_1 is true. The probability of false alarm in equation (3.3) refers to the probability of accepting H_1 when H_0 is true. According to the limit theorem and with direct computation of (3.2) and (3.3), we have [107]

$$P_{d,i} = Q\left(\left(\frac{\lambda}{N\sigma_w^2} - \gamma - 1\right)\frac{\sqrt{N}}{(2\gamma 1 + 1)}\right) \tag{3.4}$$

$$P_{f,i} = Q\left(\left(\frac{\lambda}{N\sigma_w^2} - 1\right)\sqrt{N}\right) \tag{3.5}$$

where λ is the decision threshold, σ_w^2 is the noise power, $Q(.)$ is the Q function, γ is the average signal to noise ratio of the primary base station received by the secondary users and N is the sample number [53]. According to the information collected from secondary users, the secondary base station makes its final decision about the spectrum availability. A specified decision method is adopted in order for the secondary base station to reach its final conclusion. Decision methods are generally divided into hard and soft combination decision. In hard combination decision, each SU reports their local decision to the secondary base station, and the decision is made from a specific rule, such as logic "AND" and logic "OR". Hard combining is simple to implement, and it requires lower overhead (e.g., one-bit) [108]. For soft combination decision, the original observed data at the secondary users such as the received power, is reported to the secondary base station and the decision is obtained by using one of the available techniques, such as equal gain combining (EGC) and log likelihood ratio (LLR) [108, 109, 110]. The soft combining method outperforms the hard combining method in terms of the probability of missed opportunity. However, hard combining decisions are found to perform as well as soft decisions when the number of secondary users is high [108].

We consider the hard combination decision as the core of our cooperative spectrum sensing decision method. In order to improve accuracy of the chosen sensing method, we assume the secondary base station is aware of the secondary user's location. Secondary users can be located in high dense built areas where power measurements are less reliable due to various phenomena such as diffraction and reflection. It is important that the sensing decision method considers the secondary

users locations to determine the environmental conditions of secondary users because the sensing accuracy is a function of location in respect to the source signal. Inaccurate sensing measurements which are sent to the secondary base station can potentially degrade the sensing accuracy. In a typical cellular network, the locations are stored in the HLR (Home Location Register). The home location register is the central user database in the mobile radio network. It stores the user and subscriber information. The location of both primary base station and secondary users can be described by longitude and latitude, which are a random collection of points on a coverage area [8]. The locations of primary base stations can be obtained based on publicly available data such as the Consolidated Database System (CDBS). The locations of mobile secondary users can be determined by various location estimation techniques such as time-of-arrival (TOA), angle-of-arrival (AOA), received signal strength (RSS), pattern recognition and Bayesian filters [111].

3.3 Location-aware cooperative spectrum sensing

3.3.1 Urban Propagation

Since spectrum is a very limited commodity in mobile communication systems, particularly in urban areas, we focus our study on the urban environment [112]. Propagation of electromagnetic waves in urban areas in cellular frequencies is influenced by the geographical area and the structure of buildings in dense environment. Therefore, a detailed vector database of the buildings is required in order to establish a propagation map. Typically the multi-path propagation is very important in urban environments. Urban propagation models already play an important role in the development, planning and deployment of mobile radio

systems where coverage is the primary goal. Urban propagation models could also be used for signal detection reassessment, as we show in this chapter.

3.3.2 Proposed Scheme

We propose a scheme which is capable of improving the sensing accuracy of a cooperative cognitive radio system. In this scheme, secondary users determine their locations to measure the signal path quality in reference to the primary base station (source signal). The location data of secondary users are sent to the secondary base station for further investigation, see Figure 3.3.

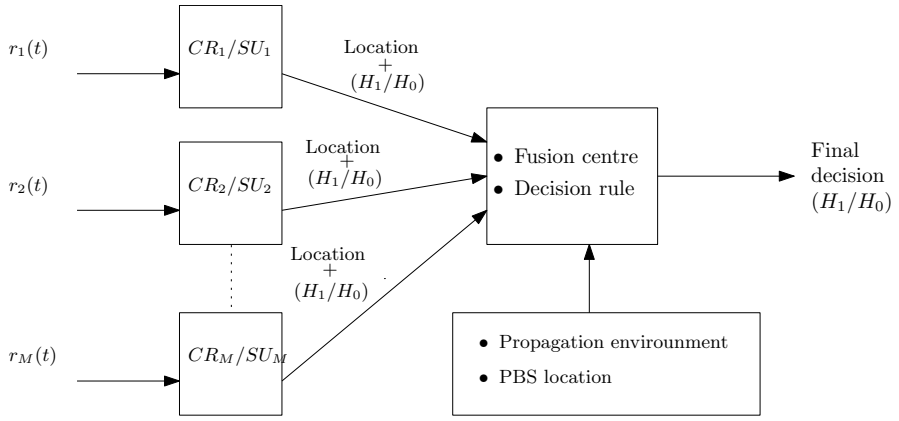

FIGURE 3.3: Proposed location aware scheme

Knowledge of secondary users location at the secondary base station can determine whether a line-of-sight (LOS) between the transmitter and receiver exists, and if the path is obstructed by large building developments and structures such as wind turbines (e.g. Non-line-of-sight (NLOS) propagation), which can potentially cause the received signal being less detectable at the secondary users. Such consequential impact can degrade the sensing quality when considering a global decision.

3.3.3 Trust Value

In the proposed scheme, the sensing results from secondary users are returned to the secondary base station along with location coordinates. We note that when secondary base station is in possession of the locations of secondary users and primary base station, and primary base station's networking information, including channel, height, transmit power antenna directionality etc. The secondary base station will have the ability to approximate a trust value. There are a number of propagation models which are well designed and give quite good accuracy of signal propagation, for example Okumura-Hata model, which is one of the most widely used empirical propagation prediction models [113]. It was developed through works of Y. Okumura and M. Hata and is based on the results of extensive measurements in certain urban and suburban areas of Japan. Such a propagation model could be used to predict the signal power at any point on a map, which could be used to assign trust values for secondary users. The pattern shown in Figure 3.4 is typical for a power law based empirical model used in an urban environment. The sector antenna patterns are clearly seen from the shape of the results. The lobes in the vertical pattern of each antenna explain the alternating colours along a radius away from each antenna [114].

The trust value accounts for the density of the surrounding structure of a given SU and the propagation environment in reference to the primary base station (source signal) and can be written as

$$\mathrm{T}_i(t) = f\left(d_{(i,PBS)}(t), h_i(t), h_B, f_0, L, C\right), \tag{3.6}$$

where $f(\cdot)$ is a function which may take a variety of shapes, for example a linear form such as the the Okumura model [115]. $\mathrm{T}_i(t) \in 0 \leq \mathrm{T}_i(t) \leq 1$, $d_{i,PBS}(t)$ denotes the distance between the ith SU and the primary base station at time t, $h_i(t)$ denotes the ith SU's antenna height, h_B denotes the primary base station's

height, L denotes the propagation loss, f_0 denotes the central frequency of the target signal and C is any physical constant (such as type of environment, water surfaces, isolated obstacle etc.).

The coverage area of the secondary base station can be divided into smaller sectors and a trust value is assigned for each sector to represent the environmental propagation in respect to the relevant primary base station. The trust value reassesses the sensing data before the fusion process to obtain the global decision. The motivation is to make a comparison between the real sensed signal power which is received at the secondary users and the expected signal power at each corresponding sector in the coverage area. The trust value contributes to enhance the accuracy of the secondary base station when the global decision of a particular channel status is calculated.

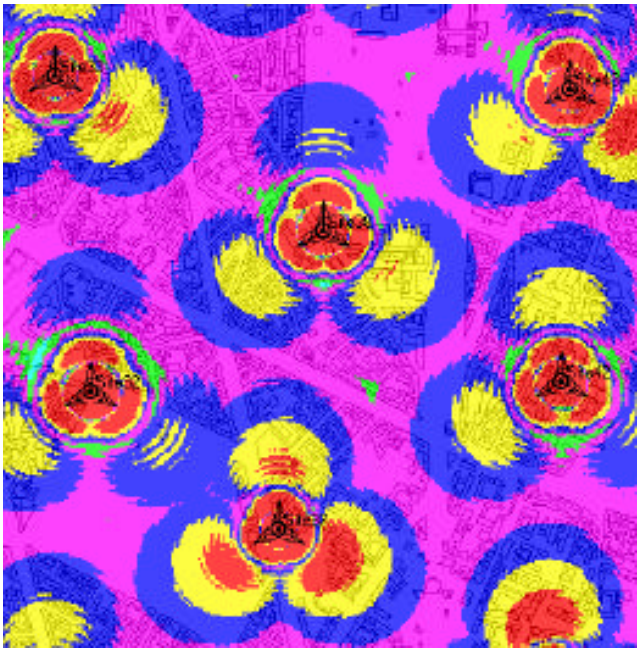

FIGURE 3.4: Signal strength from empirical propagation predictions

3.3.4 Elimination

A SU can be assigned either a low or high trust value. A low trust value indicates that a SU is located in a shadowed area (e.g. highly dense urban area) whereas a high trust value indicates that a SU is located in a less dense environment (e.g., LOS propagation is predicted). If a SU is assigned a low trust value it will be eliminated from subsequent procedures. This step ensures that such a SU does not make any significance when considering a global decision at the secondary base station. Secondary users submit the locations and the sensing results simultaneously, therefore, assigning trust values to secondary users is time and space dependent. When SU moves to a new location, a new trust value is assigned, which reflects the current location of the SU.

We assume all secondary users in the coverage area of the secondary base station follow the same process. Further steps are taken to secondary users which are assigned a high trust value. Secondary users measure the received power using the energy detection technique, which we briefly discussed in section 3.2. Secondary users submit their local decision to the secondary base station in a form of hard decision (1 if the energy detected is greater than a certain threshold and 0 otherwise.). These measurements are further processed at the secondary base station. Based on the results obtained from the secondary users, the secondary base station determine whether the corresponding channel is free from any primary transmission.

We list the detailed procedure in Algorithm 3.1.

3.3.5 Proposed Fusion Rule

In cooperative spectrum sensing, and in hard combining scheme, secondary users send their final one-bit decision to the secondary base station. $u_i \in \{0, 1\}$ is the binary decision made by the ith SU, which in essence is a logical decision metric. In

Algorithm 3.1 Proposed Spectrum Sensing

Initialisation
Number of secondary users in the network = M
$\mathbf{R} \leftarrow Empty$
for $i = 1 : 1 : M$ **do**
    Obtain SU's Location
    if ith SU is assigned low trust value **then**
        Eliminate ith SU from further analysis
    else
        $\mathbf{R} \leftarrow i$th SU
        where $\mathbf{R}$ is a vector containing all secondary users with high trust value
    end if
end for
Collect sensing results from secondary users in $\mathbf{R}$
Run log likelihood ratio test for all secondary users in $\mathbf{R}$
Calculate detection and false alarm probabilities
return

this context, 0 and 1 indicate the absence and the presence of the primary signal, respectively. There can be a number of fusion rules at the secondary base station that are represented by k-out-of-K rule and for such rule the overall detection and false alarm probabilities are, respectively [64, 56, 107]

$$Q_d = \sum_{q=k}^{K} \binom{K}{q} \left\{ \prod_{i=1}^{q} P_{d,i} \cdot \prod_{j=1}^{K-q} (1 - P_{d,i}) \right\}, \tag{3.7}$$

and

$$Q_f = \sum_{q=k}^{K} \binom{K}{q} \left\{ \prod_{i=1}^{q} P_{f,i} \cdot \prod_{j=1}^{K-q} (1 - P_{f,i}) \right\}, \tag{3.8}$$

where

$$\binom{K}{q} = \frac{K!}{q! \cdot (K-q)!} \tag{3.9}$$

Secondary base station receives decisions from M secondary users and decides H_1 if any of the total M individual decisions is H_1 and decides H_0 otherwise. This fusion rule is known as the OR-rule or 1-out-of-M rule. While AND rule corresponds to the case where secondary base station receives decisions from M secondary users and decides H_1 if all of the total M individual decisions are H_1 and decides H_0 otherwise. The global probabilities of false alarm and detection for the two fusion rules can be obtained as [64, 56, 107]

OR fusion rule:

$$Q_{d,or} = 1 - (1 - P_d)^M \tag{3.10}$$

and

$$Q_{f,or} = 1 - (1 - P_f)^M. \tag{3.11}$$

AND fusion rule:

$$Q_{d,and} = (P_d)^M \tag{3.12}$$

and

$$Q_{f,and} = (P_f)^M. \tag{3.13}$$

Fusion of incoming local decisions and decisions which are made at the secondary base station is considered in this section. In the scenario discussed here, secondary users could make only hard decisions such that u_i could take only two values 0 or 1 based on its local observation, such that $u_i \in \{0, 1\}$. Each SU makes a local decision u_i, where $\{i = 1, \ldots, M\}$ based on the local observation. The secondary

base station produces the global decision $u_o \in \{0, 1\}$. This problem is known as the binary hypothesis test (or statistical decision) since the secondary base station chooses between two hypothesis, where H_0 and H_1 are the noise-only hypothesis and signal-plus-noise hypothesis, respectively. The fusion rule which represents the AND rule in which $u_o = 1$ if all the local decisions are 1, i.e.,

$$u_o = \begin{cases} 1, & u_i = 1, i = 1, 2, \cdots, N \\ 0, & \text{otherwise.} \end{cases} \tag{3.14}$$

The OR rule in which $u_o = 1$ if at least one of the local decisions is 1, i.e.,

$$u_o = \begin{cases} 0, & u_i = 0, i = 1, 2, \cdots, N \\ 1, & \text{otherwise.} \end{cases} \tag{3.15}$$

The optimum fusion rule for this problem is given by the likelihood ratio test (LRT) as

$$\frac{\Pr(u_1, u_2, \ldots, u_M|H_1)}{\Pr(u_1, u_2, \ldots, u_M|H_0)} \underset{u_o=0}{\overset{u_o=1}{\gtrless}} \eta, \tag{3.16}$$

where η is the decision threshold, which is determined by the specified values of P_f and P_d. Next, we assume that $P_{d,i} \geq P_{f,i}$, where $\{i = 1, \ldots, M\}$. This assumption is common in cooperative cognitive radio networks sensing scenarios. We also make the following definitions

$$P_{f,i} = \Pr\left(u_i = 1|H_0\right) \tag{3.17}$$

and

$$P_{d,i} = \Pr\left(u_i = 1|H_1\right), \tag{3.18}$$

where u_i is the local decision at the secondary base station. The global probability of false alarm and detection, at the secondary base station, denoted by Q_f and Q_d are given by

$$Q_f = \Pr\left(u_o = 1|H_0\right), \tag{3.19}$$

and

$$Q_d = \Pr\left(u_o = 1|H_0\right) \tag{3.20}$$

Because the local decisions are independent, the left hand side of equation (3.16) can be written as

$$\begin{aligned}
\frac{\Pr\left(u_1, u_2, \ldots, u_M|H_1\right)}{\Pr\left(u_1, u_2, \ldots, u_M|H_0\right)} &= \prod_{i=1}^{M} \frac{\Pr\left(u_i|H_1\right)}{\Pr\left(u_i|H_0\right)} \\
&= \prod_{S_1} \frac{\Pr\left(u_i = 1|H_1\right)}{\Pr\left(u_i = 1|H_0\right)} \cdot \prod_{S_0} \frac{\Pr\left(u_i = 0|H_1\right)}{\Pr\left(u_i = 0|H_0\right)} \\
&= \prod_{S_1} \frac{Pd_i}{Pf_i} \cdot \prod_{S_0} \frac{1 - Pd_i}{1 - Pf_i}.
\end{aligned} \tag{3.21}$$

where S_j is the set of all local decisions, which are received by the secondary base station and are equal to j, $j = 0, 1$. The fusion rule that minimises the false alarm probability and maximises the probability of detection is given by

$$\prod_{S_1} \frac{P_{d,i}}{P_{f,i}} \cdot \prod_{S_0} \frac{1 - P_{d,i}}{1 - P_{f,i}} \underset{u_o=0}{\overset{u_o=1}{\gtrless}} \eta \tag{3.22}$$

So far we have discussed the fusion rules for the binary hypothesis problem without considering the reliabilities of the locations of the secondary users. Next, we include the case in which the SU are assigned a trust value which represents the expected signal strength in their respective region. The trust values and the threshold are determined by the reliability of the local decisions (by the probabilities of false alarm and detection of the secondary users). Trust values are modelled as the probability of a SU to be located in the region of acceptable reception, e.g. $T_i = j$, and $j \in [0, 1]$, where T_i is spatially independent and $T_i = 0$ represents that the respective SU location is in high shadowed area, while $j = 1$ indicates that a user is located within a line of sight in respect to the sensed signal (source signal). Assume that the trust values at each SU can take J values. The fusion rule in this case is given by the LRT in (3.23) since it indicates for each value of T_i the likelihood of H_1 versus the likelihood of H_0 and can be expressed as

$$\frac{\Pr\left(T_1, T_2, \ldots, T_M | H_1\right)}{\Pr\left(T_1, T_2, \ldots, T_M | H_0\right)} \cdot \frac{\Pr\left(u_1, u_2, \ldots, u_M | H_1\right)}{\Pr\left(u_1, u_2, \ldots, u_M | H_0\right)} \underset{u_o=0}{\overset{u_o=1}{\gtrless}} \eta \tag{3.23}$$

Now, let us define the following probabilities:

$$\alpha_{i,j} = \Pr\left\{T_i = j | H_0\right\} \tag{3.24}$$

$$\beta_{i,j} = \Pr\left\{T_i = j | H_1\right\} \tag{3.25}$$

The ratio $\frac{\Pr(T_1, T_2, \ldots, T_M | H_1)}{\Pr(T_1, T_2, \ldots, T_M | H_0)}$ in equation (3.23) can be expressed as

$$\begin{aligned}\frac{\Pr\left(T_1, T_2, \ldots, T_M|H_1\right)}{\Pr\left(T_1, T_2, \ldots, T_M|H_0\right)} &= \prod_{i=1}^{M} \frac{\Pr\left(T_i|H_1\right)}{\Pr\left(T_i|H_0\right)} \\ &= \prod_{j=0}^{J-1} \prod_{S_j} \frac{\Pr\left(T_i = j|H_1\right)}{\Pr\left(T_i = j|H_0\right)}\end{aligned} \tag{3.26}$$

Substituting (3.24) and (3.25) in (3.26), we obtain the following expression:

$$\frac{\Pr\left(T_1, T_2, \ldots, T_M|H_1\right)}{\Pr\left(T_1, T_2, \ldots, T_M|H_0\right)} = \prod_{j=0}^{J-1} \prod_{S_j} \left(\frac{\beta_{j,i}}{\alpha_{j,i}}\right) \tag{3.27}$$

Subsequently, by substituting (3.27) and (3.22) in (3.23) we obtain the following fusion rule:

$$\prod_{j=0}^{J-1} \prod_{S_j} \left(\frac{\beta_{j,i}}{\alpha_{j,i}}\right) \cdot \prod_{S_1} \frac{P_{d,i}}{P_{f,i}} \cdot \prod_{S_0} \frac{1 - P_{d,i}}{1 - P_{f,i}} \underset{u_o=0}{\overset{u_o=1}{\gtrless}} \eta, \tag{3.28}$$

where S_j is the set of all trust values T_i that are equal to $j, j \in [1, 0]$.

and by taking the logarithm of both sides, we obtain the optimum fusion rule that minimises the false alarm and maximise the probability of detection as

$$\sum_{j=0}^{J-1} \sum_{S_j} \log\left(\frac{\beta_{ji}}{\alpha ji}\right) + \sum_{S_1} \log \frac{P_{d,i}}{P_{f,i}} + \sum_{S_0} \log \frac{1 - P_{d,i}}{1 - P_{f,i}} \underset{u_o=0}{\overset{u_o=1}{\gtrless}} \log\ \eta \tag{3.29}$$

This fusion rule can also be expressed as

$$\sum_{i=1}^{M}\left[u_i \log\frac{P_{d,i}}{P_{f,i}} + (1-u_i)\log\frac{1-P_{d,i}}{1-P_{f,i}}\right] + \sum_{j=0}^{j-1}\sum_{S_j}\log\left(\frac{\beta_{ji}}{\alpha ji}\right) \underset{u_o=0}{\overset{u_o=1}{\gtrless}} \log\ \eta, \quad (3.30)$$

where (3.30) is a generalised form of (3.29).

3.4 Analysis and results

In order to evaluate the performance of our scheme, analytical results are given in this section. In our analysis, it is assumed that the secondary base station is aware of the relevant primary network parameters as well as locations of secondary users and primary base station and the trust value can be calculated, i.e., by equation (3.6). The simulations are performed using MATLAB, where we assumed the number of cooperative secondary users to be 30 and number of sampling equal to 128. For the analytical results, it is reasonable that we compare our proposed scheme with conventional cooperative spectrum sensing scheme. In the comparison presented in Figure 3.5, we varied the signal to noise ratio (SNR)[5] from -2.5dB to 2.5dB, according to [56], to investigate all the possible cases within this range. In Addition two false alarm probability P_f values are considered and are set to be 0.1 and 0.2. The secondary users which are located in high trust value is set to be 0.75. Figure 3.5 shows the improved performance of our proposed scheme when eliminating the secondary users which are considered to be located in high shadowed areas which is 25% of all participating secondary users. Because these secondary users are eliminated from further processing, they have no impact on final global decisions. It is clear that for both values of false alarm probabilities that the probability of detection P_d increased when we apply our proposed scheme. Results also indicate a slight improvement in terms of required average SNR for detection.

[5]SNR is defined as the ratio of the primary base station signal power to noise power.

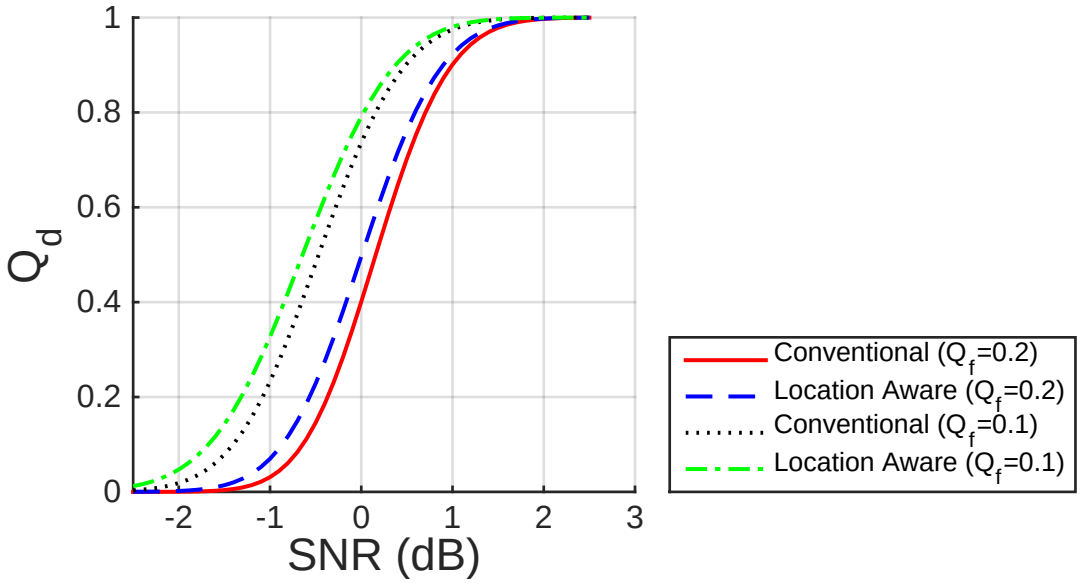

FIGURE 3.5: Probability of detection comparison of the proposed location-aware scheme and conventional hard combining scheme for different SNR when the false alarm probability constraint is 0.1 and 0.2

The results in Figure 3.6 show the ROC performance comparison of the proposed location-aware and conventional (or the case where location and propagation models are not considered) cooperative spectrum sensing scheme when $T = 0.78$ and $T = 0.6$. $T = 0.78$ indicate that 22% of the SU are located in a highly shadowed areas. These secondary users are eliminated from further processing at the secondary base station. The location-aware scheme slightly outperforms the conventional scheme when most of the secondary users are located in the same environment. However, Figure 3.6 shows that the performance has improved further when $T = 0.6$, which indicates 40% of the secondary users are in unreliable locations.

In Figure 3.7, we plot the probability of detection against the SNR. The figure presents the probabilities of detection for different numbers of cooperative cognitive radios in the network. It is evident that the detection improves with an increased number of cognitive radios, since more accurate results means better performance for the network.

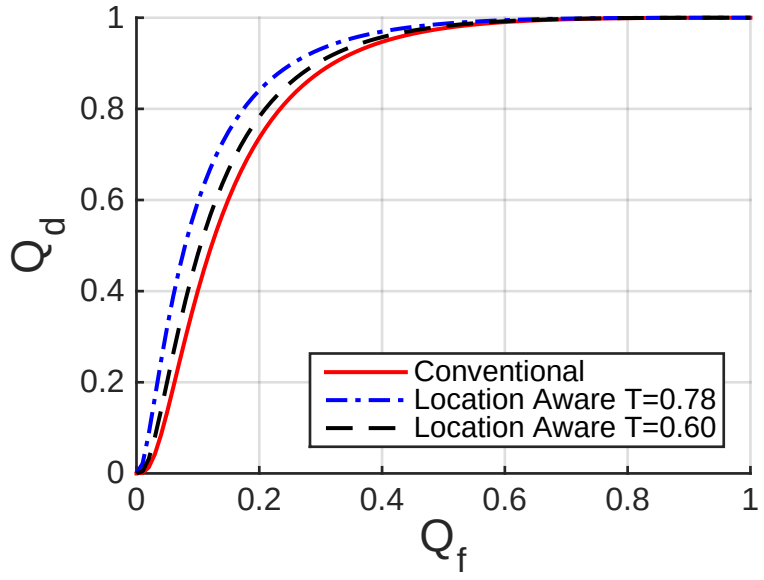

FIGURE 3.6: ROC comparison of the proposed location-aware scheme and conventional hard combining scheme under Gaussian channel when the number of cooperative users = 30 for different trust values

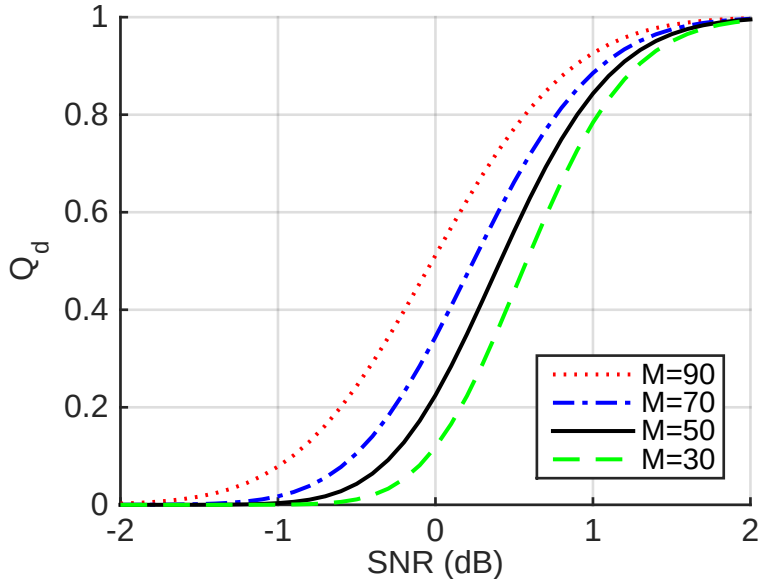

FIGURE 3.7: ROC of proposed location-aware scheme with different number of cognitive radio users under Gaussian channel and 35% of secondary users are located in highly shadowed areas

Table 3.2: Sensing Procedure Comparison

	Proposed Scheme	Conventional Schemes
SUs make local decisions	✓	✓
SUs send decision to SBS	✓	✓
SUs send geo-location to SBS	✓	
SBS calculate distance from PBS to SUs	✓	
SBS calculate channel condition	✓	
SBS calculates trust value for each SU	✓	
SBS calculates global decision	✓	✓

The number of cognitive radios is typically large in the case of urban networks. However, the proposed scheme can eliminate the s with low trust value from participating in the cooperative sensing. The proposed scheme not only improves performance of detection, but also reduces sensing time. Cooperative spectrum sensing may become impractical in cognitive radio networks with a large number of secondary users, because in a time slot only one SU sends its local decision to the secondary base station in order for the decisions to be separated easily. Hence, it may make the whole sensing time intolerably long. The scheme proposed here does not take into account the users that are located in low trust value regions, therefore it minimises the number of participating secondary users in a selective manner. Consequently, the processing time for the global decision at the secondary base station will be minimised while not compromising spatial diversity. It implies that secondary base stations have the incentive to adapt the proposed sensing decision method since it can achieve higher reliability and lower sensing time. The fundamental differences between our proposed scheme and the conventional methods are shown in Table 3.2.

3.5 Summary

We have studied the performance of cooperative cognitive spectrum sensing with energy detection in cognitive radio networks. Cooperative spectrum sensing with

location-aware secondary users have been investigated. We have derived the optimum fusion rule as well as the probability of detection which takes location reliability into consideration. The proposed scheme has been proved to exhibit better ROC especially in highly shadowed regions (e.g. Under NLOS propagation conditions). Analytical results of the proposed location-aware scheme show an improved performance over the conventional hard combination scheme (e.g. [116]), highlighting the requirements of location knowledge in cognitive radio networks especially in urban environments. Since this sensing accuracy is mainly related to the signal propagation environment, the more accurate the propagation models are, the better the expected performance will be from the proposed scheme. Moreover, for a cognitive radio network, high probability of detection results in less interference to the primary network which means more capacity and so more offered service and/or at a high quality. A major issue concerning the practical implementation of the proposed scheme is the availability of complete statistical information corresponding to source signal parameters, and particularly their variation with distance. However, lack of spectrum resources encourages the adoption of new ways of sharing including sharing of specific data related to the incumbent operators.

Chapter 4

Radio resource sharing for cooperative networks

4.1 Introduction

Most of the current radio spectrum resource distributions are based on the static spectrum allocation principles which has been identified as a major concern of spectrum scarcity within the future generations of cellular networks [54]. Efficient spectrum sharing is considered as one of the promising approaches to enhance networks' Grade of Service (GoS). In order to cope with increasing demand of wireless services and applications and to improve the spectrum utilisation, dynamic spectrum sharing (DSS) and other technologies, such as spectrum aggregations, are proposed in the literature to solve these current spectrum inefficiency problems [8, 4, 117, 118, 119, 120].

With DSS, the primary networks benefit economically by leasing their unused spectrum resources to secondary networks at the expense of marginal performance degradation while the secondary network increases GoS to a desired level. However, the marginal performance degradation of a primary network depends on its

current GoS. The current GoS of primary networks and the required GoS of secondary networks along with the overall GoS requirement defines the basis of DSS agreements between networks.

In this chapter we propose three different DSS models to analyse three spectrum sharing mechanisms by embedding overflow modelling, where operators are able to acquire portions of spectrum bandwidths from coexisting network operators. We focus on the analytical generalisation and robustness of the models during the interaction between network operators, and investigating the potential benefits of such interactions.

The remainder of the chapter is organised as follows. The detailed description of the system model is given in Section 4.2. The proposed dynamic resource sharing algorithm is presented in Section 4.4, while the scenario specific DSA mechanism with overflow models are studied in Subsections 4.4.1, 4.4.2, 4.4.3 and 4.4.4. Analytical results are provided in Section 4.5, followed by the summary and discussion in Section 4.6.

4.2 System model and assumptions

In the context of this investigation, we have considered an infrastructure-based wireless network architecture where the system that owns the spectrum property rights (called the primary system) willingly and actively attempts to share its spectrum with secondary systems to enhance the global spectrum utilisation within a given geographical area. We assume that the network operators own spectrum property rights of bandwidths (contiguous and/or non-contiguous) in order to supply different kinds of services. In this context, we further assume that network operators can act both as primary or secondary systems, depending on whether they lease or borrow spectrum bandwidths, respectively. Network operators are expected to interact with each other by acquiring or leasing spectrum bandwidths

TABLE 4.1: Symbols Used for the Analytical Modelling

Notations	Descriptions
N	Number of network operators in the network
M_i	Types of services at the ith operator
n_i^j	jth number of services at the ith operator
W_i	Allocated bandwidth of the ith operator
$\mathcal{A}_i$	Set of the available services for ith operator
n_i	Number of channel requests in progress at ith operator
$P(b_i)$	Blocking probability at ith operator
λ_i	Arrival rate at ith operator
μ_i	Services rate at ith operator
c_i	Capacity at the ith operator
$X_i(t)$	Number of channels required by ith operator at time t
Ω	State space
$\mathbf{I}_i$ and $\mathbf{I}_{ij}$	Unit vectors
$\pi(\mathbf{n})$	Steady state

owned by coexisting network operators in the same region. Secondary systems are not expected to use the infrastructure of primary system, but only acquire the right to use the incumbent spectrum of primary networks on temporal and spatial basis. Notations used in this chapter are described in Table 4.1.

In this system model, the operators are expected to interact with each other by adjusting their actions to enhance mutual benefits. This is carried out by employing the best possible strategy for secondary and primary system with a given set of constraints to control their blocking probabilities.

As shown in Figure 4.1, a given geographical area is covered with radio signals by a set of network operators. The operators are working in an overlapped manner to provide their respective users with a preset number of services.

The proposed system model is formulated to support heterogeneous radio networks. Heterogeneous networks are comprised of a mix of femto/pico/micro cells,

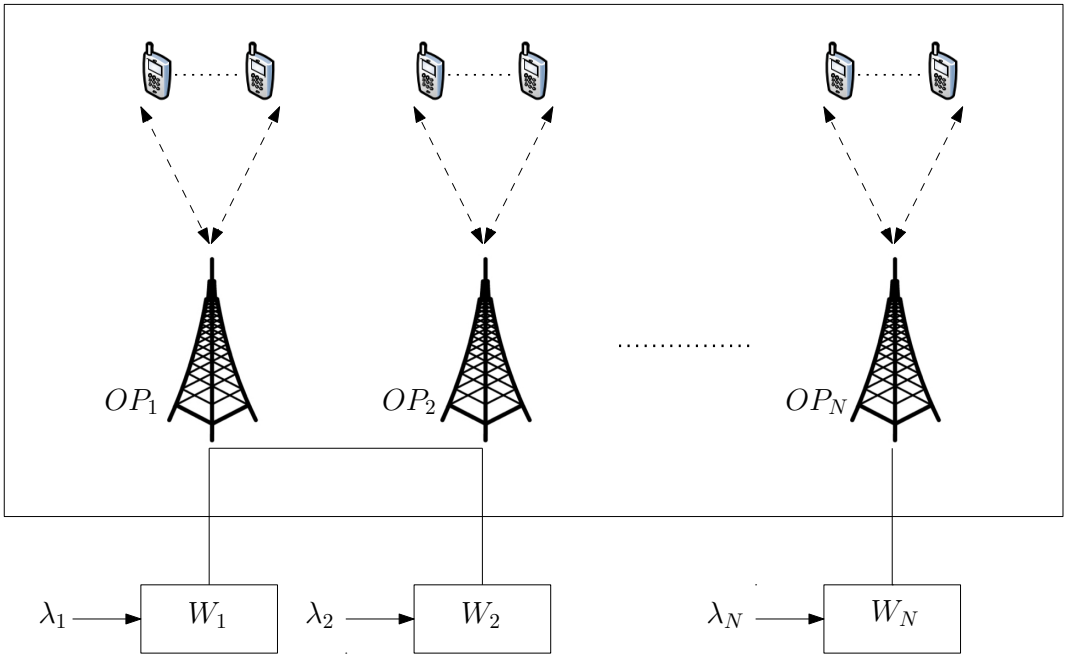

FIGURE 4.1: System Model: Coexisting Network Operators in a DSA

and are either consumer-deployed or operator-deployed [121]. In this report heterogeneous networks refers to operator deployment of cellular networks. Heterogeneity relates to the ability of a network operator to support a number of different services (e.g., 4G, 5G) in various locations. For example, one network operator could deploy 5G services in one area while it only offers 4G services in different locations. The reason could be related to several factors such as the investment versus revenue for the operators and/or service quality versus price of the offered services to users [122]. Heterogeneous radio networks substantially enhance the coverage and spatial reuse of spectrum. According to [123], 58% of mobile traffic will be offloaded to either small cells or Wi-Fi during 2019, which highlights the continuing significance of heterogenous networks. One advantage of heterogenous networks is its ability to support the future cellular systems to deliver higher GoS, while preserving mobility of cellular networks and harmonious connectivity [121]. This means that the networks will continue to experience different types of spectrum demand in different locations, hence the system model discussed here is formulated to accommodate the practical deployment of heterogenous networks.

We assume that each network operator supports n_i^j services, $i = 1, 2, \ldots, N$, $j = 1, 2, \ldots, M_i$.

Each service supported by the network is realised by a particular data rate, which are only supportive of particular operating bands such as 791-821 MHz, 880-915 MHz, and 1920-1980 MHz. Each n_i^j has a capacity c_i^j, $i = 1, 2, \ldots, N$, $j = 1, 2, \ldots, M_i$.

We assume that the network operators consider a loss model, where there are no waiting places (buffer value is equal to zero) in the system, and it blocks the arriving channel requests when all servers are busy [124]. Unlike the queueing type models, loss models are stable and the closed form analytical solution of blocking probability exists irrespective of traffic intensity. However, no closed form solution exists for infinite buffer queueing models if traffic intensity is greater than one, that is, if arrival rate is greater than departure rate.

Although multiple network operators are serving in the same geographical area, due to the variation of the service provision options among networks, there may exist a variation of services which feature specific peak time slots. Subsequently, the overall spectrum utilisation may vary from one operator to another at certain intervals. This may lead the network operators into a situation when one operator experiences high demand while the resources of other coexisting operators in the region are under-utilised. This means overloaded operators may utilise the underloaded spectrum resources of adjacent operators. In this chapter we present an analytical framework to enhance the overall GoS among the network operators. Such GoS enhancement is achieved by cooperative resource sharing between network operators in the form of dynamic traffic overflow modelling.

In the proposed overflow traffic modelling, a set of classification of operators is introduced on the basis of their cooperation agreements and traffic handling scenarios. Let us assume there are two types of network operators: the first one is willing to share resources when they are under-utilised, and the second one is

unwilling to cooperate with other operators. The first type can be further divided into primary and secondary operators. Overflow traffic from the secondary operator to the primary operator formulates a uni-directional overflow model. In the case where the same network operator can act both as primary and secondary, then such traffic handling scenarios formulate a bi-directional overflow model. We also consider a bi-directional overflow model with reserved capacity where additional capacity is accessible for operators. For analytical tractability, in this chapter, only one operator in the network is considered to have access to the reserved capacity. The case where multiple primary operators have access to a reserved capacity is discussed in Chapter 5.

The overflow mechanisms and the interactions between networks operators come with the expense of more communication overhead. Information about the extent of spatial region for spectrum use and maximum power, need to be exchanged between involved operators in order to avoid interference, and as a consequence, higher exchange of information will introduce more overhead. Moreover, the realisation of the models presented in this chapter may require new technologies in the form of coordination, signalling protocols, network elements and client devices which will entail additional computational power. Measurements and analysis of such communication and computation overheads would be of great value, but are beyond the scope of this thesis.

4.3 Formulation of Agreements

One assumption in this chapter is that the network operators involved in the cooperation are in some form of agreement to share their resources as predicted in the future generations of cellular networks [125, 126]. The nature of such resource sharing agreements depends on several factors such as service quality and resource availability. The agreements facilitate more control over trade-offs between GoS

provision and pricing. Examples of such spectrum sharing agreements which may be motivated by monetary compensation are found in [90, 102, 127, 128].

The level of cooperation and terms of agreements can have many forms depending on the policy of the operators. In this context, overflow traffic can be initiated from an Operator i to Operator j when the blocking probability $P(b_i)$ at the Operator i is

$$P(b_i) \geq \epsilon_i, \tag{4.1}$$

where ϵ_i is a very small blocking probability *threshold* of the Operator i. Under an agreement, Operator j receives some monetary compensation for leasing resources to the Operator i. The amount of reward that Operator j will receive from Operator i can be written in the mathematical form given by

$$r_{ij}(t) = r_{0j} + f\big(d(b_j)(t), r^*_{ij}(t), q_{ij}(t)\big), \tag{4.2}$$

subject to

$$P(b^*_j) < \epsilon_j, \tag{4.3}$$

where $r_{0j} \geq 0$ is a fixed reward received by the Operator j due to the agreement, $P(b_j)(t)$ is the blocking probability of Operator j due to its own arrivals at time t, $P(b^*_j)(t)$ is the new blocking probability of Operator j as a result of its own arrivals as well as the overflow traffic from Operator i at time t, $r^*_{ij}(t)$ is the reward received from Operator i due to the admission of a unit arrival to Operator j at time t, $q_{ij}(t)$ is the amount of traffic overflowed from Operator i to j during time period t, ϵ_j is the blocking probability *threshold* for the Operator j and

$$d(b_j) = P(b_j^*)(t) - P(b_j)(t). \tag{4.4}$$

The second part of the reward function $f\big(d(b_j)(t), r_{ij}^*(t), q_{ij}(t)\big)$ may take any form (for instance, linear, exponential, etc.) agreed by both the Operator i and j during the contractual period. In the simplest case, the function may be a linear function which can be defined as

$$f(.) = r_{ik}^*(t) \cdot q_{ij}(t) \cdot [1 + d(b_j)(t)]\,. \tag{4.5}$$

In the event where $P(b_j^*) = \epsilon_j$, operator j could decide to block any further overflow traffic from Operator i. Obviously in this case, Operator j will not suffer from any further performance degradation. The monetary compensation $r_{ij}(t)$ is proportional to the performance degradation incurred by overflow traffic form Operator i to Operator j. In this form of agreement, both operators may have incentives to participate in spectrum sharing: either to improve the performance, represented in reducing the blocking probability, or increase in revenues at the expense of marginal performance degradation. In this agreement, Operator j charges higher rate $r_{ij}(t)$ as $P(b_j^*) \to \epsilon_j$. Note that a more realistic approach is when Operator i considers modifying the reward according to the benefit gained by overflow traffic, such that equation (4.2) can be written as

$$r_{ij}(t) = r_{0j} + f\Big(\alpha_i(t), P(b_i^*)(t), d(b_j)(t), r_{ij}^*(t), q_{ij}(t)\Big), \tag{4.6}$$

subject to

$$P(b_j^*) < \epsilon_j, \tag{4.7}$$

and

$$r_{ij}(t) < \alpha_i(t), \tag{4.8}$$

where $\alpha_i(t)$ is the revenue due to overflow traffic from Operator i to Operator j at time t and $P(b_i^*)(t)$ is the blocking probability of Operator i at time t. Such agreements are dynamic in nature and they change at each time slot t as a function of the demands and rewards paid to Operator j. The best sharing agreement cannot be determined without analysing the blocking probabilities for each network individually. In the next section, we present four possible scenarios with different overflow mechanisms in order to focus on the impact of spectrum sharing on the blocking probabilities.

4.4 Proposed dynamic resource sharing algorithm

A predefined level of GoS is essential for network operators when designing or upgrading a cellular network. It constitutes one of the incentives for network operators to participate in spectrum sharing. As the number of users increases, the network operators are required to provide the users with fixed radio resources. Cooperation among network operators in the form of dynamic resource sharing is a solution to maintain such a predefined GoS. There are two fundamental aims of such dynamic resource sharing:

- Enhanced network wide GoS with efficient spectrum utilisation.
- Additional revenue generation by negotiated dynamic sub-contracting of under-utilised spectrum within each network operator.

Algorithm 1 describes a generic service selection which is used by Operator i to select the accessible service, where $\mathcal{A}$ is the total number of accessible services

in the network, known to every operator in advance. In this service selection algorithm, an operator continues to use its allocated resources for as long as the arrival rate is lower than the capacity of the operator (e.g., $\lambda_i < c_i$). We will show in this section that the Algorithm 4.1 ensures that if operator i experiences high traffic demand, the blocking probability increases, and thus Operator i can overflow to the available spectrum of adjacent operator(s), subject to accessibility and availability.

Algorithm 4.1 Generic service selection

Initialisation: Number of Operators in the network = N
for $i = 1 : 1 : N$ **do**
    if ith operator is blocked and jth operator is available **then**
        $\mathcal{A}_i$=$\{C_i^k\} \cup \{C_j^k\}$ $\forall$ $j \in \{1, 2, \ldots, N\}$ and $j \neq i$
        where $\mathcal{A}_i$ is the set of accessible services for operator i
        Apply overflow Model 1 & 2.
        % If reserved capacity is available.
    else if ith operator & jth operator are blocked **then**
        $\mathcal{A}_i$=$\{C_i^k\} \cup \{R\}$
        Where R denotes to a reserved capacity
        Apply overflow (Model 3) with reserved capacity
    else
        Apply Non-Sharing formula
    end if
end for
return

To study the proposed algorithm, we have developed four different models based on a loss system with overflow and evaluated and compared each of these models through numerical analysis.

4.4.1 Non-Sharing Model

Consider a network consisting of two operators for a cellular communications network. We assume that the two operators are in an agreement to share the spectrum if they can both support the same services. However in this model there are no services in common in order for the operators to deploy resource sharing.

Hence, we name this model a Non-Sharing Model. A state of this network is a vector $\mathbf{n} = (n_1, n_2)$, where n_i is the number of channel requests in progress in ith operator. The topology of the network is depicted in Figure 4.2.

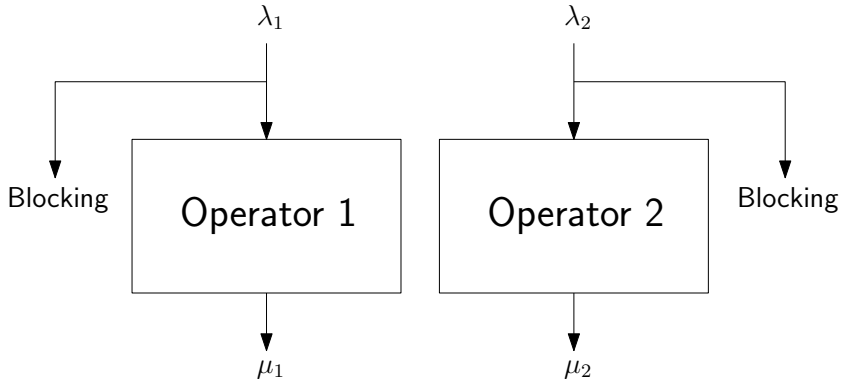

FIGURE 4.2: Non-Sharing network with two operators

Let λ_1 and λ_2 be the arrival rates to Operator 1 and 2 respectively, and the service rates be μ_1 and μ_2 and capacity c_1 and c_2, where both inter-arrival and service times are exponentially distributed random variables. The blocking probability at the ith operator ($i = 1, 2$) for such an Erlang loss system, can be calculated by [100, 129]

$$P(b_i) = \frac{1}{c_i!}\left(\frac{\lambda_i}{\mu_i}\right)^{c_i}\left[\sum_{n_i=0}^{c_i}\frac{1}{n_i!}\left(\frac{\lambda_i}{\mu_i}\right)^{n_i}\right]^{-1}. \tag{4.9}$$

The blocking probability $P(b_i)$ is defined as the probability that an arrival of user at Operator i is blocked because the capacity is saturated. Loss system is the key modelling approach in wireless telecommunication networks and blocking probability is the main performance measure to study the blocking behaviour of traffic such as voice and live video streaming. Voice and multimedia in wireless networks are arguably the highest experienced traffic demand by operators. Such real-time (elastic) traffic is modelled using a loss system as opposed to delay (buffered) system and hence it is used in this chapter.

4.4.2 Sharing Model 1 (Uni-directional overflow)

We now consider a network with two operators with capacity c_1 and c_2 for Operator 1 and Operator 2, respectively. As assumed for the Non-Sharing Model, (discussed in subsection 4.4.1), here we assume that the two operators are in an agreement to share the spectrum if they can both support the same service. However, in this model, we consider a case where only Operator 1 can have access to the resources of Operator 2, while Operator 2 is not allowed to overflow to Operator 1 resources. Channel requests for Operator 1 and 2 follow Poisson processes with rate λ_1 and λ_2 for Operator 1 and 2, respectively, i.e. inter-arrival times are exponentially distributed random variables. The service rate at Operator 1 (Operator 2) is exponentially distributed with mean μ_1^{-1} (respectively μ_2^{-1}). If all c_1 capacity are occupied at Operator 1, a channel request arriving at Operator 1 is overflowed to Operator 2 if capacity is available, and blocked otherwise. Our goal is to minimise the proportion of blocked channel requests for each operator. Figure 4.3 shows a detailed flow of channel requests for such network.

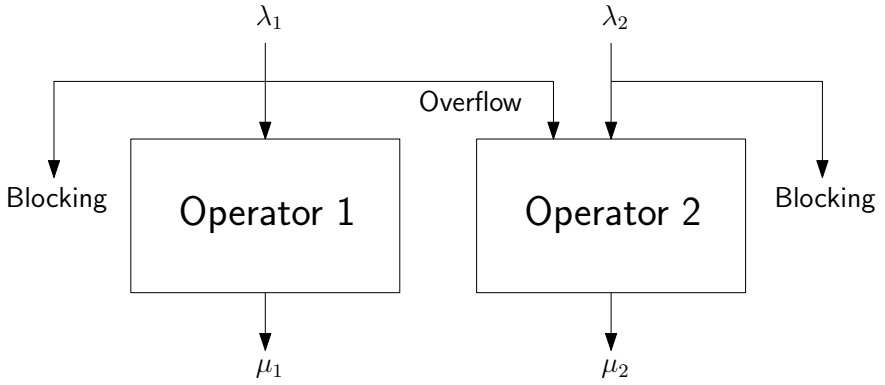

FIGURE 4.3: A two-operator network with uni-directional overflow (Model 1)

Let $X_1(t)$ be the number of channels required by Operator 1 and $X_2(t)$ by Operator 2 at time t. Also $X_{12}(t)$ denotes the number of channels required by Operator 2 overflowed from Operator 1 at time t. The assumption of exponential distribution enables us to model the network as a continuous-time Markov chain

$$\mathbf{X} = \big(X_1(t), X_{12}(t), X_2(t), t \geq 0\big)$$

with state space given by

$$\Omega = \big\{\mathbf{n} = (n_1, n_{12}, n_2) : n_1 \leq c_1, n_2 + n_{12} \leq c_2\big\}, \tag{4.10}$$

where n_i, $i = 1, 2$, is the number of channels required at the ith operator and n_{12} is the number of channels required at Operator 2 overflowed from Operator 1. The transition rates $\mathbf{Q} = \big(q(\mathbf{n}, \mathbf{n}'), \mathbf{n}, \mathbf{n}' \in \ \Omega\big)$ are given by

$$q(\mathbf{n}, \mathbf{n}') = \begin{cases} \lambda_1 & \mathbf{n}' = \mathbf{n} + \mathbf{I}_1 \text{ or } \ \mathbf{n}' = \mathbf{n} + \mathbf{I}_{12}, \text{ if } n_1 = c_1 \\ \lambda_2 & \mathbf{n}' = \mathbf{n} + \mathbf{I}_2 \\ n_i\mu_i & \mathbf{n}' = \mathbf{n} - \mathbf{I}_i, \quad i = 1, 2 \\ n_{12}\mu_1 & \mathbf{n}' = \mathbf{n} - \mathbf{I}_{12} \\ 0 & \text{otherwise,} \end{cases} \tag{4.11}$$

where $\mathbf{I}_1 = (1, 0, 0)$, $\mathbf{I}_2 = (0, 1, 0)$ and $\mathbf{I}_{12} = (0, 0, 1)$ denote the unit vectors. We are interested in deriving the blocking probability, i.e. the probability that a new channel request finds all capacities are occupied in both Operators 1 and 2.

Let $\pi(\mathbf{n}) = lim_{t\to\infty} P\big(\mathbf{X}(t) = \mathbf{n}\big)$ denote the equilibrium distribution that there are $\mathbf{n}$ channel requests in progress in both operators. Since the network is Ergodic stochastic process, we can use

$$\text{Out rate} = \text{In rate} \tag{4.12}$$

which is a commonly used method to get the steady state probability and the blocking probabilities of the network.

This equilibrium distribution of $\mathbf{X}$ is the unique distribution $\pi(\mathbf{n}), \mathbf{n} \in \Omega$ that satisfies the *global balance equation* as shown in (4.13), where $\mathbf{1}_{\{\cdot\}}$ denotes the indicator function of the event or set of $\{\cdot\}$, i.e. $\mathbf{1}_{\{\mathbf{A}\}} = 1$ if event A is satisfied and $\mathbf{1}_{\{\mathbf{A}\}} = 0$ if not. The LHS of equation (4.13) represents the "Total out rate"

$$\Big[\lambda_1\big(\mathbf{1}_{\{n_1<c_1\}}(\mathbf{n})+\mathbf{1}_{\{n_1=c_1,\, n_{12}+n_2<c_2\}}(\mathbf{n})\big)+\lambda_2(\mathbf{n})+\sum_{i=1}^{2}n_i\mu_i+n_{12}\mu_1\Big]\cdot\pi(\mathbf{n})= \\ \lambda_1\big[\pi(\mathbf{n}-\mathbf{I}_1)+\pi(\mathbf{n}-\mathbf{I}_{12})\mathbf{1}_{\{n_1=c_1,\, n_{12}+n_2<c_2\}}(\mathbf{n})\big]+\lambda_2\big[\pi(\mathbf{n}-\mathbf{I}_2)\big]+ \\ \sum_{i=1}^{2}(n_i+1)\mu_i\pi(\mathbf{n}+\mathbf{I}_i)+(n_{12}+1)\mu_1\pi(\mathbf{n}+\mathbf{I}_{12}), \tag{4.13}$$

and the RHS represents the "Total in rate" as shown in equation (4.14) and (4.15), respectively.

$$\text{Total out rate}\begin{cases}\lambda_1\big(\mathbf{1}_{\{n_1<c_1\}}(\mathbf{n})+\mathbf{1}_{\{n_1=c_1,\, n_{12}+n_2<c_2\}}(\mathbf{n})\big)+\lambda_2(\mathbf{n}) \coloneqq \mathbf{n}\xrightarrow{\lambda}(\mathbf{n}+1)\\ \sum_{i=1}^{2}n_i\mu_i+n_{12}\mu_1\cdot\pi(\mathbf{n}) \coloneqq \mathbf{n}\xrightarrow{\mu}(\mathbf{n}-1)\end{cases} \tag{4.14}$$

$$\text{Total in rate}\begin{cases}\lambda_1\big[\pi(\mathbf{n}-\mathbf{I}_1)+\pi(\mathbf{n}-\mathbf{I}_{12})\mathbf{1}_{\{n_1=c_1,\, n_{12}+n_2<c_2\}}(\mathbf{n})\big]+\lambda_2\big[\pi(\mathbf{n}-\mathbf{I}_2)\big] \coloneqq \\ \qquad\qquad (\mathbf{n}-1)\xrightarrow{\lambda}\mathbf{n}\\ \sum_{i=1}^{2}(n_i+1)\mu_i\pi(\mathbf{n}+\mathbf{I}_i)+(n_{12}+1)\mu_1\pi(\mathbf{n}+\mathbf{I}_{12}) \coloneqq (\mathbf{n}-1)\xrightarrow{\mu}\mathbf{n}\end{cases} \tag{4.15}$$

We now derive the *detailed balance equations* from the *global balance equation* (4.13),

$$\lambda_i\big(\pi(\mathbf{n}-\mathbf{I}_i)+\pi(\mathbf{n}-\mathbf{I}_{12})\big)=\big(n_i\mu_i+n_{12}\mu_1\big)\cdot\pi(\mathbf{n}) \tag{4.16}$$

Equation (4.16) has an explicit solution which is given by

$$\pi(\mathbf{n}) = K^{-1} \frac{(\lambda_1/\mu_1)^{(n_1+n_{12})}(\lambda_2/\mu_2)^{n_2}}{(n_1+n_{12})!\; n_2!}, \quad \forall \;\; \mathbf{n} \in \Omega \tag{4.17}$$

and

$$K = \sum_{\mathbf{n}\in\Omega} \frac{(\lambda_1/\mu_1)^{(n_1+n_{12})}(\lambda_2/\mu_2)^{n_2}}{(n_1+n_{12})!\; n_2!}. \tag{4.18}$$

This equilibrium distribution is a truncated multidimensional Poisson distribution from where the blocking probability can be derived. The blocking probability for Operator i, $i = 1, 2$, is then given by

$$\begin{aligned} P(b_i) &= \sum_{\mathbf{n}\in T_i} \pi(\mathbf{n}) \\ &= \sum_{\mathbf{n}\in T_i} \frac{(\lambda_1/\mu_1)^{(n_1+n_{12})}(\lambda_2/\mu_2)^{n_2}}{(n_1+n_{12})!\; n_2!} \\ &\quad \cdot \left[\sum_{\mathbf{n}\in\Omega} \frac{(\lambda_1/\mu_1)^{(n_1+n_{12})}(\lambda_2/\mu_2)^{n_2}}{(n_1+n_{12})!\; n_2!} \right]^{-1}, \end{aligned} \tag{4.19}$$

where

$$T_1 = \big\{ \mathbf{n} \in \Omega | (n_1 = c_1 \cap n_{12} + n_2 = c_2) \big\}, \tag{4.20}$$

and

$$T_2 = \big\{ \mathbf{n} \in \Omega | (n_{12} + n_2 = c_2) \big\}. \tag{4.21}$$

4.4.3 Sharing Model 2 (Bi-directional overflow)

We shall now extend Sharing Model 1 by adding an overflow strategy from Operator 2 to Operator 1, see Figure 4.4. We assume that the two operators are in an agreement to share the spectrum and both operators can support the same services. In this model, we consider a case where Operator 1 can have access to the resources of Operator 2, and likewise, Operator 2 can have access to Operator 1's resources. Therefore, this model is called a bi-directional overflow model. If all c_1 capacity are occupied at Operator 1 a channel request arriving at Operator 1 is overflowed to Operator 2 if capacity is available, and blocked otherwise. Similarly a channel request arriving at Operator 2 is overflowed to Operator 1 if capacity c_2 is occupied and there is a free capacity at Operator 1.

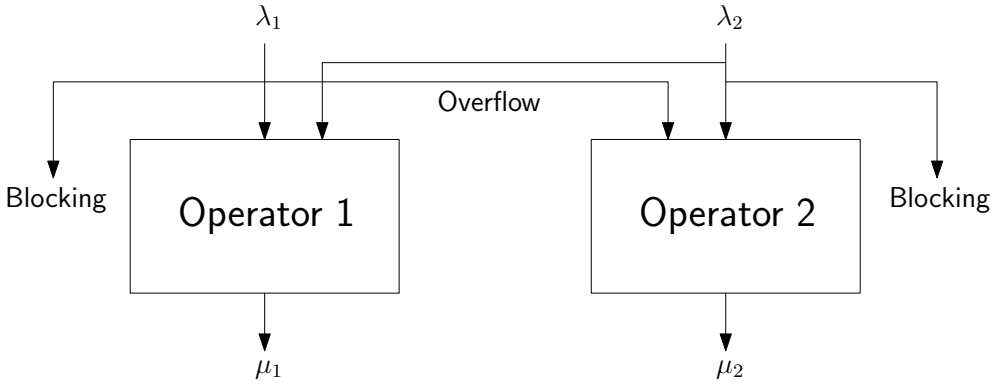

FIGURE 4.4: A two-operator network with bi-directional overflow (Model 2)

The state space for such a process can be given by

$$\Omega = \big\{\mathbf{n} = (n_1, n_{12}, n_2, n_{21}) : n_1 + n_{21} \leq c_1, n_2 + n_{12} \leq c_2\big\}. \tag{4.22}$$

Deriving the *global balance equation* and *detailed balance equations* we obtain the following solution of the steady-state distribution and the expression for blocking probability calculation for each operator

$$\pi(\mathbf{n}) = K^{-1} \frac{(\lambda_1/\mu_1)^{(n_1+n_{12})} (\lambda_2/\mu_2)^{(n_2+n_{21})}}{(n_1+n_{12})!\,(n_2+n_{21})!}, \quad \forall \ \mathbf{n} \in \Omega \tag{4.23}$$

and

$$K = \sum_{\mathbf{n}\in\Omega} \frac{(\lambda_1/\mu_1)^{(n_1+n_{12})} (\lambda_2/\mu_2)^{(n_2+n_{21})}}{(n_1+n_{12})!\,(n_2+n_{21})!}. \tag{4.24}$$

The blocking probability can be derived from the steady-state distribution (4.23). The blocking probability for operator i, $i = 1, 2$, is then given by

$$\begin{aligned} P(b_i) &= \sum_{\mathbf{n}\in T_i} \pi(\mathbf{n}) \\ &= \sum_{\mathbf{n}\in T_i} \frac{(\lambda_1/\mu_1)^{(n_1+n_{12})} (\lambda_2/\mu_2)^{(n_2+n_{21})}}{(n_1+n_{12})!\,(n_2+n_{21})!} \\ &\quad \cdot \left[\sum_{\mathbf{n}\in\Omega} \frac{(\lambda_1/\mu_1)^{(n_1+n_{12})} (\lambda_2/\mu_2)^{(n_2+n_{21})}}{(n_1+n_{12})!\,(n_2+n_{21})!} \right]^{-1}, \end{aligned} \tag{4.25}$$

where

$$T_1 = \big\{ \mathbf{n} \in \Omega | (n_1 + n_{21} = c_1 \cap n_{12} + n_2 = c_2) \big\}, \tag{4.26}$$

and

$$T_2 = \big\{ \mathbf{n} \in \Omega | (n_1 + n_{21} = c_1 \cap n_{12} + n_2 = c_2) \big\}. \tag{4.27}$$

4.4.4 Sharing Model 3 (Bi-directional overflow with reserved capacity)

We now consider a network consisting of two operators with bi-directional overflow from Operator 1 to Operator 2 and from Operator 2 to Operator 1 (Sharing Model 2). However, in the sharing model discussed here, we assume that there is a common spectrum pool for network operators. Each network operator is considered to possess a dedicated portion of this pooled spectrum. For analytical purposes, we consider a case where only Operator 2 has such a dedicated spectrum portion with a defined capacity. This is to enable a certain predictable level of GoS for Operator 2. In this chapter we refer to this spectrum portion as reserved capacity. The reserved capacity can be used to reduce the blocking probability at Operator 2.

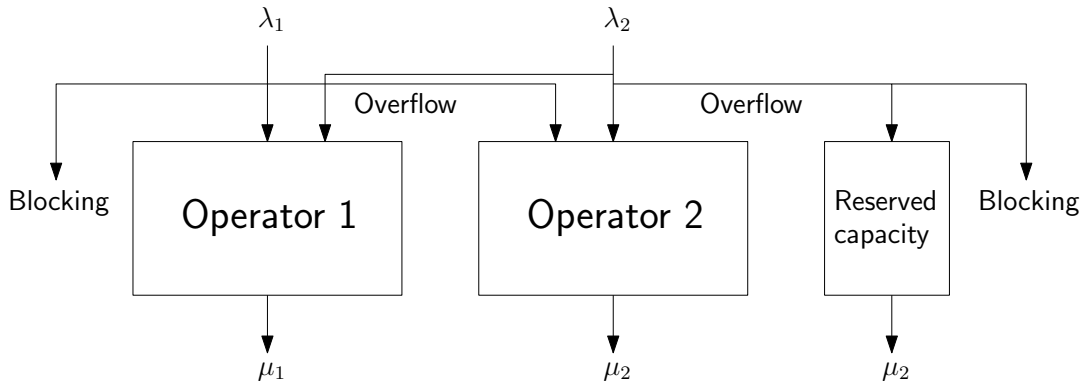

FIGURE 4.5: A two-operators network with bi-directional overflow and reserved resources (Model 3)

Let $X_1(t)$ be the number of channel requests arriving at Operator 1 and $X_2(t)$ be the number of channel requests arriving at Operator 2 at time t. Also $X_{12}(t)$ denotes the number of channel requests arriving at Operator 2 as a result of overflow from Operator 1 and $X_{21}(t)$ denotes the number of channel requests arriving at Operator 1 as a result of overflow from Operator 2 at time t. Capacity at Operator 1 and 2 are denoted by c_1 and c_2 respectively. If there is no available channels to admit the new traffic arriving at Operator 2 and Operator 1 then the

request will be transferred to the reserved resource with capacity c_3. A state of the network can be written as

$$\mathbf{X} = \big(X_1(t), X_{12}(t), X_2(t), X_{21}(t), X_{23}(t), t \geq 0\big)$$

with state space given by

$$\Omega = \big\{ \mathbf{n} = (n_1, n_{12}, n_2, n_{21}, n_{23}) : \ n_1 + n_{21} \leq c_1, n_2 + n_{12} \leq c_2, n_{23} \leq c_3 \big\}, \quad (4.28)$$

where n_i, $i = 1, 2$, is the number of channel requests at the ith operator and n_{ij} is the number of requests overflowed at Operator j from Operator i, where $i, j \in \{1, 2, 3\}$. The transition rates $\mathbf{Q} = \big(q(\mathbf{n}, \mathbf{n}'), \mathbf{n}, \mathbf{n}' \in \Omega\big)$ are given by

$$q(\mathbf{n}, \mathbf{n}') = \begin{cases} \lambda_1 & \mathbf{n}' = \mathbf{n} + \mathbf{I}_1 \ \text{ or } \ \mathbf{n}' = \mathbf{n} + \mathbf{I}_{12} \ \text{ if } \ n_1 = c_1 \\ \lambda_2 & \mathbf{n}' = \mathbf{n} + \mathbf{I}_2 \ \text{ or } \ \mathbf{n}' = \mathbf{n} + \mathbf{I}_{21} \ \text{ if } \ n_2 = c_2 \\ & \qquad \text{or } \ \mathbf{n}' = \mathbf{n} + \mathbf{I}_{23} \ \text{ if } \ n_2 = c_2 \\ & \qquad\qquad \text{and } n_1 + n_{21} = n_2 \\ n_i\mu_i & \mathbf{n}' = \mathbf{n} - \mathbf{I}_i, \ i = 1, 2 \\ n_{ij}\mu_i & \mathbf{n}' = \mathbf{n} - \mathbf{I}_{ij}, \ i, j \in \{1, 2\} \\ n_{23}\mu_2 & \mathbf{n}' = \mathbf{n} - \mathbf{I}_{23} \\ 0 & \text{otherwise.} \end{cases} \quad (4.29)$$

The *global balance equation* of the system can be derived as

The *detailed balance equations* obtained from the *global balance equation* (4.30) is given by

$$\lambda_i\big(\pi(\mathbf{n} - \mathbf{I}_i) + \pi(\mathbf{n} - \mathbf{I}_{ij} - \mathbf{I}_{23})\big) = \big(n_i\mu_i + n_{ij}\mu_i + n_{23}\mu_2\big) \cdot \pi(\mathbf{n}). \quad (4.31)$$

The explicit solution of the *detailed balance equations* after normalisation

$$
\begin{aligned}
\Big[\lambda_1\big(\mathbf{1}_{\{n_1+n_{21}<c_1\}} &+ \mathbf{1}_{\{n_1+n_{21}=c_1,\, n_{12}+n_2<c_2\}}\big) + \lambda_2\big(\mathbf{1}_{\{n_{21}+n_2<c_2\}} \\
&+ \mathbf{1}_{\{n_{12}+n_2=c_2,\, n_1+n_{21}<c_1\}} + \mathbf{1}_{\{n_{12}+n_2=c_2,\, n_1+n_{21}=c_1,\, n_{23}<c_3\}}\big) \\
&+ \sum_{i=1}^{2} n_i\mu_i + \sum_{i,j\in\{1,2\}} n_{ij}\mu_i + n_{23}\mu_2\Big]\cdot\pi(\mathbf{n}) \\
&= \lambda_1\big[\pi(\mathbf{n}-\mathbf{I}_1) + \pi(\mathbf{n}-\mathbf{I}_{12})\mathbf{1}_{\{n_1+n_{21}=c_1,\, n_{12}+n_2<c_2\}}\big] + \lambda_2\big[\pi(\mathbf{n}-\mathbf{I}_2) \\
&+ \pi(\mathbf{n}-\mathbf{I}_{21})\mathbf{1}_{\{n_{12}+n_2=c_2,\, n_{21}+n_2<c_2\}} \\
&+ \pi(\mathbf{n}-\mathbf{I}_{23})\mathbf{1}_{\{n_{12}+n_2=c_2,\, n_{21}+n_2=c_2,\, n_{23}<c_3\}}\big] \\
&+ \sum_{i=1}^{2}(n_i+1)\mu_i\pi(\mathbf{n}+\mathbf{I}_i) \\
&+ \sum_{i,j\in\{1,2\}}(n_{ij}+1)\mu_i\pi(\mathbf{n}+\mathbf{I}_{ij}) + (n_{23}+1)\mu_2\pi(\mathbf{n}+\mathbf{I}_{23}). \qquad (4.30)
\end{aligned}
$$

$(\sum \pi(\mathbf{n}) = 1)$

we get

$$\pi(\mathbf{n}) = K^{-1}\frac{(\lambda_1/\mu_1)^{(n_1+n_{12})}(\lambda_2/\mu_2)^{(n_2+n_{21}+n_{23})}}{(n_1+n_{12}+n_{23})!\,(n_2+n_{21})!}, \quad \forall\ \mathbf{n}\in\Omega \qquad (4.32)$$

and

$$K = \sum_{\mathbf{n}\in\Omega}\frac{(\lambda_1/\mu_1)^{(n_1+n_{12})}(\lambda_2/\mu_2)^{(n_2+n_{21}+n_{23})}}{(n_1+n_{12})!\,(n_2+n_{21}+n_{23})!}. \qquad (4.33)$$

The blocking probability can be derived from the steady-state distribution (4.32). The blocking probability for Operator i, where $i = 1, 2$, is then given by

$$
\begin{aligned}
P(b_i) &= \sum_{\mathbf{n}\in T_i} \pi(\mathbf{n}) \\
&= \sum_{\mathbf{n}\in T_i} \frac{(\lambda_1/\mu_1)^{(n_1+n_{12})}(\lambda_2/\mu_2)^{(n_2+n_{21}+n_{23})}}{(n_1+n_{12})!\,(n_2+n_{21}+n_{23})!} \\
&\quad \cdot \left[\sum_{\mathbf{n}\in\Omega} \frac{(\lambda_1/\mu_1)^{(n_1+n_{12})}(\lambda_2/\mu_2)^{(n_2+n_{21}+n_{23})}}{(n_1+n_{12})!\,(n_2+n_{21}+n_{23})!}\right]^{-1},
\end{aligned} \tag{4.34}
$$

where

$$
T_1 = \big\{\mathbf{n}\in\Omega | (n_1+n_{21}=c_1 \cap n_{12}+n_2=c_2)\big\}, \tag{4.35}
$$

and

$$
T_2 = \big\{\mathbf{n}\in\Omega | (n_1+n_{21}=c_1 \cap n_{12}+n_2=c_2 \cap n_{23}=c_3)\big\}. \tag{4.36}
$$

The models discussed in this chapter can be summarised by Figure 4.6.

Even though the models discussed in this section only consider the interactions between two operators, it can be extended to include more operators with added complexity, for instance, if there are more than two operators in the network, there can be a number of different interactions between operators. Multi-operator modelling and analysis is discussed thoroughly in Chapter 5 and Chapter 6.

4.5 Analysis and results

In this section we investigate the robustness of the analytical models which are discussed in Section 4.4, with different offered load $(0-30)$ assuming service rate is always 1, number of servers $(0-25)$ and reserved capacity $(0,1)$ across the

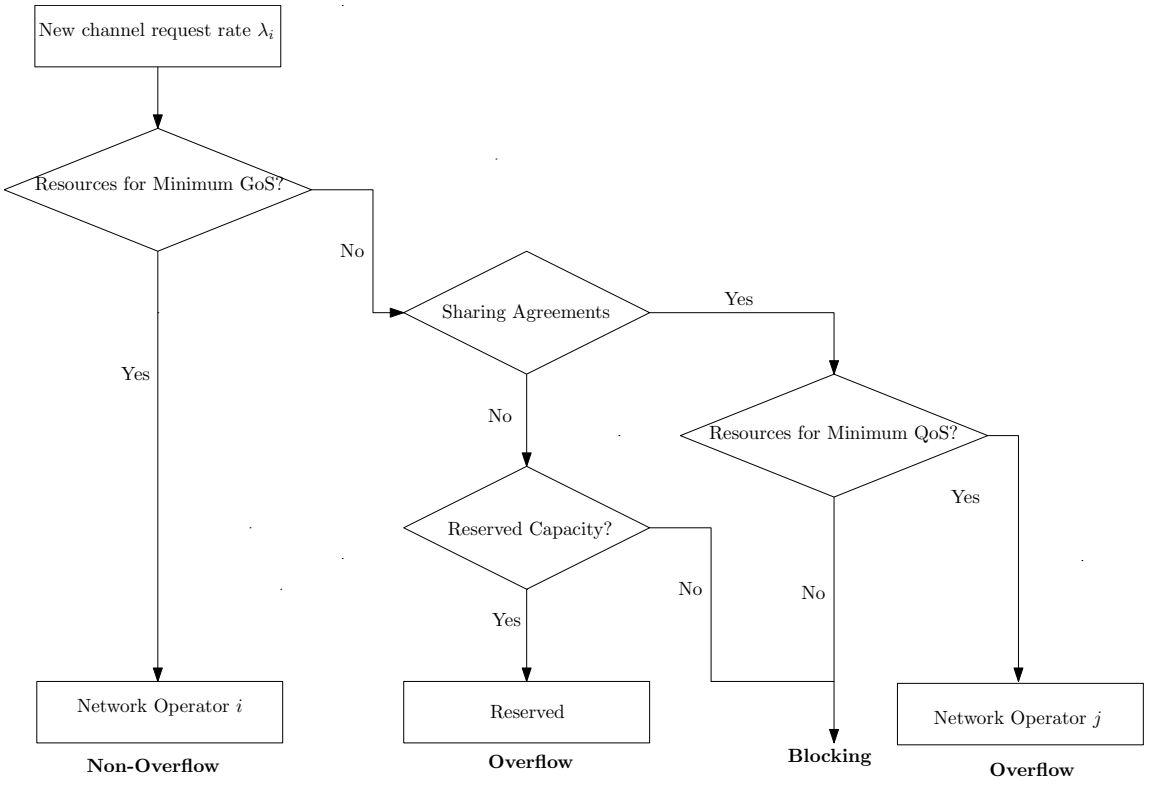

FIGURE 4.6: The flowchart for the proposed overflow models

network. The offered load values which are chosen in the simulation are considered to investigate the proposed models by various traffic load scenarios (e.g. during high, medium and low traffic intensity). In addition we further analyse our models by considering a wide range of channel availability to replicate various spectrum holdings by the operators. The performance of the proposed resource sharing framework is examined. For the analytical results, it is reasonable that we compare the four scenario specific model configurations: Non-Sharing Model, Sharing Model 1, Sharing Model 2 and Sharing Model 3.

4.5.1 Performance comparison between the Non-Sharing Model and Model 1

The comparison for the Non-Sharing Model and the proposed uni-directional overflow model at Operator 1 and Operator 2 are presented in Figure 4.7a and 4.7b, respectively. The offered load at Operator 1 varies from 0 to 30 while the offered load at Operator 2 is kept fixed at 10. Figure 4.7a shows the blocking probabilities for the Non-Sharing Model and the proposed uni-directional overflow model. According to the analytical results in Figure 4.7a, it is clear that the blocking probability for the proposed overflow model for Operator 1 is reduced in comparison to the Non-Sharing Model. However, for the overflow model, the blocking probability for both Operator 1 and 2 converges as $\lambda_1 \rightarrow 30$. This is due to the fact that the uni-directional sharing model only allows overflow from Operator 1 to Operator 2. Thus, the capacity for both operators reaches saturation gradually as the offered load increases. In addition, for the same offered load in the Non-Sharing Model and uni-directional overflow model, it is seen that at Operator 1 with our proposed overflow model when $\lambda_1 > 10$, the blocking probability is lower than those for the Non-Sharing Model. This shows the superiority of our proposed model over the Non-Sharing Model.

To realise the impact of our overflow model on Operator 2 with different offered load values, we have experimented with fixed offered load at Operator 1 as 10 and varied it for Operator 2 from 0 to 30, see Figure 4.7b. It is evident that the blocking probability of Operator 2 is higher for Model 1, except for when $\lambda_2 < 10$, because of the additional overflow load from Operator 1. Meanwhile, the blocking probability for Operator 1 has decreased as compared to when employing the Non-Sharing Model. It is evident from Figure 4.7b that the blocking probability for the uni-directional model at Operator 1 is lower than those for the Non-Sharing Model. However, in the proposed model, the blocking probability increases with

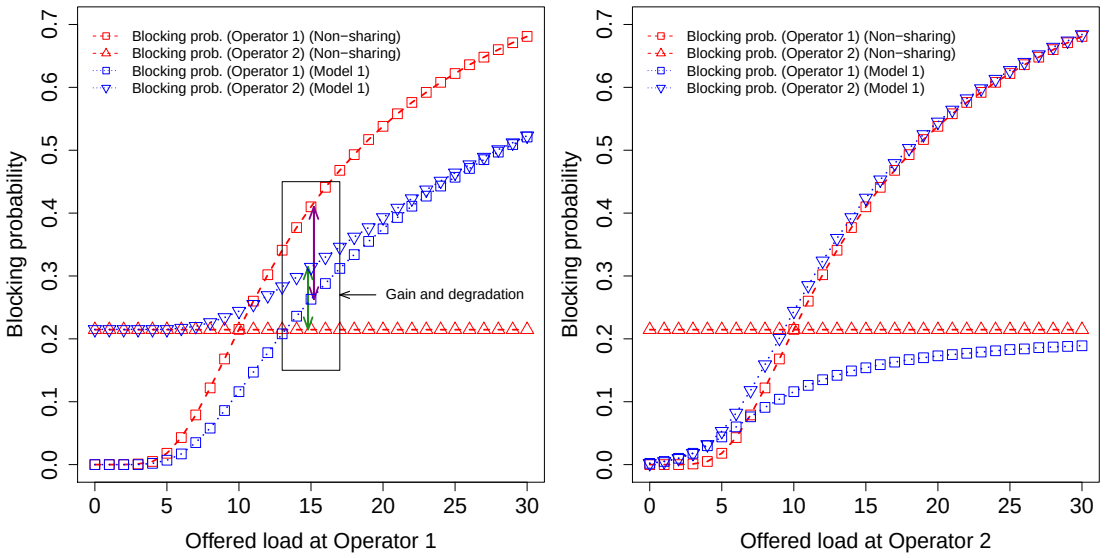

(A) (B)

FIGURE 4.7: Comparison of the blocking probability for the Non-Sharing Model with Model 1 with $c_1 = c_2 = 10$ for (A) $\lambda_1 = 0:30$, $\lambda_2 = 10$ and (B) $\lambda_1 = 10$, $\lambda_2 = 0:30$

the increase of offered load. This is due to the reason that as $\lambda_2 \to 30$, the capacity gain obtained from sharing decreases with the drop of the capacity of Operator 2.

To demonstrate the trade-off agreements between operators, Figure 4.8 shows a zoomed region from the boxed area in Figure 4.7a. We show in the figure that Operator 1 improves its blocking probability by 0.174 while a degraded performance of blocking probability reduction by 0.098 for Operator 2 with offered loads 15 and 10 for Operator 1 and 2, respectively, and capacity 10 for both operators. In this case, Operator 2 is expected to gain a monetary reward, which may be calculated by using either equation (4.2) or (4.6) according to the agreements made during a contractual period.

In terms of performance under different numbers of servers, we have compared the blocking probability for the Non-Sharing Model with the uni-directional overflow model where the number of servers at Operator 1 varies from 5 to 25. The number of server is fixed at 10 for Operator 2. For simplicity, in this configuration, we set

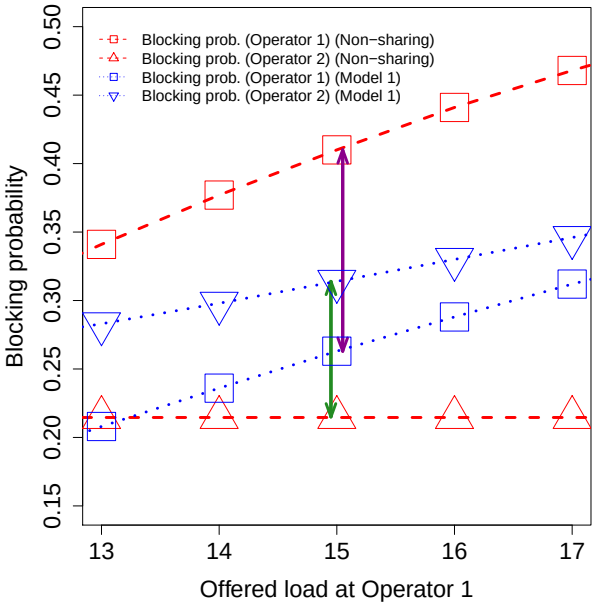

FIGURE 4.8: Gain and degradation performance trade-off between Operator 1 and 2 for the Non-sharing and Uni-directional model

$\lambda_1 = \lambda_2 = 10$ and $\mu_1 = \mu_2 = 1$. According to the analytical results, see Figure 4.9a, the blocking probability at Operator 1 for our proposed model is lower than that for the Non-Sharing Model. However, as $c_1 \rightarrow 25$, the advantage over the Non-Sharing Model becomes less visible due to the fact that Operator 1 increases its own capacity by overflow to Operator 2. Thus, it becomes less dependant on Operator 2, which results in lower overflow levels. In addition, it is also noticed that the blocking probability for Operator 2 with both models are almost the same when the number of servers exceed 10.

In order to test the impact of varying the number of servers at Operator 2, we have kept the number of servers at Operator 1 fixed at 10. For this configuration, we have fixed the offered load for Operator 1 and 2 at 10. The comparison is intended to be representative of the performance in terms of the blocking probability at Operator 2, see Figure 4.9a. It can be seen that as $c_1 \rightarrow 25$, the blocking probability of Operator 1 and 2 decreases. The overflow model performs slightly better than the Non-Sharing Model, while the overflow model at Operator 1 achieves

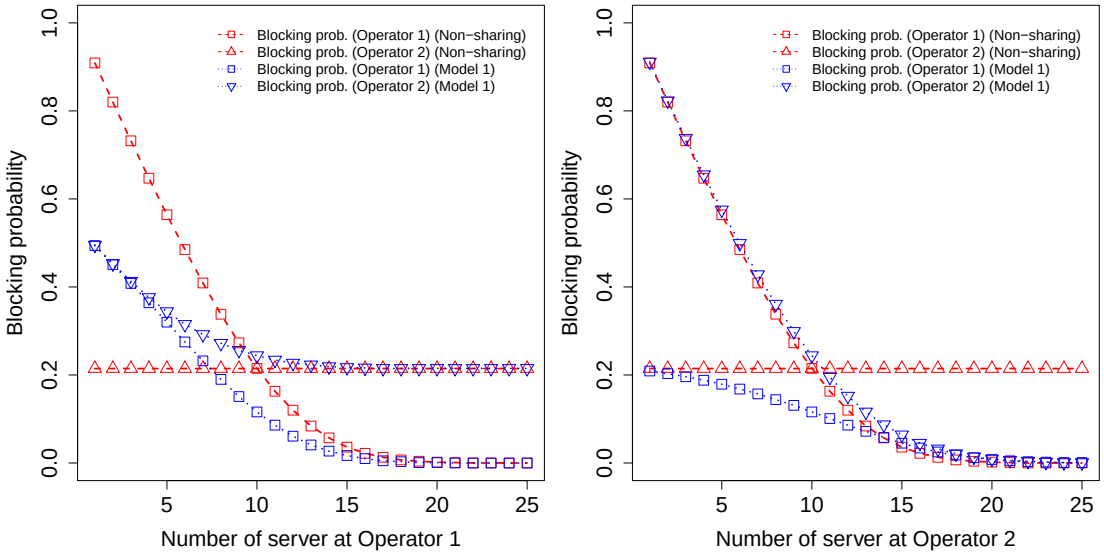

(A) (B)

FIGURE 4.9: Comparison of the blocking probability for the Non-Sharing Model with Model 1 with $\lambda_1 = \lambda_2 = 10$ for (A) $c_1 = 5 : 25$, $c_2 = 10$ and (B) $c_1 = 10$, $c_2 = 1 : 25$

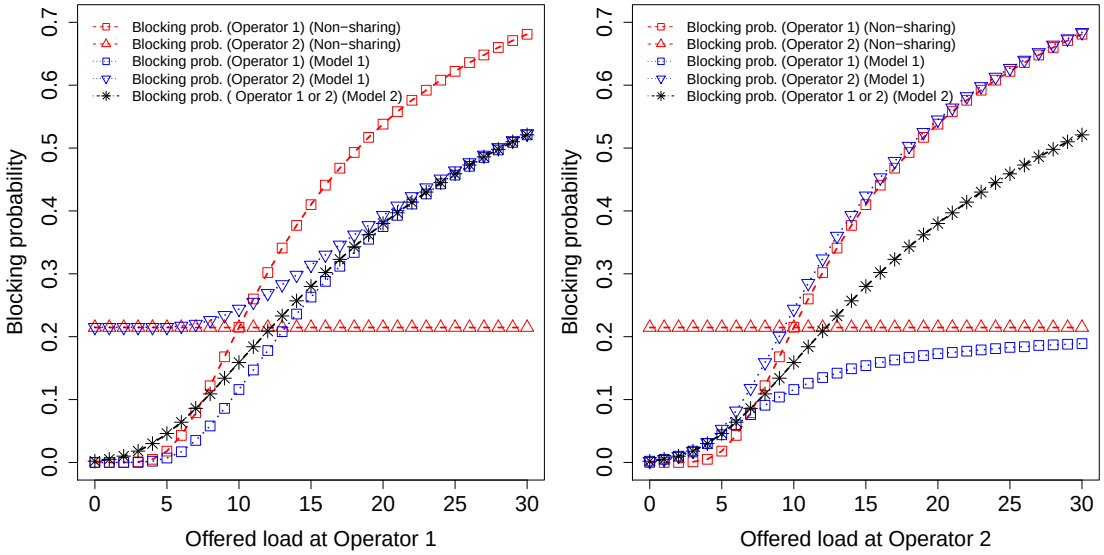

(A) (B)

FIGURE 4.10: Comparison of the blocking probability for the Non-Sharing Model with Model 1 and Model 2 with $c_1 = c_2 = 10$ for (A) $\lambda_1 = 0 : 30$, $\lambda_2 = 10$ and (B) $\lambda_1 = 10$, $\lambda_2 = 10$

the lowest blocking probability. This analysis is used to show that a non-sharing approach where the operators do not share resources, although in certain cases might perform better than the overflow model, does not perform well when the offered load is high.

4.5.2 Performance comparison between the Non-Sharing Model, Model 1 and Model 2

The results obtained in Figure 4.10a, 4.10b, 4.11a and 4.11b represent a comparison of the bi-directional model with the uni-directional and the Non-Sharing Model. Figure 4.10a shows the blocking probability for the case where the offered load is varied from $(0 - 30)$ assuming $\mu_1 = \mu_2 = 1$ and $c_1 = 10$. We see that the blocking probability for Operator 1, when considering Model 1, is lower than in Model 2, especially in the region where the offered load is between 5 and 15. The performance of Operator 2 in Figure 4.10b is identical to the performance in Figure 4.10a for Model 2 since the traffic load is always distributed uniformly over the two operators.

The other results in Figure 4.11a and 4.11b, represent a comparison of the bi-directional model with the uni-directional and the Non-Sharing Model for varying number of servers. When considering individual operators it is evident from the results that Model 1 presents better GoS as compared to the other two models. These results show comparisons in achieving a lower blocking probability for an operator using baseline assumptions for several parameters.

4.5.3 Performance comparison between the Non-Sharing Model and Model 3

Figure 4.12a and Figure 4.12b present the comparison of the blocking probabilities for the Non-Sharing Model and Model 3. Figure 4.12a shows the effect of increasing

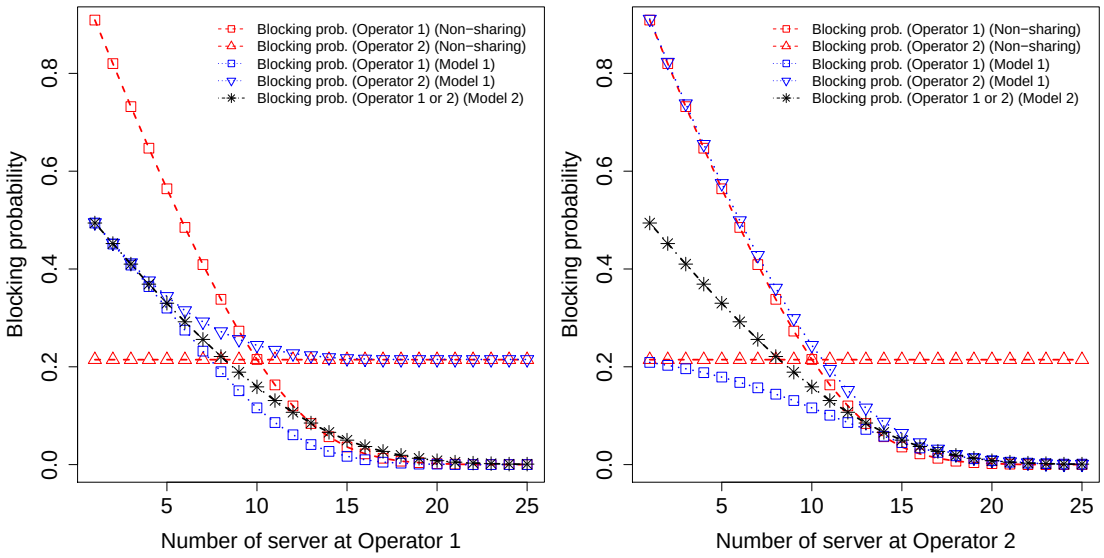

(A) (B)

FIGURE 4.11: Comparison of the blocking probability for the Non-Sharing Model with Model 1 and Model 2 with $\lambda_1 = \lambda_2 = 10$ for (A) $c_1 = 1:25$, $c_2 = 10$ and (B) $c_1 = 10$, $c_2 = 1:25$

traffic intensity at Operator 1, where we demonstrate that the blocking probability is lower when considering the Non-Sharing Model as compared to Model 3. The reason for this is that in Model 3 when the traffic at Operator 2 requires more capacity the setup allows for overflow to Operator 1 first rather than to the reserved capacity which is set to 5. This creates more traffic intensity at Operator 1, which explains the observed blocking probabilities at Operator 1 in Model 3.

In Figure 4.12b we have fixed the traffic intensity at Operator 1 while at Operator 2 the traffic is varied from $(0-30)$. In this example, with high traffic intensity (e.g., $\lambda_2 > 5$) Operator 2 in Model 3 shows significant blocking probability reduction in comparison to Non-Sharing Model due to available capacity from Operator 1 as well as the reserved capacity. At low traffic intensity (e.g., $\lambda_2 < 5$) at Operator 1, Model 3 performs better compared to Non-Sharing Model. The number of servers which is used for Figure 4.12a and Figure 4.12b are illustrated in Table 4.2.

The effect of number of servers on blocking probability at Operator 1 and Operator

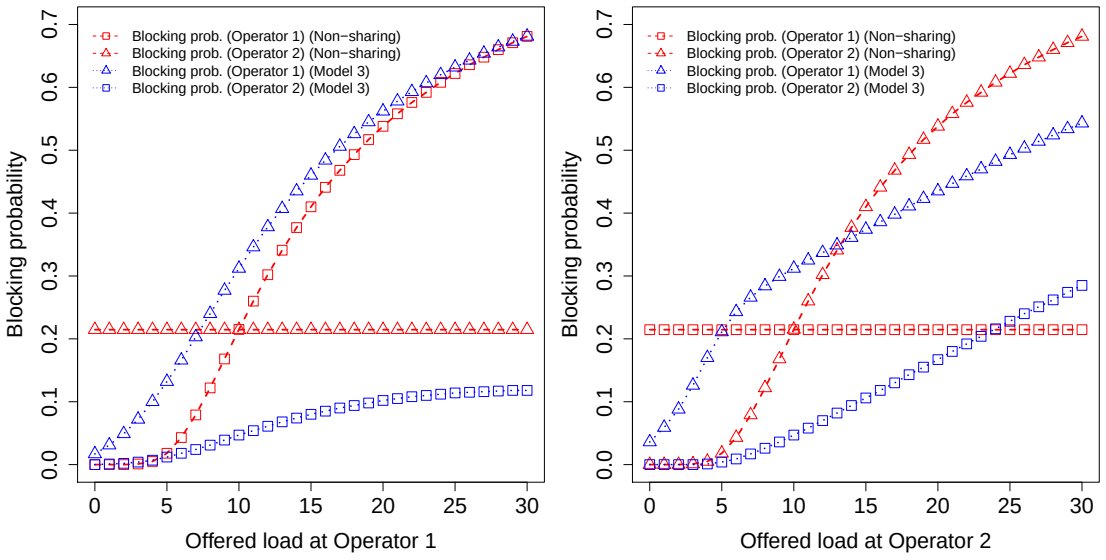

(A) (B)

FIGURE 4.12: Comparison of the blocking probability for the Non-Sharing Model ($c_1 = c_2 = 10$) with Model 3 ($c_1 = 10, c_2 = 5$, reserved capacity $= 5$) for (A) $\lambda_1 = 0:30$, $\lambda_2 = 10$ and (B) $\lambda_1 = 10, \lambda_2 = 0:30$

TABLE 4.2: Number of servers considered in Figure 4.12a and Figure 4.12b

Model	Figure 4.12a			Figure 4.12b		
	Number of servers					
	Operator 1	Operator 2	Reserved	Operator 1	Operator 2	Reserved
Non-Sharing	10	10	−−	10	10	−−
Model 3	10	5	5	10	5	5

2 for the Non-Sharing Model and Model 3 is presented in Figure 4.13a and Figure 4.13b, respectively. The traffic intensity is kept fixed for both operators. The results in Figure 4.13a show that the blocking probability for the Non-Sharing Model at Operator 1 is lower than Model 3. The reason is related to the traffic overflow from Operator 2, which adds an extra traffic at Operator 1. On the other hand, the blocking probability in Model 3 presents higher gain from the overflow flexibility, which benefits from the extra capacity provided by both Operator 1 and the reserved capacity. From Figure 4.12 and 4.13 we notice that for a particular operator, Model 3 does not always guarantee the enhancement of the grade of

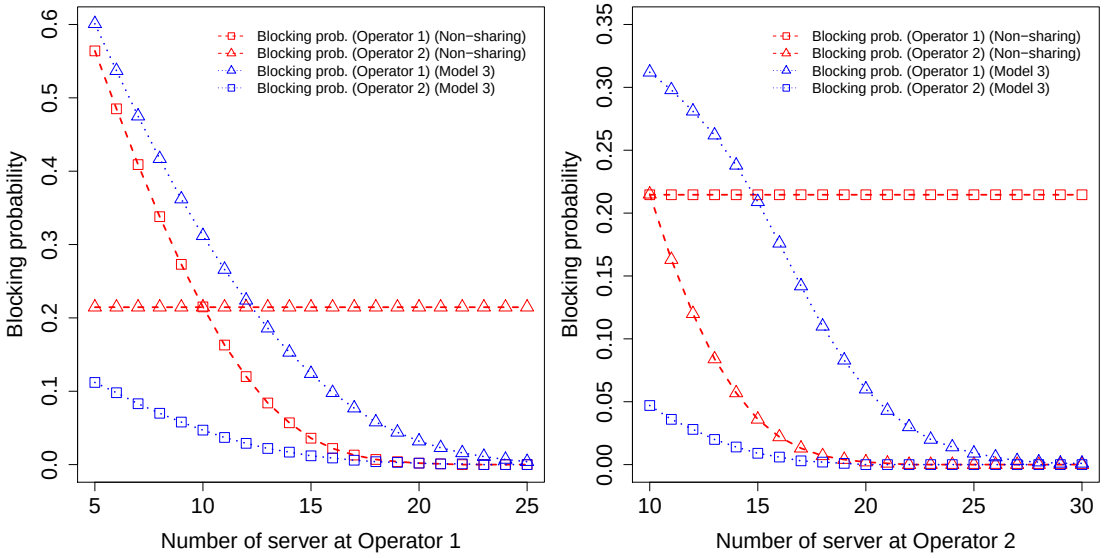

(A) (B)

FIGURE 4.13: Comparison of the blocking probability for the Non-Sharing Model with Model 3 for $\lambda_1 = \lambda_2 = 10$. See Table 4.3 for server configurations for (A) and (B).

service (GoS), instead the Non-Sharing Model can serve a higher GoS. The number of servers which is used for Figure 4.13a and Figure 4.13b are illustrated in Table 4.3.

TABLE 4.3: Number of servers considered in Figure 4.13a and Figure 4.13b

Model	Figure 4.12a			Figure 4.12b		
	Number of servers					
	Operator 1	Operator 2	Reserved	Operator 1	Operator 2	Reserved
Non-Sharing	5 : 25	10	−−	10	10 : 30	−−
Model 3	5 : 25	5	5	10	5 : 25	5

4.5.4 Evaluation of models under homogeneous traffic intensity

We have compared the blocking probability for the Non-Sharing Model, sharing Model 1, 2 and 3, see Table 4.4. The table shows the overall network blocking probability for each model configuration. Note that we defined the overall blocking probability of the networks as

$$P(b) = \sum_{i=1}^{n} P(b_1)\ g(\lambda_1, \mu_1) + P(b_2)\ g(\lambda_2, \mu_2) + P(b_n)\, g(\lambda_n, \mu_n), \tag{4.37}$$

where $P(b_i)$ is the blocking probability at operator i and $g(\lambda_i, \mu_i)$ is a function of arrival rate and service rate for the ith operator, which give the weight for the ith operator. In our case we use the weighted mean method as

$$g(\lambda_i, \mu_i) = \frac{\lambda_i/\mu_i}{\lambda_1/\mu_1 + \lambda_2/\mu_2 + \ldots + \lambda_n/\mu_n}. \tag{4.38}$$

With three different offered loads (0.25, 0.5, and 1) at Operator 1 and 2, we calculate the blocking probability for individual operators and overall network. To evaluate the models under homogeneous traffic intensity, in Table 4.4 we present a case where the four models have equal total capacity. In Model 3, $c_1 = 2$ and $c_2 = 1$, however, Operator 2 can overflow to the reserved capacity ($c_3 = 1$) in case of no capacity is available at Operator 2 and Operator 1. Table 4.4 shows that Model 3 has a clear advantage over the Non-Sharing Model and Model 1 in terms of overall blocking probability. On the other hand, Model 3 has a higher blocking probability in comparison to Model 2, this is because the overflow capacity available to Operator 1 is less in Model 3 than in Model 2 which provokes lower resource sharing efficiency.

TABLE 4.4: Comparison of the blocking probabilities for the Non-Sharing Model with Model 1, Model 2 and Model 3 with homogeneous traffic intensity

Model	Traffic intensity		Capacity			Blocking probability		
	Operator 1	Operator 2	Operator 1	Operator 2	Reserved	Operator 1	Operator 2	Overall
Non	0.25	0.25	2	2	−−	0.024	0.024	0.024
Sharing	0.50	0.50	2	2	−−	0.077	0.077	0.077
	1	1	2	2	−−	0.200	0.200	0.200
Model 1	0.25	0.25	2	2	−−	0.001	0.025	0.013
	0.500	0.500	2	2	−−	0.011	0.081	0.046
	1	1	2	2	−−	0.069	0.220	0.145
Model 2	0.250	0.250	2	2	−−	0.002	0.002	0.002
	0.500	0.500	2	2	−−	0.015	0.015	0.015
	1	1	2	2	−−	0.095	0.095	0.095
Model 3	0.250	0.250	2	1	1	0.013	0.001	0.007
	0.500	0.500	2	1	1	0.067	0.010	0.039
	1	1	2	1	1	0.225	0.058	0.142

4.5.5 Evaluation of models under heterogeneous traffic intensity

To better understand the models' behaviour, Table 4.5 shows the comparison of the blocking probabilities among the Non-Sharing Model, sharing Model 1, 2 and 3 for heterogeneous traffic intensity. Table 4.5 also includes the overall network blocking probability for each model configuration. It can be concluded from the table that sharing Model 2 and sharing Model 3 have superiority over the Non-Sharing Model and Model 1. However, if we compare Model 2 and 3 we see that Model 2 provides the lowest overall blocking probability. This indicates that even for heterogeneous traffic intensity Model 2 provides better GoS with respect to overall network performance. Since the available capacity for both operators in Model 2 is higher, the network ensures better resource utilisation compared to sharing Model 3. Even though the total capacity at Model 3 is equal to the total capacity available to Model 2, the latter performs better due to the restriction imposed on the reserved capacity which is accessible only by Operator 1. However, the results for blocking probability with respect to Operator 2 is best in Model 3 due to the reserved capacity which is available only for Operator 2.

In Summary, we have analysed and compared the performance of three different overflow models with the Non-Sharing Model. As a result, the performance achievable by the operators varies according to the operator parameters (e.g. capacity, traffic intensity) and the overflow interactions between operators. It implies that operators have the incentive to participate in the proposed sharing models since they can achieve reduced blocking probability as compared to the Non-Sharing Model.

TABLE 4.5: Comparison of the blocking probability for the Non-Sharing Model, Model 1, Model 2 and Model 3 with heterogeneous traffic intensity

Model	Traffic intensity		Capacity			Blocking probability		
	Operator 1	Operator 2	Operator 1	Operator 2	Reserved	Operator 1	Operator 2	Overall
Non	0.250	0.500	2	2	−−	0.024	0.077	0.059
Sharing	0.500	0.250	2	2	−−	0.077	0.024	0.059
	0.500	1	2	2	−−	0.077	0.200	0.159
	1	0.500	2	2	−−	0.200	0.077	0.159
Model 1	0.250	0.500	2	2	−−	0.003	0.077	0.052
	0.500	0.25	2	2	−−	0.006	0.028	0.013
	0.500	1	2	2	−−	0.021	0.204	0.143
	1	0.500	2	2	−−	0.043	0.100	0.062
Model 2	0.25	0.50	2	2	−−	0.006	0.006	0.006
	0.50	0.25	2	2	−−	0.006	0.006	0.006
	0.50	1	2	2	−−	0.048	0.048	0.048
	1	0.5	2	2	−−	0.048	0.048	0.048
Model 3	0.25	0.50	2	1	1	0.035	0.005	0.015
	0.50	0.25	2	1	1	0.035	0.002	0.024
	0.50	1	2	1	1	0.142	0.035	0.070
	1	0.500	2	1	1	0.143	0.019	0.101

4.5.6 Evaluation of Model 1 and Model 2 with reference to simulated blocking probabilities

Theoretical solution and numerical approximation analysis are compared in this section to validate our proposed mathematical approach. The same criteria were used in the analysis for the theoretical and the numerical approximation. In order to perform this validation, we have chosen the uni-directional (See Figure 4.14a) and the bi-directional overflow models (See Figure 4.14). In Figure 4.14a and 4.14b we set $c_{1,2} = 10$, λ_1 is varied between $0 : 30$, and $\lambda_2 = 10$. From the figures we observe that the simulated models are almost identical to the theoretical counterparts. In both figures it is seen that the blocking probabilities increase with the increase of λ_1.

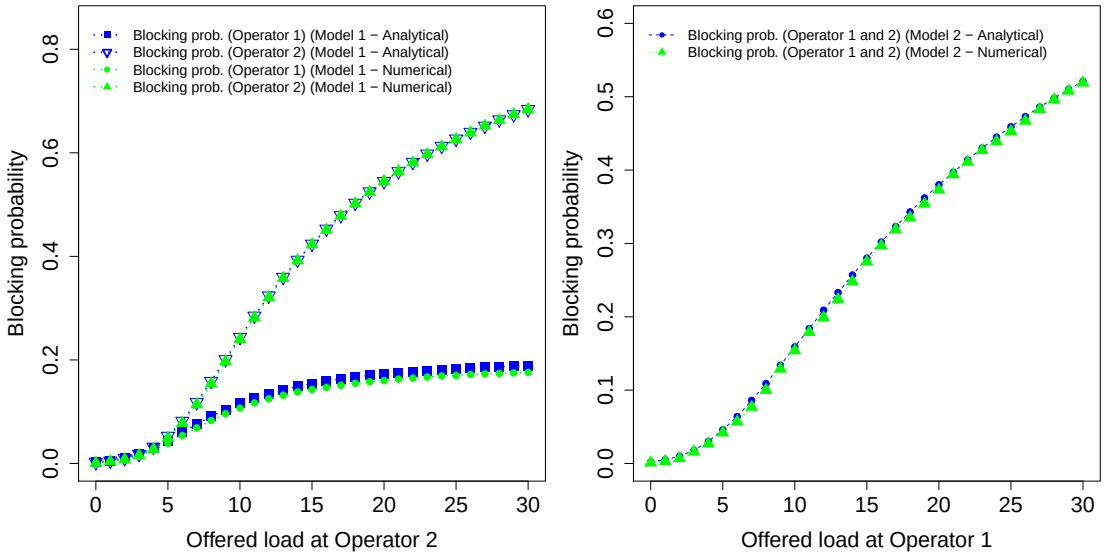

(A) (B)

FIGURE 4.14: Comparison of the blocking probability for Model 1 (A) and Model 2 (B) using analytical and numerical approaches.

4.6 Summary

Cooperative resource sharing is considered to be one of the key challenges for future generation wireless communication networks. The problem of resource allocation under the sharing environment increases as the number of cooperating network operators increases with their complex sharing agreements. Consequently, network operators have to deal with spectrum allocation for a number of service types and operators. To the best of our knowledge, there is no work which studies the resource allocation problem under different resource sharing schemes which depend on many factors such as agreements between network operators and spectrum availability between coexistent network operators.

Considering a number of overflow mechanisms we addressed the resource sharing problem and presented a robust analytical framework for DSA. We have proposed four different models: the Non-Sharing Model, the sharing model with uni-directional overflow (Model 1), the sharing model with bi-directional overflow (Model 2) and the sharing model with reserved capacity for one of the operators in the network (Operator 2) and a bi-directional overflow between both operators (Model 3). We have derived the global balance equation, and found an explicit expression of the blocking probability for each resource sharing model. Blocking probabilities are calculated for each model under various traffic scenarios. The results show that the operators can achieve a notable reduction of blocking probability under the proposed models compared with the Non-Sharing Model.

Our analytical results provide a basis for further study of this type of overflow with different configurations. The results highlight the importance of resource sharing for communication networks. The analysis provided in this chapter can be used to inform network operators to determine agreement terms for future spectrum sharing cooperation with coexisting network operators.

Chapter 5

Dynamic spectrum sharing (Multi-operator)

5.1 Introduction

In this chapter we consider the scenario emerging from spectrum sharing where one secondary operator interacts with multi-primary operators according to certain mutual agreements [1, 36, 100, 130, 131, 132]. We analyse three types of multi-operator joint spectrum management schemes by considering a loss system. Analysis and modelling of the loss system are vital for the ubiquitous real-time multimedia (voice and video) communications where delay is not tolerable. The modelling and analysis of loss systems are increasingly important due to the growing percentage of multimedia traffic. Modelling of non real-time multimedia traffic by using the queue system are also important but beyond the scope of this study.

The rest of the sections are organised as follows. The system model is described in the next Section. Section 5.3 presents the spectrum sharing models and describes our mathematical approach. In Section 5.4, we present our findings. Finally, Section 5.5 summarises our conclusions.

5.2 System model

We consider a network consisting of four operators. An operator could be a primary operator, secondary operator or both, depending on the chosen arrangement between operators, see Figures 5.1, 5.2 and 5.3. We first assume that each of the operators in the network owns a spectrum band which is divided into $c_i \in \mathbb{Z}^+$ frequency channels. Each operator serves users with Poisson distributed arrivals and mean rate λ_i and service rate μ_i. In a non-sharing model, each operator in the network would operate independently and the blocking probability in this case can be easily calculated using an Erlang system giving $E(c_i, \lambda_i, \mu_i)$ [133, 88]. However in a cooperative network if one or more operators are underloaded then it may allow other operators with high traffic to use their under-utilised resources under a mutual agreement.

A first-come-first-served scheduling system is considered to preserve the stability of the network and eliminate channel interference. As such each shared server is allowed one entry by the users of the involved operators. If a channel is being used by an operator then the primary operator waits until a channel is vacated by its current occupier. Channel requests are granted completely, in which fragmentation is not considered. The use of spectrum fragmentation where the available spectrum is fragmented into smaller channels across a wide-band, aggregation techniques are required to allocate channels to the users, which is beyond the scope of this thesis.

In the system where multi-operators cover the same geographical area, the SNO aims to find the operators with available channels in order to balance the load across all available resources without causing one operator to be overloaded while other operators are in an underloaded state. Such a set up will ensure better utilisation of spectrum as we will see later in Section 5.4. The PNOs who experiences a drop in the average arrival rate λ_i will be preferable to the SNO. Similarly, PNO who is experiencing an increase of channel request rates would not be accessible by the SNO. When all PNOs channels are busy then the SNO will have to drop the

new arrival channel requests. In this chapter we consider a non-adjustable service rate to provide a standardised service quality.

Operators benefit from temporal variation in the traffic by allowing each other to use their idle channels with mutual agreements. We discuss three possible models in cellular networks. Uni-directional cooperation; bi-directional cooperation; bi-directional cooperation with emergency capacity. The models are discussed in details in the Section 5.3

5.3 Dynamic spectrum sharing models

In this section, we develop models for dynamic spectrum sharing under different resource sharing schemes. Three models with complex sharing schemes are proposed which are described in the subsequent sections.

5.3.1 Model A: Uni-Directional cooperation

Consider a network with three primary and one secondary operators where the secondary operator aims to borrow spectrum from the primary operators under a uni-directional leasing agreement as shown in Figure 5.1. Our main objective is to find the impact of the secondary operator on the grade of service and spectrum utilisation. We assume that the channel requests follow Poisson processes with arrival rates $\lambda_i, i = 1, 2, 3$ for the ith PNO and λ_0 for the SNO and exponential channel holding time with rates $\mu_i, i = 1, 2, 3$ for the ith PNO and μ_0 for the SNO. The offered load for the ith operator is then defined as $\rho_i = \lambda_i/\mu_i$. Denote the capacity of the ith operator as $c_i, i = 0, 1, 2, 3$.

Let $X_i(t), i = 1, 2, 3$ be the number of channels in the ith primary network operator (PNO), $X_0(t)$ be the number of channels in the secondary network operator (SNO) and $X_{0i}(t), i = 1, 2, 3$ be the number of channels borrowed by the

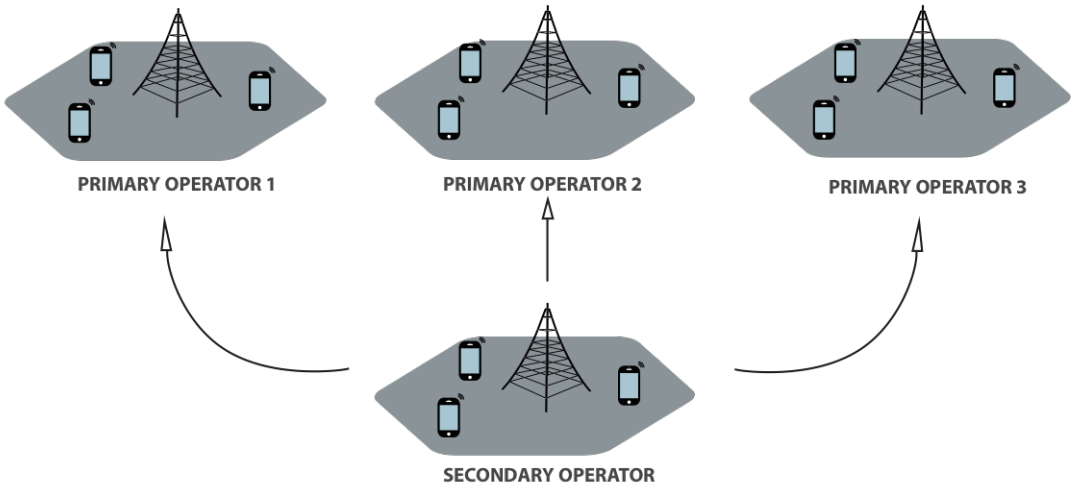

FIGURE 5.1: Uni-Directional service operators sharing network

$$q(\mathbf{n},\mathbf{n}') = \begin{cases} \lambda_0(t) & \mathbf{n}' = \mathbf{n} + \mathbf{e}_0 \text{ or } \mathbf{n}' = \mathbf{n} + \mathbf{e}_{01} \text{ if } n_0 = c_0 \cap n_1 + n_{01} < c_1 \\ & \text{or } \mathbf{n}' = \mathbf{n} + \mathbf{e}_{02} \text{ if } n_0 = c_0 \cap n_1 + n_{01} = c_1 \cap n_2 + n_{02} < c_2 \\ & \text{or } \mathbf{n}' = \mathbf{n} + \mathbf{e}_{01} \text{ if } n_0 = c_0 \cap n_1 + n_{01} = c_1 \cap n_2 + n_{02} \\ & = c_2 \cap n_3 + n_{03} < c_3 \\ \lambda_i(t) & \mathbf{n}' = \mathbf{n} + \mathbf{e}_i,\ i = 1,2,3 \\ n_i\mu_i(t) & \mathbf{n}' = \mathbf{n} - \mathbf{e}_i,\ i = 0,1,2,3 \\ n_{0i}\mu_i(t) & \mathbf{n}' = \mathbf{n} - \mathbf{e}_{0i},\ i = 1,2,3 \\ 0 & \text{otherwise} \end{cases} \tag{5.2}$$

where $\mathbf{e}_0$ and $\mathbf{e}_{0i}$ are unit vectors.

SNO from the ith PNO. Then a state of the process is a vector defined by $\mathbf{X} = (X_0(t), X_1(t), X_2(t), X_3(t), X_{01}(t), X_{02}(t), X_{03}(t))$ which is a Markov chain with state space

$$\Omega = \{(n_0, n_1, n_2, n_3, n_{01}, n_{02}, n_{03}) : n_0 \leq c_0, n_i + n_{0i} \leq c_i, i = 1,2,3\} \tag{5.1}$$

The transition rates of the process are defined in equation (5.2).

Denote the steady state distribution by $\pi(\mathbf{n}, t)$ which can be obtained by solving the Kolmogorov forward equation (5.3) given by equation (5.3).

$$\begin{aligned}\frac{\mathrm{d}\pi(\mathbf{n},t)}{\mathrm{d}t} =& \Bigg[\lambda_0(t)\cdot\Big(\mathbf{1}(n_0<c_0)+\mathbf{1}(n_0=c_0\cap_{i\in\{1,2,3\}}\mathbf{n}+\mathbf{e}_{0i})\Big)\\ &+\sum_{i=1}^{3}\lambda_i(t)\cdot\mathbf{1}(n_i+n_{0i}<c_i)\Bigg]\cdot\pi\left((\mathbf{n}-\mathbf{e}_i),t\right)\\ &+\sum_{i=0}^{3}(n_i+1)\mu_i(t)\pi\left((\mathbf{n}+\mathbf{e}_i),t\right)+\sum_{i=1}^{3}(n_{0i}+1)\mu_{i0}(t)\cdot\pi(\mathbf{n}+\mathbf{e}_{0i})\\ &-\Bigg[\lambda_0(t)\cdot\Big(\mathbf{1}(n_0<c_0)+\mathbf{1}(n_0=c_0\cap_{i\in\{1,2,3\}}\mathbf{n}+\mathbf{e}_{0i})\Big)\\ &+\sum_{i=1}^{3}\lambda_i(t)\cdot\mathbf{1}(n_i+n_{0i}<c_i)+\sum_{i=0}^{3}n_i\mu_i(t)+\sum_{i=1}^{3}n_{0i}\mu_i(t)\Big)\Bigg]\cdot\pi\left(\mathbf{n},t\right)\end{aligned} \tag{5.3}$$

Solving the Kolmogorov forward equations (5.3) by equating the RHS of equation (5.3) at 0, we obtain the closed form solution of the equilibrium distribution which is

$$\pi(\mathbf{n})=\mathcal{G}^{-1}\frac{\rho_0^{(n_0+n_{01}+n_{02}+n_{03})}}{(n_0+n_{01}+n_{02}+n_{03})!}\cdot\frac{\rho_1^{n_1}\rho_2^{n_2}\rho_3^{n_3}}{n_1!n_2!n_3!},\ \ \forall\ \ \mathbf{n}\in\Omega \tag{5.4}$$

where

$$\mathcal{G}=\sum_{\mathbf{n}\in\Omega}\left[\frac{\rho_0^{(n_0+n_{01}+n_{02}+n_{03})}}{(n_0+n_{01}+n_{02}+n_{03})!}\cdot\frac{\rho_1^{n_1}\rho_2^{n_2}\rho_3^{n_3}}{n_1!n_2!n_3!}\right]. \tag{5.5}$$

One of the main goals of deriving the equilibrium distribution is to calculate the blocking probability or call congestion rate. The formula for the blocking probability can be derived from the closed-form solution (5.4). The blocking probability for an operator $i, i=0,1,2,3$ is then given by

$$
\begin{aligned}
P_{b_i}(t) &= \sum_{\mathbf{n}\in S_R} \pi(\mathbf{n},t) \\
&= \frac{\displaystyle\sum_{\mathbf{n}\in S_R} \frac{\rho_0^{(n_0+n_{01}+n_{02}+n_{03})}}{(n_0+n_{01}+n_{02}+n_{03})!}\cdot\frac{\rho_1^{n_1}\rho_2^{n_2}\rho_3^{n_3}}{n_1!n_2!n_3!}}{\displaystyle\sum_{\mathbf{n}\in\Omega} \frac{\rho_0^{(n_0+n_{01}+n_{02}+n_{03})}}{(n_0+n_{01}+n_{02}+n_{03})!}\cdot\frac{\rho_1^{n_1}\rho_2^{n_2}\rho_3^{n_3}}{n_1!n_2!n_3!}} \quad \forall \ \mathbf{n}\in\Omega
\end{aligned} \tag{5.6}
$$

where the set S_R is the restricted state space, and varies for the SNO and PNOs. For the SNO, it is defined as

$$
S_R = \big\{\mathbf{n}\in\Omega \,|\, (n_0 = c_0 \cap n_{01}+n_{11} = c_1 \cap n_{02}+n_{22} = c_2 \cap n_{03}+n_{33} = c_3)\big\}, \tag{5.7}
$$

and for the ith PNO, S_R can be replaced by S_i and defined as

$$
S_i = \big\{\mathbf{n}\in\Omega \,|\, (n_i + n_{0i} = c_i)\big\}, \quad i = 1,2,3. \tag{5.8}
$$

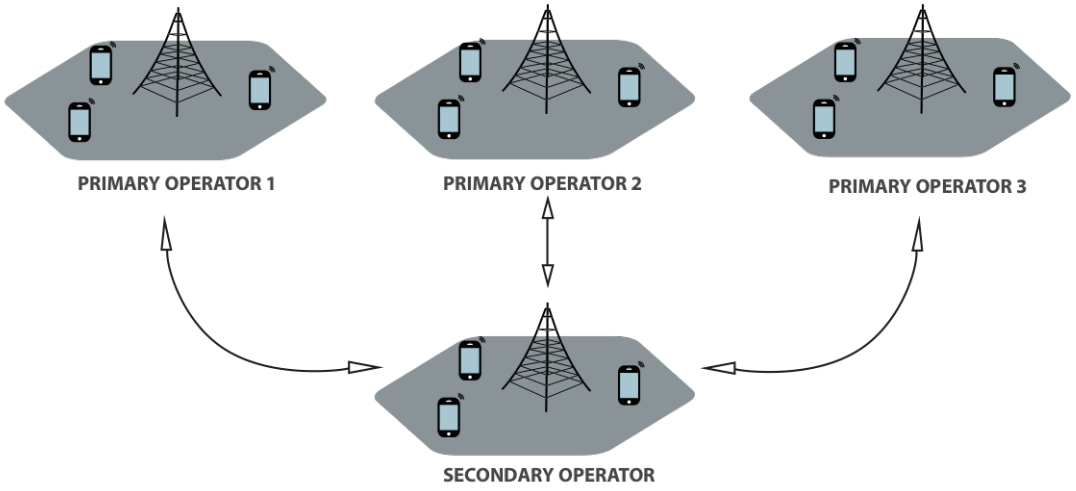

FIGURE 5.2: Bi-Directional service operators sharing network

$$
\begin{aligned}
P_{b_i}(t) &= \sum_{\mathbf{n}\in S_R} \pi(\mathbf{n},t) \\
&= \frac{\displaystyle\sum_{\mathbf{n}\in S_R} \frac{\rho_0^{(n_0+n_{01}+n_{02}+n_{03})}}{(n_0+n_{01}+n_{02}+n_{03})!} \cdot \frac{\rho_1^{(n_1+n_{10})}\rho_2^{(n_2+n_{20})}\rho_3^{(n_3+n_{30})}}{(n_1+n_{10})!(n_2+n_{20})!(n_3+n_{30})!}}{\displaystyle\sum_{\mathbf{n}\in\Omega} \frac{\rho_0^{(n_0+n_{01}+n_{02}+n_{03})}}{(n_0+n_{01}+n_{02}+n_{03})!} \cdot \frac{\rho_1^{(n_1+n_{10})}\rho_2^{(n_2+n_{20})}\rho_3^{(n_3+n_{30})}}{(n_1+n_{10})!(n_2+n_{20})!(n_3+n_{30})!}} \quad \forall \ \mathbf{n}\in\Omega
\end{aligned}
\tag{5.11}
$$

where the set S_R is the restricted state space for all operators.

5.3.2 Model B: Bi-Directional cooperation

In bi-directional cooperative model, in addition to uni-directional operation primary operators are also allowed to borrow spectrum from the secondary operators when they require as shown in Figure 5.2.

Deriving Kolmogorov forward equation and solving we obtain the equilibrium probability distribution as given in equation (5.9).

$$
\pi(\mathbf{n}) = \mathcal{G}^{-1} \frac{\rho_0^{(n_0+n_{01}+n_{02}+n_{03})}}{(n_0+n_{01}+n_{02}+n_{03})!} \cdot \frac{\rho_1^{(n_1+n_{10})}\rho_2^{(n_2+n_{20})}\rho_3^{(n_3+n_{30})}}{(n_1+n_{10})!(n_2+n_{20})!(n_3+n_{30})!}, \quad \forall \ \mathbf{n}\in\Omega
\tag{5.9}
$$

where

$$
\mathcal{G} = \sum_{\mathbf{n}\in\Omega} \left[\frac{\rho_0^{(n_0+n_{01}+n_{02}+n_{03})}}{(n_0+n_{01}+n_{02}+n_{03})!} \cdot \frac{\rho_1^{(n_1+n_{10})}\rho_2^{(n_2+n_{20})}\rho_3^{(n_3+n_{30})}}{(n_1+n_{10})!(n_2+n_{20})!(n_3+n_{30})!} \right]
\tag{5.10}
$$

The blocking probability formula for quantifying the GoS can be given by 5.11

For the SNO, it is defined as

$$S_R = \{\mathbf{n} \in \Omega \,|\, (n_0 = c_0 \cap n_{01} + n_{11} = c_1 \cap n_{02} + n_{22} = c_2 \cap n_{03} + n_{33} = c_3)\}, \tag{5.12}$$

and for the ith PNO, S_R can be replaced by S_i and defined as

$$S_i = \{\mathbf{n} \in \Omega \,|n_0 + n_{i0} = c_0 \cap (n_i + n_{0i} = c_i)\}, \quad i = 1, 2, 3. \tag{5.13}$$

5.3.3 Model C: Bi-Directional cooperation with pooled resources

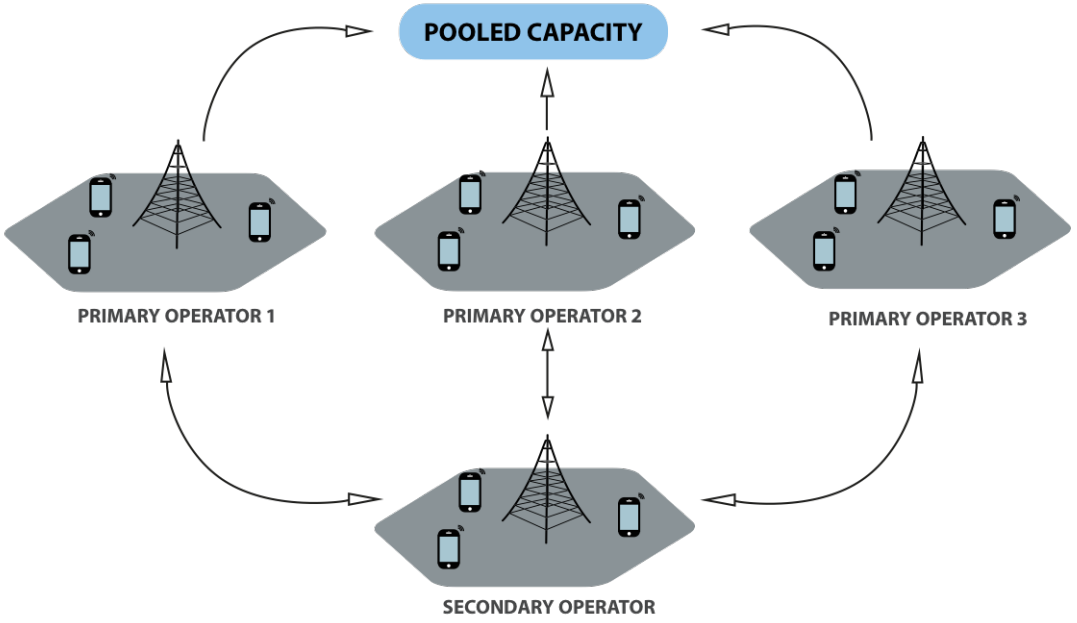

FIGURE 5.3: Bi-Directional with pooled capacity service operators sharing network

The bi-directional cooperation with pooled resources model is similar to Model B with additional pooled resources denoted by c_p, which can be accessed by any of the PNOs under *first-come-first-served* discipline, see Figure 5.3. The pooled

The blocking probability formula for Model C can be given by

$$P_{b_i}(t) = \sum_{\mathbf{n}\in S_R} \pi(\mathbf{n},t)$$
$$= \frac{\displaystyle\sum_{\mathbf{n}\in S_R} \frac{\rho_0^{(n_0+n_{01}+n_{02}+n_{03})}}{(n_0+n_{01}+n_{02}+n_{03})!} \cdot \frac{\rho_1^{(n_1+n_{10}+n_{1p})}\rho_2^{(n_2+n_{20}+n_{2p})}\rho_3^{(n_3+n_{30}+n_{3p})}}{(n_1+n_{10}+n_{1p})!(n_2+n_{20}+n_{2p})!(n_3+n_{30}+n_{3p})!}}{\displaystyle\sum_{\mathbf{n}\in\Omega} \frac{\rho_0^{(n_0+n_{01}+n_{02}+n_{03})}}{(n_0+n_{01}+n_{02}+n_{03})!} \cdot \frac{\rho_1^{(n_1+n_{10}+n_{1p})}\rho_2^{(n_2+n_{20}+n_{2p})}\rho_3^{(n_3+n_{30}+n_{3p})}}{(n_1+n_{10}+n_{1p})!(n_2+n_{20}+n_{2p})!(n_3+n_{30}+n_{3p})!}} \quad \forall\, \mathbf{n}\in\Omega \quad (5.16)$$

where the set S_R is the restricted state space for all operators.

resources is considered as a last resort for the PNOs when the SNO's channels are also occupied.

$$\pi(\mathbf{n}) = \mathcal{G}^{-1} \frac{\rho_0^{(n_0+n_{01}+n_{02}+n_{03})}\rho_1^{(n_1+n_{10}+n_{1p})}\rho_2^{(n_2+n_{20}+n_{2p})}\rho_3^{(n_3+n_{30}+n_{3p})}}{(n_0+n_{01}+n_{02}+n_{03})!(n_1+n_{10}+n_{1p})!(n_2+n_{20}+n_{2p})!(n_3+n_{30}+n_{3p})!} \quad \forall\ \mathbf{n}\in\Omega \quad (5.14)$$

where

$$\mathcal{G} = \sum_{\mathbf{n}\in\Omega} \left[\frac{\rho_0^{(n_0+n_{01}+n_{02}+n_{03})}\rho_1^{(n_1+n_{10}+n_{1p})}\rho_2^{(n_2+n_{20}+n_{2p})}\rho_3^{(n_3+n_{30}+n_{3p})}}{(n_0+n_{01}+n_{02}+n_{03})!(n_1+n_{10}+n_{1p})!(n_2+n_{20}+n_{2p})!(n_3+n_{30}+n_{3p})!} \right] \quad (5.15)$$

For the SNO, it is defined as

$$S_R = \big\{\mathbf{n} \in \Omega \,|\, (n_0 = c_0 \cap n_{01} + n_{11} = c_1 \cap n_{02} + n_{22} = c_2 \cap n_{03} + n_{33} = c_3)\big\}, \tag{5.17}$$

and for the ith PNO, S_R can be replaced by S_i and defined as

$$S_i = \big\{\mathbf{n} \in \Omega \,|n_0 + n_{i0} = c_0 \,\cap\, (n_i + n_{0i} = c_i \,\cap \sum_{i=1}^{3} n_{ip} = c_p)\big\}, \;\; i = 1, 2, 3. \tag{5.18}$$

5.3.4 Bi-Directional cooperation with multi-primary operators and pooled capacity

Up to this point we have considered spectrum sharing between one secondary operator and three primary operators, however, in practical scenarios, the number of primary operators may vary, according to the agreements between the operators and also the availability of spectrum resources. For this reason, in this section we extend the analytical model to count for N primary operator[6].

Let us define the unique invariant distribution $\pi(\mathbf{n})$ using the transition rates of the operators (Secondary and primary operators) as

$$\pi(\mathbf{n}) = \mathcal{G}^{-1}(\mathcal{D}) \qquad\qquad \forall \;\; \mathbf{n} \in \Omega \tag{5.19}$$

where (for N primary operators and 1 secondary operator)

$$\mathcal{D} = \frac{\left[\rho_0^{(n_0+n_{01}+\cdots+n_{0N})}\right]\left[\rho_1^{(n_1+n_{10}+n_{1p})}\right]\cdots\left[\rho_N^{(n_N+n_{N0}+n_{Np})}\right]}{(n_0+n_{01}+\cdots+n_{0N})!(n_1+n_{10}+n_{1p})!\cdots(n_N+n_{N0}+n_{Np})!} \qquad \forall \;\; \mathbf{n} \in \Omega \tag{5.20}$$

[6]The analytical sharing model with multiple-secondary and multiple-primary operators is addressed in the Appendix.

and

$$\mathcal{G} = \sum_{\mathbf{n}\in\Omega} \mathcal{D} \tag{5.21}$$

The blocking probability for N primary operators and 1 secondary operator can be written as

$$P_{(b_i)(t)} = \sum_{\mathbf{n}\in\mathbf{S}} \pi(\mathbf{n}, \mathbf{t})$$

$$= \frac{\sum\limits_{\mathbf{n}\in\mathbf{S_R}} \mathcal{D}}{\mathcal{G}} \tag{5.22}$$

where the set S is the restricted state space, and varies for the SNO and PNOs. For the secondary network operator it is defined as

$$S = \big\{\mathbf{n} \in \Omega \,|\, (n_0 = c_0 \cap n_{01} + n_{11} = c_1 \cap n_{02} + n_{22} = c_2 \cap \cdots \cap n_{0N} + n_{NN} = c_N)\big\}, \tag{5.23}$$

and for the i PNO, S can be replaced by S_i and defined as

$$S_i = \big\{\mathbf{n} \in \Omega \,|n_0 + n_{i0} = c_0 \,\cap\, (n_i + n_{0i} = c_i \,\cap \sum_{i=1}^{N} n_{ip} = c_p)\big\}, \;\; i = 1, 2, 3. \tag{5.24}$$

5.3.5 Marginal probability distribution and spectrum utilisation

Spectrum utilisation as the ratio of the average number of busy channels and the overall available number of channels in the network is an important parameter. As we aim to quantify the spectrum utilisation we first calculate the marginal probability distribution of number of channels for each operator. The marginal probability distribution can be given by

$$\pi(n_i) = \sum_{\mathbf{n}\in\{\Omega\setminus n_i\}} \pi(\mathbf{n})$$

$$\forall \begin{cases} i \in \{0,1,2,3,01,02,03\} \text{ for Model A} \\ i \in \{0,1,2,3,01,02,03,10,20,30\} \text{ for Model B} \\ i \in \{0,1,2,3,01,02,03,10,20,30,1p,2p,3p\} \text{ for Model C} \\ i \in \{0,1,\cdots,N,01,\cdots,0N,10,\cdots,N0,1p,\cdots,Np\} \text{ for Model C and } N \text{ PNO} \end{cases} \tag{5.25}$$

Therefore, expected spectrum utilisation of each model can be obtained as

$$u(n_i) = \sum_{n_i\in\Omega} \frac{1}{c}\big[n_i \cdot \pi(n_i)\big] \quad \forall\, n_i \in \Omega \tag{5.26}$$

where

$$c = \begin{cases} (c_0 + c_1 + c_2 + c_3) \text{ for Model A and B} \\ (c_0 + c_1 + c_2 + c_3 + c_p) \text{ for Model C} \\ (c_0 + c_1 + \cdots + c_N + c_p) \text{ for Model C and } N \text{ PNO} \end{cases} \tag{5.27}$$

5.4 Analysis and results

In this section, we show the impact of system parameters on the models performance and verify our theoretical analysis presented in Section 5.3.

5.4.1 Effect of traffic intensity at the secondary operator on blocking probability

The *first-come-first-served* scheduling system, which we have used in our models, means that at saturation the primary operators have their bandwidth allocation reduced and hence we observe an increase in blocking probability, as shown in Figure 5.4. Below the saturation point between an offered load of ($\rho_0 = 2 : 3$), the uni-directional cooperation outperforms the bi-directional counterpart, see the zoomed part of Figure 5.4. However, when the network starts to reach saturation, the blocking probability of uni and bi-directional cooperation models are approximately equal and they increase exponentially as $\rho_0 \rightarrow 10$. By deploying the bi-directional with pooled capacity model (Model C), we notice that as the x-axis of Figure 5.4 continues and with more traffic diverted to the primary operators' channels, the latter begins to rely on the pooled capacity (where $c_p = 1$). This provides additional channels to the PNOs, which results in lower blocking probability compared to the first two models.

5.4.2 Effect of traffic intensity at the secondary operators on blocking probability

The blocking probability of the primary operators as a function of secondary operators traffic intensity is plotted in Figure 5.5 and 5.6. From Figure 5.5, we observe that a continuous increase in the blocking probability at Operator 1 and 2 of new user requests as the traffic intensity of secondary operator increases while keeping

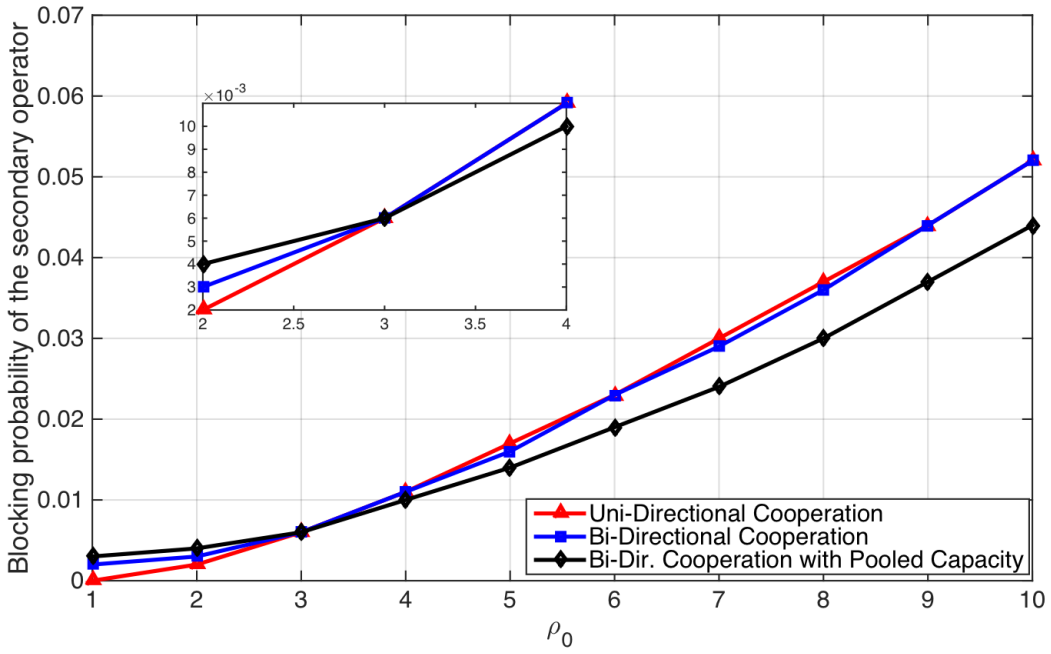

FIGURE 5.4: Comparison of the blocking probability for the secondary operator using the proposed models with $\rho_0 = 1 : 10$, see Table 5.1 for full configuration details.

the capacity of each operator constant. When the majority of the channels are occupied by respective licensed users, the primary operators use the pooled resources which is why we see Model C outperform Model A and B when the traffic is high. At low traffic Model B performs well compared to Model A and C. In Figure 5.6 the blocking probability of operator 3 is quantified using the three proposed models. From the figure, we find similar trends in blocking probability to Figure 5.5 with a slight difference, which is caused by the variation in the parameters used in Operator 2 and 3, as shown in the highlighted row of Table 5.1.

The crossover point in the performance can be seen in Figure 5.6 which is more visible than in figures 5.4 and 5.5. This crossover point is because the total channels available at the primary operators for the secondary access is larger in Model B than in Model C. Hence we see that model B performs better when the traffic is low. However, when the traffic increase, Models C outstrip Model B due to the primary operators recourse to the pooled capacity (only available to the primary

operators), leaving more channels available to the secondary operator. In that case Model C have advantage over Model B when the network experiences high traffic when considering the proposed pooled capacity.

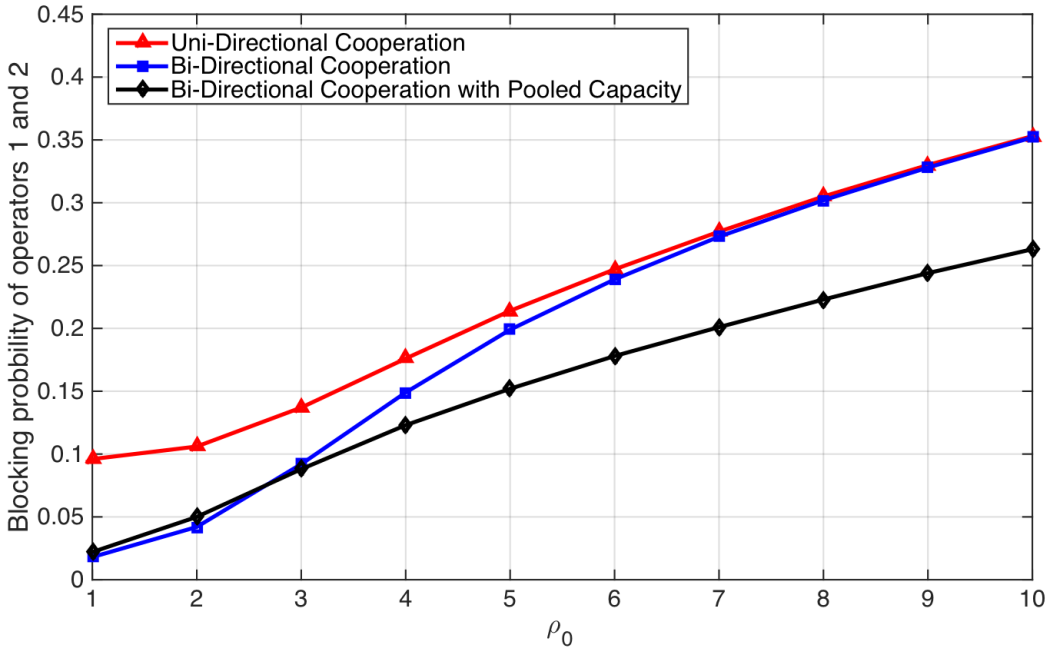

FIGURE 5.5: Blocking probability for Operator 1 and 2, see Table 5.1 for full configuration details.

TABLE 5.1: Configurations used in Figure 5.4, 5.5 and 5.6

	Number of channels					Traffic intensity			
Model	SNO	PNO 1	PNO 2	PNO 3	Pooled Capacity	SNO	PNO 1	PNO 2	PNO 3
Model A	4	4	4	4	−−	1 : 10	2	2	4
Model B	4	4	4	4	−−	1 : 10	2	2	4
Model C	4	4	4	4	1	1 : 10	2	2	4

5.4.3 Effect of the number of available channels on blocking probability

Figure 5.7 shows the blocking probability of the secondary operator for each model when PNO 1 has different number of channels ($c_1 = 1 : 10$). In the network each

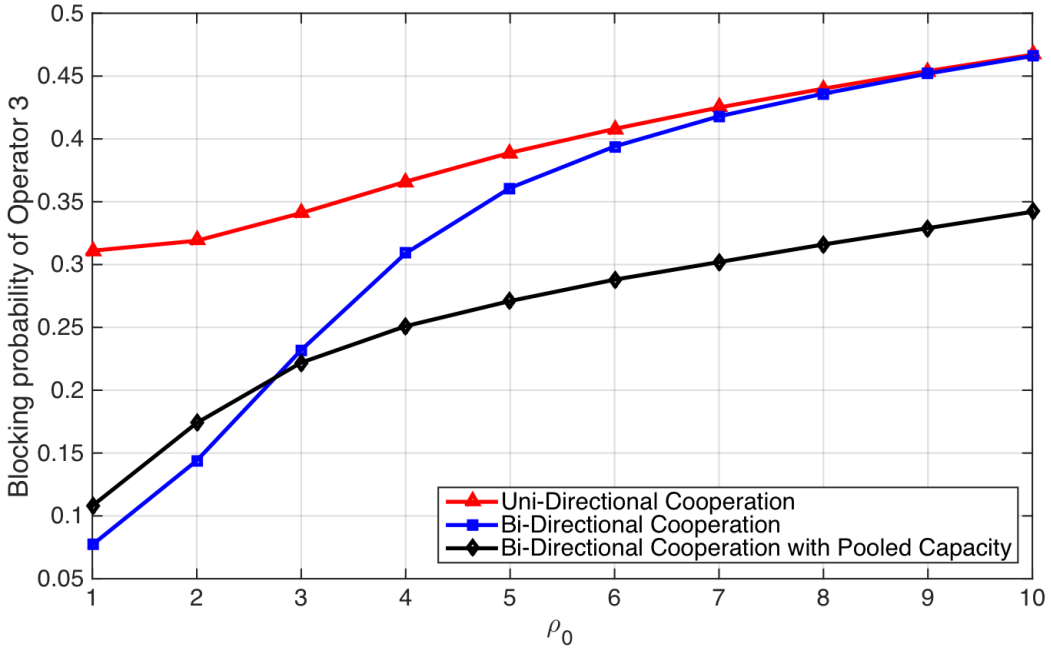

FIGURE 5.6: Blocking probability for (a) Operator 1 and 2 and (b) Operator 3, see Table 5.1 for full configuration details.

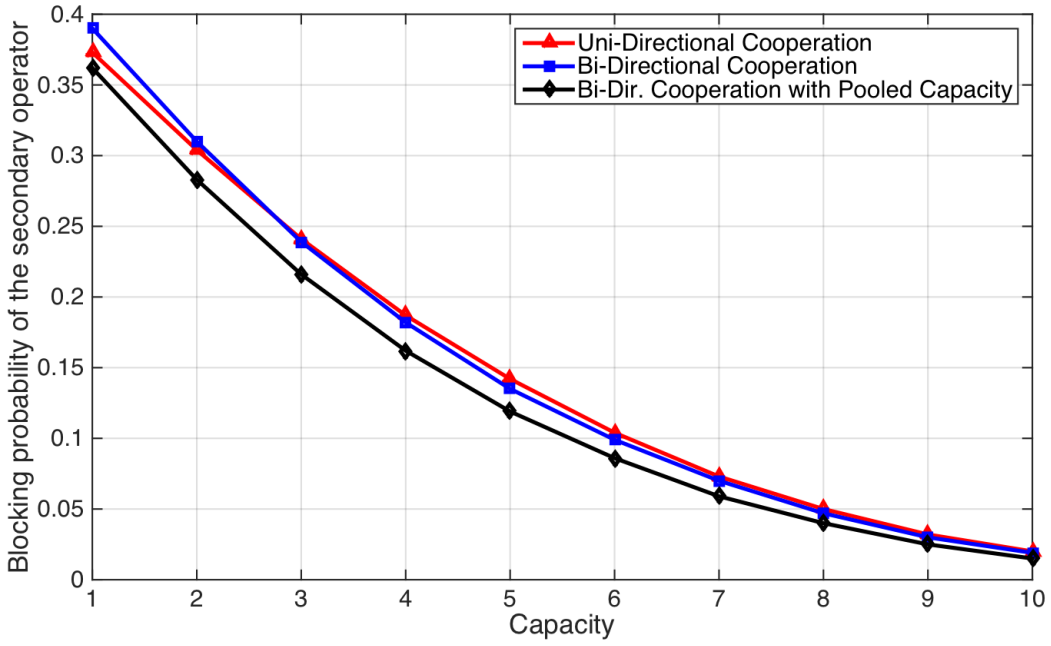

FIGURE 5.7: Comparison of blocking probability for the secondary operator with the varying number of channels using the proposed models when $\rho_s = 5, \rho_1 = 3, \rho_2 = 4, \rho_3 = 5, c_{0,2,3} = 2, c_1 = 1:10, c_p = 1$.

operator has its own licensed channels, service rate and offered load as shown in the figure caption. This result indicates that Model A and B show similar performances of blocking probability. Model C in this case has the advantage due to the higher number of channels.

5.4.4 Evaluation of spectrum utilisation

The performance measure discussed so far is concerned with the call congestion and focuses on the performance of each individual operator. In this subsection we analyse the proposed model's efficiency in terms of spectrum utilisation. We use the formulae derived in Subsection 5.3.5 and the simulation parameters shown in Table 5.2. We show the change in the spectrum utilisation against the traffic intensity at the SNO ($\rho_0 = 1 : 10$). In Figure 5.8 we can see that Model C is superior compared to the other two models especially when $\rho_0 < 4$. We also notice that Model C performance deteriorates when the traffic intensity is high $\rho_0 > 5$. When traffic load is less than 5 Model A and Model B provide similar performance due to increased saturation of channels. On average Model B performs best at 85% spectrum utilisation with 2% higher than the uni-directional cooperation model and 0.5% higher than Model C.

We also investigate the spectrum utilisation of the proposed models against the change in traffic intensity at the operators 1, 2 and 3, see Figure 5.9. Keeping ρ_0 fixed at 10, we vary the traffic intensity of PNO 1, 2 and 3 ($\rho_1 = \rho_2 = \rho_3 = 5 : 14$). For a fair comparison, the total number of channels available is kept fixed for all Models as $\sum_i c_i = 12 \ \forall i \in \{0, 1, 2, 3\}$.

For traffic intensity below 6 the utilisation of channels under Model A and B are equal. With excess offered load the difference between Model A and B becomes wider and considerably more for $\rho > 13$. Under any offered load Model C shows the lowest level of efficiency. Considering that traffic conditions occur at equal

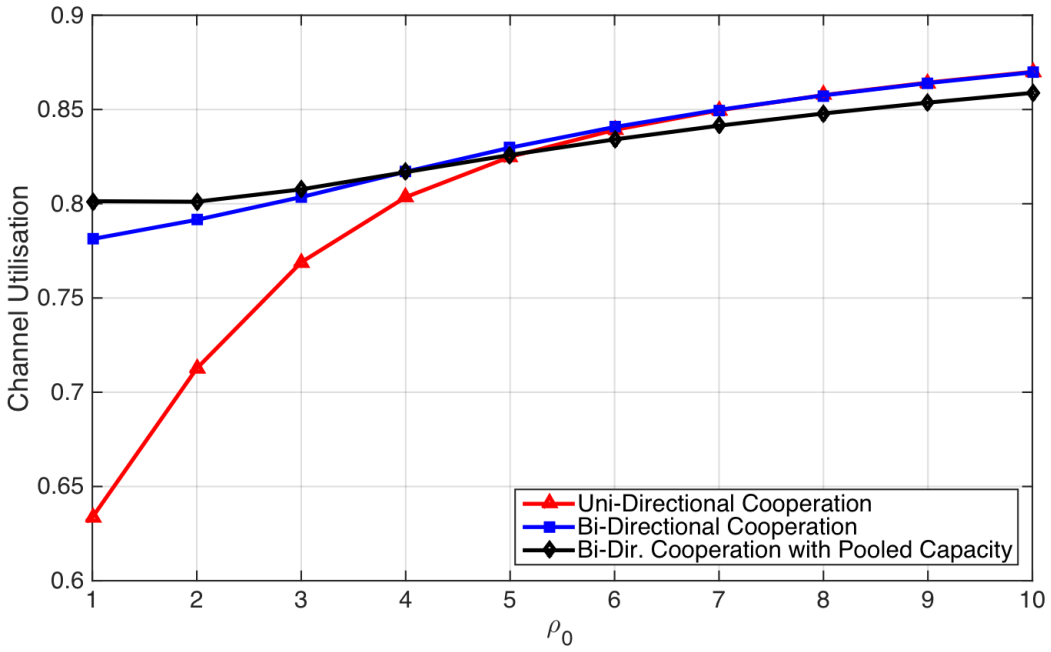

FIGURE 5.8: Comparison of channel utilisation for the secondary operator using the proposed models with $\rho_0 = 1:10$.

probability one could see that Model B provides the network with the highest spectrum utilisation at 92.6%.

TABLE 5.2: Configurations used in Figure 5.8

	Number of channels					Traffic intensity			
Model	SNO	PNO 1	PNO 2	PNO 3	Pooled Capacity	SNO	PNO 1	PNO 2	PNO 3
Model A	3	3	3	3	−−	1 : 10	4	4	4
Model B	3	3	3	3	−−	1 : 10	4	4	4
Model C	3	2	2	2	4	1 : 10	4	4	4

5.5 Summary

Spectrum sharing in cellular networks has received much attention in recent years due to its efficiency in spectrum utilisation and capability to improve the grade of service to subscribers. The efficiency is defined by spectrum utilisation as the

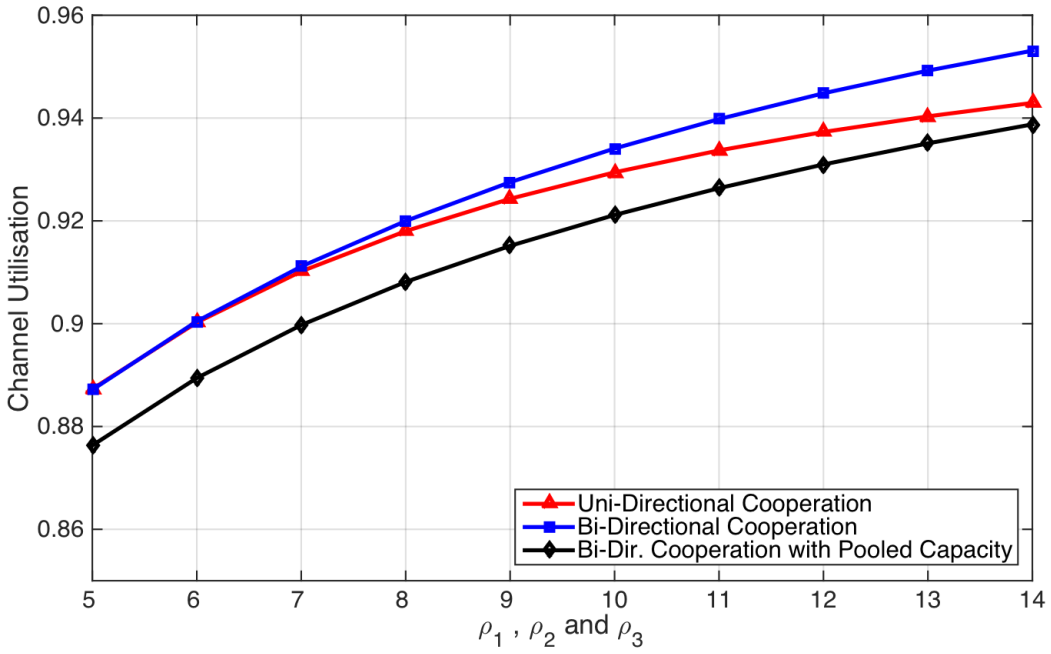

FIGURE 5.9: Comparison of channel utilisation for the secondary operator using the proposed models with ρ_1, ρ_2 and $\rho_3 = 1 : 10$.

ratio of the average number of busy channels and the overall available number of channels in the network while the grade of service is defined by the blocking probability. In this chapter we have presented three different models for dynamic spectrum sharing management in multi-operator cellular networks, operating with different spectrum holdings. Each model is defined by its own terms of sharing and interactions among the operators. The models represent the expected practical implementations of the next generation of cellular wireless networks. For each of the proposed models we have derived the blocking probability of the individual operators and spectrum utilisation to quantify and analyse the benefits of the proposed models. The formulation of the models applies whether the operators adopts FDM, TDMA, W-CDMA or TD-CDMA radio technologies. In addition, the models apply to the downlink as well as the uplink. The analysis provides a way to quantify the benefits to operators when they adopt spectrum sharing.

Chapter 6

Dynamic spectrum sharing optimisation and post-optimisation analysis

6.1 Introduction

It has been noted in the many research papers that the current static spectrum management must give way to a new approach that breaks down artificial spectrum access barriers and enables networks and their subscribers to dynamically access the spectrum [10, 130, 134]. As a response, for example, in the UK there are plans for spectrum liberalisation between operators with different spectrum holdings [131]. Liberalisation of spectrum of the incumbent holders and mandatory spectrum release may lead to some spectrum being under the control of a third party for secondary use. It is also possible that the spectrum might be redistributed not only because of such a mandate and realisation but also as a result of secondary market trading [99, 135, 136, 36]. Secondary trading of spectrum enhances the overall spectrum utilisation. As a result, network operators would be allowed to release their under-utilised commodities to potential operators [137, 138, 139, 140].

With the large number of service providers in the mobile cellular network industry, each with their own policy and strategy, a variety of spectrum opportunities could be available for secondary use. To this end, in order to distinguish between options of different bandwidth opportunities, incumbent holders of spectrum licenses may broadcast information in relation to these available bandwidths for possible leasing to secondary operators [141]. Part of the information broadcast by the spectrum holders are in the form of available spectrum size, location boundaries, maximum allowable transmit power, duration of the lease, type of band and admission cost [96, 1, 142].

Operators aim to provide a stable grade of service (GoS) to their end users with their limited allocated spectrum. However, in high demand periods, operators would require additional spectrum. A solution to increase the spectrum by means of sharing has been addressed in the research domain [21, 22, 23]. Spectrum sharing between operators often results in a significant improvement of GoS, although it would incur additional costs to the operators [24]. Since network operators often operate with a limited budget, the borrowing decisions of a network operator would be affected. Consequently, the operators would need to make dynamic, on-demand and correct choices of borrowing additional bandwidths from other operators.

Given a market scenario with several operators, rules and conditions of spectrum access, spectrum requirement and their prices, and other parameters, our main idea is to optimise the resource sharing under a target GoS and budget restriction. We propose two algorithms: the first is to optimise the amount of savings that secondary operator could achieve when they engage in spectrum trading with primary operators (incumbent holders of spectrum licenses) to gain a certain threshold of GoS. Second is to optimise the profit of secondary operator under budget restrictions. However, due to the mutual spectrum sharing agreement between the operators, the targeted GoS cannot be always guaranteed. Therefore, a post-optimisation analysis is needed to calculate the actual GoS in terms of blocking probability. Hence, we derive the blocking probability formulae under a

mutual agreement to share spectrum where the leased spectrum bandwidth may be claimed back by the primary operators according to the operators internal demand. We allow operators to dynamically access or handover part of the shared spectrum according to their internal demand state.

The chapter is organised as follows: the proposed dynamic spectrum management model is described in Section 6.2. Section 6.3 addresses the problem of spectrum allocation in cellular networks and describes our mathematical programming formulations to the problem. Section 6.3.8, presents blocking probability analysis under resource sharing with multiple PNOs. In Section 6.4, we present our findings. Finally, Section 6.5 summarises our conclusions.

6.2 Dynamic spectrum management model

We consider a cellular network to consists of S secondary network operators (SNOs) and $\mathcal{N}$, with size $|\mathcal{N}| = N$, denote the set of primary network operators (PNOs) serving a region $\mathcal{R}$, see Figure 6.1. Let $\mathcal{L}$, with size $|\mathcal{L}| = L$, be the set of cells in the region.

Each operator in the network is licensed with an incumbent bandwidth consisting of a set of component carriers, each of which can be allocated to support the operators' subscribers. The antenna towers/masts at the centre of each cell $i \in \mathcal{L}$ are shared among the operators. In the context of this cellular networks arrangement, we only consider cells with an almost identical radio environment, which is visible to all providers in each cell. An example of this setup is when a town or city requires operators to use common towers for their antennas, due to the economy of scale property of telecommunication industry.

Due to spectrum liberalisation, the PNOs $|\mathcal{N}|$ will have the freedom to lease their spectrum bandwidths to the SNO. Leasing spectrum bandwidths would mean that the secondary operator will have to pay a certain compensation to the primary

operator for using the spectrum bandwidths, and naturally the amount of compensation is expected to be proportional to the amount of allowed spectrum leasing by the primary system. We assume that the compensation paid to the PNO is in form of monetary value. The PNOs broadcast specific information about their available bands for leasing and admission cost (per unit bandwidth) at each cell $i \in \mathcal{L}$ at fixed identical intervals (e.g., every 2 hours). The lease conditions may specify additional parameters such as the extent of spatial region for spectrum use and maximum power. The compliant use of leased spectrum requires that the SNO returns the spectrum to the PNO at the end of the lease interval. The duration of each lease could be decided by the network providers under a mutual agreement, and/or any other regulatory bodies' conditions (e.g., minutes, hours, days).

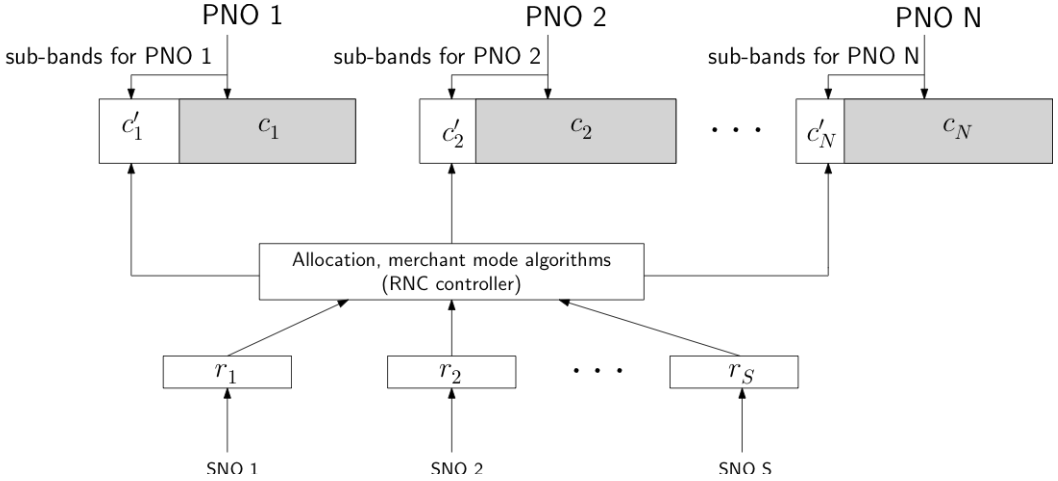

FIGURE 6.1: Network model for cellular network with N PNOs and S SNOs

6.2.1 Spectrum trading

We consider a spectrum market based on the *merchant mode* where PNOs independently determine the size of the available spectrum for lease along with the associated monetary value. The price of the available primary spectrum can be determined by estimating the utilisation and demand in time and space [143].

The available number of channels and the associated prices are then advertised according to a *take-it or leave-it* policy and channels are assigned on a first-come, first-served basis. No negotiation or bidding is conducted among network operators. *Merchant mode* is appropriate when the demand from the SNO is less than the available spectrum [10]. For analytical purposes, in the analysis section we have evaluated the proposed algorithms even for the case where the demand is higher than the available spectrum, but only in a fraction of the controlled cells.

6.2.2 Service type and channel characteristics

New technologies such as the Universal Mobile Telecommunications System (UMTS) and Long Term Evolution (LTE) have made possible a number of new services. In addition to the voice telephone service with good speech quality, these include in particular multimedia data services based on the Internet Protocol. In this system model, secondary and primary network operators are assumed to support M types of services, with $|\mathcal{M}| = M$ denotes the set of supported services. This is a realistic assumption in today's and future wireless cellular networks, where most network operators can only support one service in a single location. For simplicity, we consider all operators to support the same number of services, e.g., $M = 3$. The cells $|\mathcal{L}|$ in region $\mathcal{R}$ are categorised by their type of supported service, which represents the operating bandwidth range. As such, the SNO at cell i that support service j, may only borrow spectrum bandwidths from other operators, which support the same service category in the respective cell. Each PNO $k \in |\mathcal{N}|$ with services of type j has the same channel size (e.g. 200 KHz).

The users which belong to the SNO are assumed to be capable of transmitting and receiving over any spectrum band borrowed from the PNOs. This could be achieved using non-contiguous OFDM technology [144]. The default cellular networking rule is that the users of a particular cell are restricted to access bandwidth

allocated for the same cell. However, in resource sharing scenarios, the rule is relaxed, enabling the users to access the borrowed channels, which are acquired for that cell by the Radio Network Controller (RNC). Borrowed channels are only used by the SNOs in one cell which implies that spectrum spatial re-use is not allowed in this work. The borrowed bandwidth is essentially to gain the rights to use the spectrum bandwidth temporarily and spatially. The SNOs are not allowed to use the spectrum bands which is borrowed in one cell for use in another cell to eliminate possible interference.

6.2.3 Spectrum request processing

The SNO will continue to own their licensed spectrum and operate their existing networks unaffected. However, they can utilise new spectrum bandwidths, which can be dynamically obtained and configured from PNOs bands. The sharing process begins when heavily loaded cells request additional resources from a lightly or moderately loaded resource supply owned by the PNOs. This enables the SNOs to enhance their bandwidth access and translate such spectrum sharing into cost savings, which otherwise would need to split existing cells into smaller cells.

The SNO have temporal and spatial spectrum demand from their respective users, which arrive according to a Poisson process with potential rate $\lambda_{i_j} \forall i, j \in |\mathcal{L}|$ and $|\mathcal{M}|$, respectively. At each cell i in the operating area, the expected demand λ_i at the SNO (e.g. for calls, video calls and mobile data applications) requires dedicated channels. Inter-arrival times of a given cell is assumed to be independent of other cells. However, during high demand periods for particular cells, SNO suffers GoS degradation, where the blocking probability is high. In such periods, the SNO opportunistically attempts to minimise its blocking probability to a certain target value (e.g. 0.01). This requirement determines the spectrum resources (e.g. number of orthogonal channels) for all $i \in |\mathcal{L}|$ have certain GoS to the end users.

To obtain a suitable bandwidth that fulfils the necessary GoS, the SNO aims to borrow spectrum channels from PNOs, which share the same cell. The SNO pays the PNO(s) admission fees for the spectrum resource access per unit bandwidth, for a predetermined interval of time. A secondary operator can borrow frequency spectrum from the set of primary operators $|\mathcal{N}|$ simultaneously or in short succession. The available spectrum channels and the associated admission cost can be viewed as a function of cell index (location), type of band, incumbent network operator and time. Typically, the admission cost is proportional to the number of the operator's own occupied channels, however, for simplicity in this paper we model this process as a discrete random variable with non-negative real values. The PNOs announce their available spectrum size and the associated admission costs. Such information is advertised at the beginning of each trading window. The PNOs periodically determine the maximum available spectrum for release and the associated cell location. However, in this system model we do not set a minimum release requirement, also called relaxed release threshold, which enables the SNO to borrow the appropriate spectrum size without the need for over-borrowing. This further increases the efficiency of spectrum borrowing. The available spectrum bandwidth is modelled as a discrete with non-negative integer values. Spectrum demand can be obtained by using a predictive model based on historical traffic measurements or from expected subscribers' bandwidth inputs. The spectrum demand is used to generate acquisitions for various combination of channels from the PNOs. SNO determines the selection of bandwidths depending on the objectives of the network and the resources available. Allocation and de-allocation of spectrum is done at fixed intervals, allowing the network to predict transitions and permit higher level protocols to adapt to a certain connectivity disruptions [10].

Once the leased spectrum is active and operational, users, who are subscribed to the respective SNO cells recognise the borrowed bandwidth as part of their respective network resources and are allowed to operate over the newly borrowed

spectrum for the entire duration of the lease. The duration of each lease could be decided by the network providers (e.g., minutes, hours, days).

6.3 Problem formulation

Considering the system model described in Section 6.2, the problem now becomes how the RNC of an SNO acquires additional spectrum from the PNOs. The spectrum borrowing can be performed by considering one of the following objectives:

- to minimise borrowing cost in each time slot by selecting the lowest cost combinations of available spectrum from the primary networks to achieve a specified GoS and
- to maximise profit in each time slot by borrowing the highest profit combinations of available spectrum from the primary networks under restricted budget to achieve a specified GoS.

In principle, the RNC's objective is to minimise overall operating cost or to maximize revenue for an SNO as well as to maximize utility to the end users.

6.3.1 Modelling assumptions

In this subsection we identify the part of network information which is assumed to be known to the SNOs:

- arrival rate of the sth SNO at ith cell for jth type of spectrum band $\lambda_{si_j},\ \forall s, i, j,$
- service rate of the sth SNO at ith cell for jth type of spectrum band $\mu_{si_j},\ \forall s, i, j,$

- available bandwidth of the sth SNO at ith cell for jth type of spectrum band $w_{si_j},\ \forall s, i, j$,
- borrowing cost of the sth SNO for unit bandwidth from the PNOs at ith cell for jth type of spectrum band $c_{i_jk},\ \forall i, j, k$ (which are assumed to be announced periodically by the PNOs),
- allocated budget for borrowing bandwidths to the sth SNO at ith cell for jth type of spectrum band from the PNOs $b_{si_j},\ \forall s, i, j$, and
- available bandwidth of the kth PNO at ith cell for jth type of spectrum band $a_{i_jk},\ \forall i, j, k$, (which are assumed to be announced periodically by the PNOs).

Time is divided into equal-length slots $\mathcal{T} = \{0, 1, 2, \ldots\}$. At each time slot $t \in \mathcal{T}$ the process of aggregated channel borrowing is repeated. We use the time indicator (t) to emphasise the vector's dependency on time. Trading of bandwidth is done between primary and secondary providers separately in each of successive time windows of a particular duration. Henceforth, we focus on the process of channel borrowing and optimisation in a single window.

6.3.2 Notations used in Problem 1 and Problem 2:

Let us define the following quantities which are used later in the mathematical the programming problems (*Problem 1* and *Problem 2*):

$c_{i_jk}(t) :=$ cost of unit bandwidth to be borrowed from the kth PNO for the j type spectrum bandwidth at the ith cell during time interval t, where $c_{i_jk}(t) \in \mathbb{R}_{\geq 0}^{L \times N_{i_j}}$ $\big(c_{i_jk}(t) > 0\big)$ and N_{i_j} is the number of PNOs in the ith cell for the jth type of spectrum bandwidth and L is the number of cells in the region $\mathcal{R}$.

$x_{i_jk}(t) \coloneqq$ unit of spectrum bandwidths (or sub-bands) to be borrowed from the kth PNO for the j type of spectrum bandwidth at the ith cell during time interval t, where $x_{i_jk}(t) \in \mathbb{R}_{\geq 0}^{L \times N_{i_j}}$.

$\theta_{i_jk}(t) \coloneqq$ intrinsic quality of the PNOs' spectrum (e.g. the extent of the coverage area and/or maximum allowable transmit power), where $\{\theta_{i_j1}, \theta_{i_j2}, \ldots, \theta_{i_jk}, \ldots, \theta_{L \times N}\}$.

$p_{si_j}(t) \coloneqq$ target blocking probability for the j type of spectrum bandwidth at the ith cell during time interval t for the secondary network operator.

$a_{i_jk}(t) \coloneqq$ unit bandwidth available from the kth PNO to be leased to the sth SNO for the jth type of spectrum bandwidth at the the ith cell during time interval t, where $a_{i_jk}(t) \in \mathbb{R}_{\geq 0}^{L \times N_{i_j}}$.

$r_{si_j}(t) \coloneqq$ unit bandwidth required to satisfy the target blocking probability $p_{i_j}(t)$ for the the sth SNO for the jth type of spectrum bandwidth at the ith cell during time interval t, where $r_{i_j}(t) \in \mathbb{R}_{\geq 0}^{L}$.

$\gamma_{i_jk}(t) \coloneqq$ the expected profit for the borrowing unit bandwidth from the kth PNO for the jth type of spectrum bandwidth at the ith cell during time interval t, where $\gamma_{i_jk}(t) \in \mathbb{R}^{L \times N_{i_j}}$.

6.3.3 Spectrum allocation by minimising borrowing cost

We now formulate the spectrum allocation problem, that is, how much spectrum bandwidths to be borrowed from each PNO to keep the blocking probability at a specific level, for instance, at 1%. Given a set of possible available spectrum resources $\{a_{i_jk}(t)\}$ and their associated prices $\{c_{i_jk}(t)\}$, the problem is to find the feasible set of spectrum bandwidths $\{x_{i_jk}(t)\}$ by minimising the total borrowing cost. The PNOs set their prices according to the maximum allowed transmit power

$\varpi_{i_j k}$ and the pricing coefficient $\varphi_{i_j k}$, which can be expressed as [24]

$$c_{i_j k} = \left(\sum_{k \in a_{i_j k}} \left[\log \left(1 + \frac{h_{i_j}\, \varpi_{i_j k}}{\varrho_i} \right) - (\varpi_{i_j k} \cdot \varphi_{i_j k}) \right] \right) \cdot (a_{i_j k})^{-1} \tag{6.1}$$

where h_{i_j} is the average aggregated channel gain for the ith cell and jth type of spectrum bandwidth, ϱ_i is the additive noise received by SNO users at cell i and $\varphi_{i_j k}$ represents pricing coefficient of PNO k for the SNO in the ith cell for causing each unit of interference. Equation (6.1) shows that PNOs select prices in a way such that the collective preference order of transmit power, channel gain and noise are retained. This cancels the intuition that prices are selected so that all channels available for borrowing are equally preferable to a secondary. In addition, each PNO incurs a minimum cost $X_{(min)}$ when it leases its channel to the SNOs and therefore it is not possible to select a price lower than $X_{(min)}$ such that

$$c_{i_j k} = \begin{cases} \text{RHS of Eq. (6.1)}, & \text{RHS of Eq. (6.1)} \geq X_{(min)} \\ X_{(min)}, & \text{otherwise.} \end{cases} \tag{6.2}$$

Resource acquisition in this case for the sth SNO is obtained by solving the following optimisation problem:

Problem 1:

$$\text{minimise} \left[\sum_{i_j=1}^{L} \sum_{k=1}^{N_{i_j}} c_{i_j k}(t) \cdot x_{i_j k}(t) \cdot \theta_{i_j k}(t) \right], \tag{6.3}$$

subject to

$$\arg\min_{x_{i_jk}\forall i,j,k} \Pr\left(\lambda_{si_j}(t), \mu_{si_j}(t), \omega_{si_j}\right) \leq p_{si_j}(t), \quad \forall s, i_j, k \tag{6.4}$$

$$x_{i_jk}(t) \leq a_{i_jk}(t), \quad \forall i_j, k \tag{6.5}$$

$$\sum_{k=1}^{N_{i_j}} x_{i_jk}(t) \leq r_{si_j}(t), \quad \forall s, i_j, k \tag{6.6}$$

where $\omega_{si_j} = \sum_{k=1}^{N_{i_j}} x_{i_jk}(t) + w_{si_j}$ is the total bandwidth (available and borrowed bandwidth from the PNOs). In contrast to the formulation of *Problem 1*, borrowing cost for each cell i can be calculated as $\sum_{k=1}^{N_{i_j}} c_{i_jk}(t) \cdot x_{i_jk}(t) \cdot \theta_{i_jk}(t)$. The parameter $\theta_{i_jk}(t)$ $(0 \leq \theta_{i_jk}(t) \leq 1)$ defines the intrinsic quality by weighing the cost of borrowing spectrum bandwidths. The intrinsic quality represents the quality of the available heterogeneous aggregated channels to carry the data for transmission. Therefore, the price per unit bandwidth in each PNO can vary, i.e., $c_{i_jk}(t) \lesseqgtr c_{i_jl}(t)$, $\forall i_j$ and $\forall k, l$ with $k \neq l$. We thus refer to this pricing scheme as *non-uniform pricing*.

The constraint (6.4) in *Problem 1* guarantees that the sth SNO is borrowing enough to fulfil its demand. The blocking probability in constraint (6.4) is a non-linear function of spectrum bandwidth for each cell. Therefore, the above optimisation problem is considered as a non-linear optimisation, which can be solved in two phases:

- ***Phase 1:*** *Stochastic modelling*

  In this phase the SNOs set the target blocking probability for each cell (e.g., $p_{si_j} = 0.01,\ \forall i_j$). Then SNOs calculates the bandwidth $r_{si_j}(t)$ required to achieve the target blocking probability $p_{si_j}(t)$ for each cell i. Next the SNO finds the amount of bandwidth required to borrow from primary networks. We assume that the channel request rates and service rates follow Markov processes (i.e., inter-arrival and service times are exponential) for all PNOs and SNOs. A channel request is immediately lost if it finds the system busy,

which implies that networks operate independently in a non-cooperative way. This is referred to as an Erlang loss system [100, 129]. Loss system is the key modelling approach in wireless telecommunication networks and blocking probability is the main performance measure to study the blocking behaviour of traffic such as voice and live video streaming. Voice and multimedia in wireless networks are arguably the highest experienced traffic demand by operators. Such real-time (elastic) traffic is modelled using a loss system as opposed to delay (buffered) system and hence it is used in this paper. Under a loss system the well-known blocking probability for the jth type of spectrum bandwidth at the ith cell of the sth SNO can be given by the Erlang B formula as

$$p_{si_j}(t) = \frac{1}{w_{si_j}!}\left(\frac{\lambda_{si_j}(t)}{\mu_{si_j}(t)}\right)^{w_{si_j}} \left[\sum_{n=0}^{w_{si_j}} \frac{1}{n!}\left(\frac{\lambda_{si_j}(t)}{\mu_{si_j}(t)}\right)^{n}\right]^{-1}. \tag{6.7}$$

where $\lambda_{si_j}(t), \mu_{si_j}(t)$ and w_{si_j} are arrival rate, service rate and existing capacity of the sth SNO, respectively. Note that during the post-optimisation analysis new blocking probability formula are developed to accommodate sharing and interaction between operators in Section 6.3.8

Now with the existing bandwidth w_{si_j}, we first calculate the total required bandwidth $\tau_{si_j}(t)$ to achieve the target blocking probability for the ith cell of the SNO

$$\tau_{si_j}(t) = f^{-1}\left(\Pr\left(\lambda_{si_j}(t), \mu_{si_j}(t), w_{si_j}\right)\right). \tag{6.8}$$

where $f^{-1}(\cdot)$ is the inverse function of $P_{(b)}(t)$ (equation 6.7) used to derive the required capacity over the existing capacity. As the function is non-linear in $\lambda_{si_j}(t)$, $\mu_{si_j}(t)$ and $\tau_{si_j}(t)$, it is not easy to get an explicit expression for $\tau_{si_j}(t)$ for a given target blocking probability. However, it is possible to calculate $\tau_{si_j}(t)$ iteratively for given values of $\lambda_{si_j}(t)$, $\mu_{si_j}(t)$ and a target blocking probability $p_{si_j}(t)$. Subtracting the existing bandwidth w_{si_j} from

the total required $\tau_{si_j}(t)$, we obtain the required bandwidth $r_{si_j}(t)$ at the ith cell of the SNO during time interval t

$$r_{si_j}(t) = \tau_{si_j}(t) - w_{si_j}. \tag{6.9}$$

Now the problem is to find the feasible set of bandwidth $x_{i_jk}(t)$ from the PNOs which minimises the borrowing cost. This is done in the next mathematical programming phase.

- ***Phase 2:*** *Mathematical programming*

  In this phase, we set up the borrowing cost $c_{i_jk}(t)$ and the maximum possible bandwidth available $a_{i_jk}(t)$. The borrowing decisions of the SNO are made subject to the lowest price from the set $\{a_{i_jk}(t)\}$. The decision variable $x_{i_jk}(t)$ in this context can be a combination of a number of acquisitions, e.g., SNO selects the lowest price from the available set of bandwidths from the PNOs. If the acquired resources $a_{i_jk}(t)$ are insufficient to reach the target blocking probability $p_{i_j}(t)$ (i.e., $r_{i_jk}(t) - a_{i_jk}(t) > 0$), then the SNO borrows from the remaining bandwidths from the set $a_{i_jk}(t) \notin \{a_{i_j1}(t), a_{i_j2}(t), \ldots, a_{i_jN}(t)\}$ for which the cost is minimum. If the required blocking probability $p_{i_j}(t)$ is reached, then the SNO stops acquiring new spectrum bandwidths until the next time interval $(t+1)$.

Once the problem is solved, the new blocking probability for the sth SNO can be calculated as

$$\begin{aligned} P_{(b_{si_j}^{new})}(t) &= \Pr\left(\lambda_{si_j}(t), \mu_{si_j}(t), \left(w_{si_j} + \sum_{k=1}^{N_{i_j}} x_{i_jk}(t)\right)\right) \\ &= \frac{1}{\omega_{si_j}!}\left(\frac{\lambda_{si_j}(t)}{\mu_{si_j}(t)}\right)^{\omega_{si_j}} \left[\sum_{n=0}^{\omega_{si_j}} \frac{1}{n!}\left(\frac{\lambda_{si_j}(t)}{\mu_{si_j}(t)}\right)^{n}\right]^{-1}, \end{aligned} \tag{6.10}$$

where

$$\omega_{si_j} = w_{si_j} + \sum_{k=1}^{N_{i_j}} x_{i_jk}(t). \tag{6.11}$$

Consequently, the sth SNO will achieve the blocking probability with the required amount of bandwidths satisfying the target blocking probability $p_{si_j}(t)$ or with the highest possible borrowed bandwidths which is mathematically expressed as

$$P_{(b_{si_j}^{new})}(t) = \begin{cases} p_{si_j}(t), & \sum_{k=1}^{N_{i_j}} a_{i_jk}(t) \geq r_{si_j}(t) \\ P_{(b_{si_j}^{new})}(t), & \text{otherwise.} \end{cases} \tag{6.12}$$

Algorithm 6.1 Optimal spectrum borrowing

1: **Initialisation**: Number of cells in the network = L, number of operators in the network = N and number of types of spectrum bands = M.
2: Calculate $r_{i_j}\ \forall i, j$ which satisfies p_{i_j}, and get c_{i_jk} and $a_{i_jk}\ \forall i, j, k$.
3: **for** every time slot (t) **do**
4: **for** all cells $i \leftarrow 1 : L$ **do**
5: **for** all PNOs $k = 1 : N$ **do**
6: Solve the nonlinear stochastic *Problem 1* s.t. constraints (6.4), (6.5) and (6.6)
7: **end for**
8: **end for**
9: **end for**
10: **return**

6.3.4 Spectrum allocation using the heuristic algorithm

In this approach, spectrum acquisition is performed randomly as illustrated in Algorithm 6.2. The optimal borrowing cost using this algorithm can only be found randomly from the set of capacity values a_{i_jk} by satisfying the constraints in equation (6.5) and (6.6).

Algorithm 6.2 Heuristic spectrum borrowing

Initialisation: Number of cells in the network = L, number of operators in the network = N and number of types of spectrum bands = M.
Calculate $r_{i_j}\ \forall i, j$ which satisfies p_{i_j}, and get c_{i_jk} and $a_{i_jk}\ \forall i, j, k$.
for every time slot (t) **do**
    for all cells $i \leftarrow 1 : L$ **do**
        Set $x_{i_jk} \leftarrow \{\phi\}$, where $\{\phi\}$ is an empty set.
        Set counter $\leftarrow \sum_k x_{i_jk}$.
        Choose a random integer $n \in \{1, 2, \ldots, N\}$.
        for all PNOs $k = n : N \quad 1 : (n-1)$ **do**
            if $0 < a_{i_jk} > (r_{i_j} - \text{counter})$ **then**
                $x_{i_jk} \leftarrow (r_{i_j} - \text{counter})$.
                BREAK
            else if $a_{i_jk} > 0$ & counter $< r_{i_j}$ **then**
                $x_{i_jk} \leftarrow a_{i_jk}$.
                counter $\leftarrow$ counter $+ x_{i_jk}$.
            else
                $x_{i_jk} \leftarrow 0$.
            end if
        end for
    end for
end for
return

For all i, j and k, equation (6.6) ensures that the SNO does not borrow more than the network's bandwidths demand by controlling the borrowed spectrum bandwidth size in each iteration, which can be expressed mathematically as

$$x_{i_jk}(t) = \begin{cases} a_{i_jk}(t), & r_{i_j}(t) \geq a_{i_jk}(t) \\ r_{si_j}(t), & \text{otherwise.} \end{cases} \tag{6.13}$$

This scenario can also be regarded as round-robin scheduling algorithm, where SNOs randomly gain access to the PNOs' available spectrum, and the PNOs serve one SNO in each turn. The resource allocation in algorithm 6.2 evolves in two main discrete steps:

- compute the spectrum demand in each cell r_{i_j}, $\forall i, j$ from equation (6.9)
- randomly obtain x_{i_jk} subject to equations (6.5) and (6.6) from the vector a_{i_jk}

In the heuristic formulation, the cost of spectrum access is not considered, where spectrum acquisition is performed randomly from the set $\{a_{i_jk}\}$. Note that when $\sum a_{i_jk} \leq r_{i_j}$ the feasible set $\{x_{i_jk}\}$ is equal for both formulations. We also note that when $\sum_{k=1}^{N_{i_j}} a_{i_jk}(t) > r_{i_j}(t)$, the optimal and heuristic algorithm may achieve the same outcome in terms of total borrowing cost, however, this is a result of randomness in the selection process with probability

$$P(\text{selecting optimal bandwidths}) \quad = \begin{cases} \dfrac{1}{N} & a_{i_jk} \geq r_{i_j}, \forall i_j \\ \dfrac{1}{\left|\{\bar{a}_{i_j}..\}\right|} & \sum_m \{\bar{a}_{i_jlm},\ \forall l, m\} \geq r_{i_j}, \forall i_j \\ 1 & \sum_{k=1}^{N_{i_j}} a_{i_jk} \leq r_{i_j}, \forall i_j \end{cases} \tag{6.14}$$

where $\{\bar{a}_{i_jlm},\ \forall l, m\} \subset \{a_{i_jk,\,\forall i_j,\,k}\}$, and $\left|\{\bar{a}_{i_j}..\}\right|$ is the number of subsets in the set $\{\bar{a}_{i_j}..\}$ which satisfy the bandwidth requirement for the ith cell with the jth type of spectrum band.

Remark 6.1. In *Problem 1*, the objective function and all constraints are linear except for the constraint (6.4). Once we calculate the required bandwidth for the ith cell using the non-linear constraint (6.4) iteratively we then solve the optimization Problem 1 using Algorithm 6.1. With the remaining constraints the optimization problem is solved by the well-known revised simplex method. However, the computational complexity in Algorithm 6.1 is polynomial time, i.e. $O(n)$ time. The computational time increases linearly with number of cells and number of PNOs. The heuristic counterpart, Algorithm 6.2, arbitrarily borrows bandwidths from the PNOs until the target blocking probability of the SNO is achieved. Since the algorithm finds a solution by performing a combinatorics satisfying a set of constraints, the computational complexity is quadratic time, i.e. $O(n^2)$ with number of PNOs (N) and exponential time, i.e. 2^n with number of cells (L). Note that the Algorithm 6.2 does not guarantee the optimal solution and the probability of finding an optimal solution by the heuristic algorithm is given in equation (6.14).

6.3.5 Expected profit maximisation under a restricted budget

In this section, we formulate the second spectrum allocation problem that illustrates how much spectrum bandwidths is to be borrowed from each PNO to keep the blocking probability at a specific level. Given a set of possible available spectrum resources $\{a_{i_jk}(t)\}$, their associated prices $\{c_{i_jk}(t)\}$ and expected profit $\{\gamma_{i_jk}(t)\}$, the problem is to find the feasible set of spectrum bandwidths $\{x_{i_jk}(t)\}$ by maximising the total profit of the SNO, under an allocated budget and performing the selection according to the highest possible profit combination. Resource acquisition in this case is obtained by solving the following optimisation problem:

Problem 2:

$$\text{maximise} \left[\sum_{i=1}^{L} \sum_{j=1}^{M} \sum_{k=1}^{N_j} \gamma_{i_j k}(t) \cdot x_{i_j k}(t) \right] \tag{6.15}$$

subject to

$$\begin{aligned}
\underset{x_{i_j k} \forall i,j,k}{\arg\min} \Pr\left(\lambda_{si_j}(t), \mu_{si_j}(t), \omega_{si_j}\right) &\leq p_{si_j}(t), \quad \forall s, i_j, k && (6.16)\\
x_{i_j k}(t) &\leq a_{i_j k}(t), \quad \forall i_j, k && (6.17)\\
\sum_{k=1}^{N_{i_j}} x_{i_j k}(t) &\leq r_{si_j}(t), \quad \forall s, i_j, k && (6.18)\\
\sum_{k=1}^{N_{i_j}} c_{i_j k}(t) \cdot x_{i_j k}(t) &\leq b_{si_j}, \quad \forall s, i_j, k, && (6.19)
\end{aligned}$$

where $\gamma_{i_j k}(t)$ consists of two parts: the expected revenue $v_{i_j}(t)$ and cost $c_{i_j k}(t)$, which can be obtained as

$$\gamma_{i_j k}(t) = v_{i_j k}(t) - c_{i_j k}(t). \tag{6.20}$$

Here

$$v_{i_j k}(t) = f\left(\beta_{i_j}(t), \theta_{i_j k}(t)\right), \tag{6.21}$$

where $\beta_{i_j}(t)$ is the selling price per unit bandwidth for the ith cell and jth type service during time period t. In equation (6.21), the expected revenue $v_{i_j k}(t)$ is the function $f(\cdot)$ of the selling price $\beta_{i_j k}(t)$ and the intrinsic quality ($\theta_{i_j k}(t)$) which may take, in general, a non-linear form. In the simplest case, the function can be defined as

$$v_{i_j k}(t) = \beta_{i_j k}(t) \cdot \left[-e^{-\theta_{i_j k}(t)}\right]. \tag{6.22}$$

We consider the the intrinsic quality per unit bandwidth ($\theta_{i_j k}(t)$) for each PNO, which can vary, i.e., $\theta_{i_j k}(t) \lesseqgtr \theta_{i_j l}(t)$, $\forall\ i_j$ and $\forall\ k, l$ with $k \neq l$ according to the

spatial structure of the base stations, allowed transmission power, bandwith types, etc. In this problem formulation, the parameter $\theta_{i_jk}(t)$ influences the optimal spectrum borrowing decisions.

The revenue earned through the sale of the borrowed bandwidth can be equal, higher or lower than the cost. However, for simplicity, we model the revenue $v_{i_jk}(t)$ earned through the sale of the borrowed bandwidth to exceed the borrowing cost, i.e., $v_{i_jk}(t) > c_{i_jk}(t)$ due to the assumption that the profit of the SNO for borrowing a unit bandwidth is always positive.

The inequality constraint in equation (6.19) implies that the SNO maximises its profit by taking into account the limitations imposed by the cost of the utility and the maximum allowable expenditure which the SNO can spend for borrowing spectrum demand in each cell. Next, we solve the above non-linear optimisation problem in two phases:

- ***Phase 1:*** *Stochastic modelling*

  In the first phase, the same steps are performed using equation (6.16) as for solving Problem 1. The SNO calculates the spectrum demand to meet its time varying target blocking probability over time and location. The spectrum demand is adjusted dynamically based on the network information provided by the expected cell demand, service rate and existing spectrum bandwidth.

- ***Phase 2:*** *Mathematical programming*

  In the second phase, we set up the vectors $\{c_{i_jk}(t)\}$, $\{a_{i_jk}(t)\}$ and $\{\gamma_{i_jk}(t)\}$. The borrowing decisions of the SNO are made subject to achieving the maximum profit for each acquisition from the PNOs. In Problem 1, the budget restriction is not considered, where the SNO is allowed to make spectrum bandwidth borrowing until it meets the spectrum demand, i.e.,

$$\sum_{k=1}^{N_j} x_{i_j k}(t) = r_{i_j}(t), \text{ assuming } \sum_{k=1}^{N_j} a_{i_j k}(t) \geq r_{i_j}(t). \tag{6.23}$$

Algorithm 6.3 Optimal spectrum borrowing under restricted budget

1: **Initialisation**: Number of cells in the network = L, number of operators in the network = N and number of types of spectrum bands = M.
2: Calculate r_{i_j} $\forall i, j$ which satisfies p_{i_j}, and get $c_{i_j k}$, $a_{i_j k}$, $\gamma_{i_j k}$ and $\theta_{i_j k}(t)$ $\forall i, j, k$.
3: Set maximum allowed budget expenditure for every cell b_{i_j}.
4: **for** every time slot (t) **do**
5: **for** all cells $i \leftarrow 1 : L$ **do**
6: **for** all PNOs $k = 1 : N$ **do**
7: Solve the nonlinear stochastic *Problem 2* s.t. (6.16), (6.17), (6.18) and (6.19)
8: **end for**
9: **end for**
10: **end for**
11: **return**

However, in this formulation, the borrowing capacity of the SNO is restricted to budget allocation b_{i_j}. Note that in the case where the SNO's budget is too small to provide the required GoS, then Problem 2 is infeasible. The SNO only achieves a best effort service to minimise the blocking probability so far as the budget permits.

6.3.6 Spectrum allocation using the heuristic algorithm under budget constraint

In this subsection, we solve the problem of spectrum allocation under budget constraint by a heuristic bandwidth selection algorithm (Algorithm 6.4). The algorithm performs all the steps as in Algorithm 6.3. However, Algorithm 6.4 does not perform spectrum selection according to the highest possible profit combination from the set $\{a_{i_jk}\}$, rather runs on randomly selected combination from the set $\{a_{i_jk}\}$ to satisfy the spectrum demand r_{i_j}. The optimal profit using Algorithm 6.4 can only be found from the set of capacity values $\{a_{i_jk}\}$ satisfying the constraints in equation (6.17), (6.18) and (6.19) with probability given in equation (6.14). To satisfy the constraints in equation (6.17), (6.18) and (6.19) we use

$$x_{i_jk}(t) = \begin{cases} a_{i_jk}(t), & r_{si_j}(t) \geq a_{i_jk}(t),\ b_{si_j} \geq c_{i_jk}, \\ r_{si_j}(t), & r_{si_j}(t) < a_{i_jk}(t),\ b_{si_j} \geq c_{i_jk}, \\ 0, & b_{si_j} < c_{i_jk} \text{ or } r_{si_j}(t) = 0. \end{cases} \tag{6.24}$$

Algorithm 6.4 Heuristic spectrum borrowing under restricted budget

Initialisation: Number of cells in the network = L, number of operators in the network = N and number of types of spectrum bands = M.
Calculate r_{i_j} $\forall i, j$ which satisfies p_{i_j}, and get c_{i_jk}, a_{i_jk}, γ_{i_jk} and $\theta_{i_jk}(t)$ $\forall i, j, k$.
Set maximum allowed budget expenditure for every cell b_{i_j}.
for every time slot (t) **do**
    for all cells $i \leftarrow 1 : L$ **do**
        Set $x_{i_jk} \leftarrow \{\phi\}$, where $\{\phi\}$ is an empty set.
        Set counter $\leftarrow \sum_k x_{i_jk}$.
        Choose a random integer $n \in \{1, 2, \ldots, N\}$.
        for all PNOs $k = n : N$ and $1 : (n-1)$ **do**
            if $(0 < a_{i_jk}) \leq (r_{i_j} - \text{counter})$ & $(c_{i_jk} * a_{i_jk}) \leq b_{i_j}$ **then**
                $x_{i_jk} \leftarrow a_{i_jk}$.
                counter $\leftarrow$ counter $+ \sum x_{i_jk}$.
                $b_{i_j} \leftarrow b_{i_j} - \sum(x_{i_jk} * c_{i_jk})$.
            else if $(a_{i_jk} > 0)$ & $c_{i_jk} \leq (b_{i_j} - \text{counter})$ & $(a_{i_jk} * c_{i_jk}) \geq b_{i_j}$ **then**
                $x_{i_jk} \leftarrow \left\lfloor \frac{b_{i_j}}{c_{i_jk}} \right\rfloor$ where $\lfloor x \rfloor$ means the floor of x.
                counter $\leftarrow$ counter $+ \sum x_{i_jk}$.
                $b_{i_j} \leftarrow b_{i_j} - \sum x_{i_jk}. * c_{i_jk}$.
            else if counter $\leq r_{i_j}$ & $a_{i_jk} > 0$ & $a_{i_jk} \geq (r_{i_j} - \text{counter})$ & $(a_{i_jk} * c_{i_jk}) \leq b_{i_j}$ **then**
                $x_{i_jk} \leftarrow r_{i_j} - \text{counter}$.
                counter $\leftarrow$ counter $+ \sum x_{i_jk}$.
                $b_{i_j} \leftarrow b_{i_j} - \sum x_{i_jk}. * c_{i_jk}$.
                break
            else if counter $\leq r_{i_j}$ & $a_{i_jk} > 0$ & $a_{i_jk} \geq (r_{i_j} - \text{counter})$ & $(a_{i_jk} * c_{i_jk}) \geq b_{i_j}$ **then**
                $x_{i_jk} \leftarrow min\left\{\left\lfloor \frac{b_{i_j}}{c_{i_jk}} \right\rfloor\right\}$.
                counter $\leftarrow$ counter $+ \sum x_{i_jk}$.

Algorithm 6.4 (continued) Heuristic spectrum borrowing under restricted budget

$b_{i_j} \leftarrow b_{i_j} - \sum x_{i_j k} * c_{i_j k}$.
else if
then
$x_{i_j k} \leftarrow 0$.
end if
end for
end for
end for
return

Remark 6.2. Like *Problem 1*, in *Problem 2* we have the non-linear constraint which is solved iteratively and then the whole problem is solved by the revised simplex method. Therefore, Algorithm 6.3 is polynomial time and the heuristic counterpart (Algorithm 6.4) is again quadratic time/exponential time depending on number of cells and PNOs.

6.3.7 Spectrum demand-supply strategy

In general, due to large amount of cells and small borrowing time, SNOs will demand spectrum at different trade windows in different cells. However, when multiple SNOs demand spectrum at the same trade window t and the same cell i, the available spectrum is shared in a distributed manner between SNOs to ensure fairness in resource allocation. This can be accomplished by the following steps:

1. calculation of the required demand of each SNO in the network $\{r_{1i_j}(t,m), \ldots, r_{si_j}(t,m), \ldots, r_{Si_j}(t,m)\}$ where m indicates the iteration count and t represents the trade window,

2. calculation of the available spectrum by the following formula

$$a_{i_j k}(t, m) = \frac{a_{i_j k}(t, (m-1))}{\left[S(t) - g_{i_j}(t, m)\right]} \tag{6.25}$$

where $S(t)$ is the number of SNOs that demand resources at trade window t, and

$$g_{i_j}(t, m) = g_d(t, m-1) + g_b(t, m-1), \tag{6.26}$$

where $g_d(t, m-1)$ is the number of SNOs in the cell with satisfied bandwidth demands in the previous step and $g_b(t, m-1)$ is the number of SNOs which have reached the budget threshold (with $g_b(t, \cdot) = 0$ for optimization Problem 1),

3. optimization is performed by the SNOs to acquire resources from the PNOs, and

4. adjustment occurs on the allocation of spectrum bandwidths considering the supply from the PNOs and demand of the SNOs and repeated until all demand has been allocated.

Note that the proposed approach handles demands by giving equal access to the available channels to the secondary operators. This solution allows us to optimally allocate every spectrum in an on-line manner. The model which captures the competition between operators by evaluating competing bids has been addressed by several authors, for instance, Lin Gao et al. in [145] who used Vickrey-Clarke-Groves (VCG) auction which may yield an optimal solution.

6.3.8 Performance analysis under resource sharing between the SNO and PNOs

In the optimisation problems above, the PNOs lease part of their spectrum resources to the SNO for monetary benefits. The leasing and borrowing was based

on expected demand and available spectrum resources. However, the demand in the PNOs may change during trading window causing one or more of PNOs' state to change from the underloaded to overloaded and their blocking probability would increase. As a consequence, a PNO may react by deviating part or all of its leased spectrum resources under mutual agreement, which results in reducing the size of the shared spectrum resources. This dynamic mechanism affects the performance of all operators involved in the trading. The complexity of the problem depends primarily on the number of PNOs involved and the level of interactions between them. In this chapter we will consider three cases as follows:

6.3.8.1 Case 1: SNO is sharing with three PNOs

Consider a cell consisting of an SNO with capacity c_0 and three PNOs with capacity c_1, c_2 and c_3. Under a sharing agreement all three PNO share part of their resources c_1', c_2' and c_3', respectively with the SNO determined using the optimisation approach discussed in the previous sections. These resources may also be used by the corresponding PNO under mutual agreement. A state of this network is a vector

$$\mathbf{n} = (n_0, n_1, n_2, n_3, n_{01}, n_{02}, n_{03}, n_{11}, n_{22}, n_{33})$$

where n_i are the number of channel requests in progress in the secondary operator and primary operators $1, 2, 3$ respectively, $n_{0i}, i = 1, 2, 3$ are the number of channel requests in the shared resources of the ith primary operator from the secondary operator and $n_{ii}, i = 1, 2, 3$ are the number of calls of the ith primary operator on its own shared resources. The states $\mathbf{n}$ are restricted due to resource sharing constraints. The set of feasible states can be written as

$$\Omega_s = \{\mathbf{n} : A\mathbf{n} \leq \mathbf{s}\} \tag{6.27}$$

where A is a $d \times 10$ matrix, and $\mathbf{s}$ is a d-vector, where d is the number of constraints. The network topology is reflected in the matrix A, and the vector $\mathbf{s}$.

Let calls arrive to the secondary and ith primary operators according to a non-homogeneous Poisson process, with rates $\lambda(t)$ and $\lambda_i(t)$ at time t. These calls are admitted if $\mathbf{n} + \mathbf{e}_i \in \Omega_s$, where $\mathbf{e}_i$ is the ith unit vector with 1 in place i and 0 elsewhere. When all c_0 resources of the secondary operator is full then calls are diverted and admitted to the ith primary operator if $\mathbf{n} + \mathbf{e}_{0i} \in \Omega_s$, where $\mathbf{e}_{0i}$ is the ith unit vector. Similarly, being all c_i resources occupied calls are diverted to its shared resources c_i' for the ith primary network if $\mathbf{n} + \mathbf{e}_{ii} \in \Omega_s$, where $\mathbf{e}_{ii}$ is the ith unit vector. Assume that admitted calls in secondary and primary operators i have exponential holding times with rates $\mu(t)$ and $\mu_i(t)$ respectively at time t. Under these assumptions, the network can be modeled as a non-homogeneous continuous time Markov chain $\mathbf{X}(t) = (X_i(t), X_{0i}(t), X_{ii}(t);\ i = 1, 2, 3,\ t \geq 0)$ that records the number of channel requests in progress from all operators. The state space of the Markov chain is specified in (6.27), and its transition rates $\mathbf{Q}(t) = (q(\mathbf{n}, \mathbf{n}', t), \mathbf{n}, \mathbf{n}' \in \Omega_s)$ are given by

$$q(\mathbf{n}, \mathbf{n}', t) = \begin{cases} \lambda(t) & \mathbf{n}' = \mathbf{n} + \mathbf{e}_1 \ \text{ or } \ \mathbf{n}' = \mathbf{n} + \mathbf{e}_{0i}, \quad \text{if } \ n_0 = c_0,\ i = 1, 2, 3 \\ \lambda_i(t) & \mathbf{n}' = \mathbf{n} + \mathbf{e}_i \ \text{ or } \ \mathbf{n}' = \mathbf{n} + \mathbf{e}_{ii}, \quad \text{if } \ n_i = c_i,\ i = 1, 2, 3 \\ n\mu(t) & \mathbf{n}' = \mathbf{n} - \mathbf{e}_1 \\ n_i\mu_i(t) & \mathbf{n}' = \mathbf{n} - \mathbf{e}_i,\ i = 1, 2, 3 \\ n_{0i}\mu_i(t) & \mathbf{n}' = \mathbf{n} - \mathbf{e}_{0i},\ i = 1, 2, 3 \\ n_{ii}\mu_i(t) & \mathbf{n}' = \mathbf{n} - \mathbf{e}_{ii},\ i = 1, 2, 3 \\ 0 & \text{otherwise.} \end{cases} \tag{6.28}$$

Theorem 6.3. *The closed-form solution of* $\mathbf{n}$ *channel requests in progress at time* t *is given by equation (6.29).*

$$P(\mathbf{n},t) = \mathcal{K}^{-1}\frac{\left[\rho^{(n+n_{01}+n_{02}+n_{03})}(t)\right]\cdot\left[\rho_1^{(n_1+n_{11})}(t)\right]\cdot\left[\rho_2^{(n_2+n_{22})}(t)\right]\cdot\left[\rho_3^{(n_3+n_{33})}(t)\right]}{(n_0+n_{01}+n_{02}+n_{03})!\,(n_1+n_{11})!\,(n_2+n_{22})!\,(n_3+n_{33})!} \quad \forall\ \mathbf{n}\in\Omega_s \tag{6.29}$$

where $\mathcal{K}$ is the normalising constant and given by

$$\mathcal{K} = \sum_{\mathbf{n}\in\Omega_s}\frac{\left[\rho^{(n+n_{01}+n_{02}+n_{03})}(t)\right]\cdot\left[\rho_1^{(n_1+n_{11})}(t)\right]\cdot\left[\rho_2^{(n_2+n_{22})}(t)\right]\cdot\left[\rho_3^{(n_3+n_{33})}(t)\right]}{(n_0+n_{01}+n_{02}+n_{03})!\,(n_1+n_{11})!\,(n_2+n_{22})!\,(n_3+n_{33})!}. \tag{6.30}$$

Proof. Define the state probabilities

$$P(\mathbf{n},t) := Pr(X(t)=\mathbf{n}),\ \ \mathbf{n}\in\Omega_s,\ t\geq 0 \tag{6.31}$$

with initial condition $P_0(\mathbf{n}) = Pr(X(0)=\mathbf{n})$. Since the network has a finite state space, these probabilities are the unique solution of the Kolmogorov forward equations given in (6.32) for $\mathbf{n}\in\Omega_s, t>0$.

The Kolmogorov forward equations can be defined as

$$\frac{\mathrm{d}P(\mathbf{n},t)}{\mathrm{d}t} = \Bigg[\lambda(t)\cdot\left(\mathbb{1}(n_0 < c_0) + \mathbb{1}(n_0 = c_0 \cap_{i\in\{1,2,3\}} \mathbf{n} + \mathbf{e}_{0i})\right) + \sum_{i=1}^{3}\lambda_i(t)\cdot\left(\mathbb{1}(n_i < c_i)\right.$$
$$\left. + \mathbb{1}(n_i = c_i \cap \mathbf{n} - \mathbf{e}_{ii})\right)\Bigg]\cdot P\left((\mathbf{n}-\mathbf{e}_i),t\right) + (n+1)\mu(t)P\left((\mathbf{n}+\mathbf{e}_i),t\right)$$
$$+ \sum_{i=1}^{3}(n_{0i}+1)\mu_i(t)\cdot P(\mathbf{n}+\mathbf{e}_{0i}) - \Bigg[\lambda(t)\cdot\left(\mathbb{1}(n_0 < c_0) + \mathbb{1}(n_0 = c_0 \cap_{i\in\{1,2,3\}} \mathbf{n} + \mathbf{e}_{0i})\right)$$
$$+ \sum_{i=1}^{3}\lambda_i(t)\cdot\left(\mathbb{1}(n_i < c_i) + \mathbb{1}(n_i = c_i \cap \mathbf{n} - \mathbf{e}_{ii}) + n\mu(t) + \sum_{i=1}^{3} n_{0i}\mu_i(t)\right)\Bigg] P\left(\mathbf{n},t\right) \tag{6.32}$$

where $\mathbb{1}(A)$ is the indicator function for an event A.

Equations in (6.32) can be written in the operator form as given by

$$\frac{\mathrm{d}\mathbf{P}(t)}{\mathrm{d}t} = \mathbf{P}(t)\,\mathbf{Q}(t), \quad \mathbf{P}(0) = \mathbf{P}_0,\ t > 0 \tag{6.33}$$

where $\mathbf{P}(t)$ is the vector of probabilities $\mathbf{P}(\mathbf{n},t)$. The formal solution of the equation (6.33) is given by

$$\mathbf{P}(t) = \mathbf{P}_0\,E_Q(t), \quad t \geq 0 \tag{6.34}$$

where $E_Q(t)$ is the time-ordered exponential of the generator $\mathbf{Q}(t)$, that is the unique operator solution to the equation

$$\frac{\mathrm{d}E_Q(t)}{\mathrm{d}t} = E_Q(0)\,\mathbf{Q}(t), \quad t \geq 0 \tag{6.35}$$

where $E_Q(0) = \mathbf{I}$, the identity operator. The unique solution of the Kolmogorov forward equations (6.32) is then given by the equation (6.29). □

The blocking probability formula can then be derived from the closed-form solution (6.29). The blocking probability for an operator i (ith operator could be the SNO or a PNO), is then given by

$$\begin{aligned} P_{b_i}(t) &= \sum_{\mathbf{n}\in S_R} P(\mathbf{n},t) \\ &= \frac{\displaystyle\sum_{\mathbf{n}\in S_R} \frac{\left[\rho^{(n+n_{01}+n_{02}+n_{03})}(t)\right]\cdot\left[\rho_1^{(n_1+n_{11})}(t)\right]\cdot\left[\rho_2^{(n_2+n_{22})}(t)\right]\cdot\left[\rho_3^{(n_3+n_{33})}(t)\right]}{(n_0+n_{01}+n_{02}+n_{03})!\,(n_1+n_{11})!\,(n_2+n_{22})!\,(n_3+n_{33})!}}{\displaystyle\sum_{\mathbf{n}\in\Omega_s} \frac{\left[\rho^{(n+n_{01}+n_{02}+n_{03})}(t)\right]\cdot\left[\rho_1^{(n_1+n_{11})}(t)\right]\cdot\left[\rho_2^{(n_2+n_{22})}(t)\right]\cdot\left[\rho_3^{(n_3+n_{33})}(t)\right]}{(n_0+n_{01}+n_{02}+n_{03})!\,(n_1+n_{11})!\,(n_2+n_{22})!\,(n_3+n_{33})!}} \quad \forall\ \mathbf{n}\in\Omega_s \end{aligned} \tag{6.36}$$

where the set S_R is the restricted state space, and varies for the SNO and PNOs. For the SNO, it is defined as

$$S_R = \left\{\mathbf{n}\in\Omega_s \,|\, (n_0 = c_0 \cap n_{01}+n_{11} = c_1' \cap n_{02}+n_{22} = c_2' \cap n_{03}+n_{33} = c_3')\right\}, \tag{6.37}$$

and for the ith PNO, S_R can be replaced by S_i and defined as

$$S_i = \left\{\mathbf{n}\in\Omega_s \,|\, (n_i = c_i \cap n_{0i}+n_{ii} = c_i')\right\}, \quad i = 1,2,3. \tag{6.38}$$

6.3.8.2 Case 2: SNO is sharing with two PNOs

When two primary operators (1 and 2) are sharing with the SNO, the product form solution (6.29) takes the following form

$$P(\mathbf{n},t) = \mathcal{K}^{-1}\frac{\left[\rho^{(n+n_{01}+n_{02})}(t)\right]\cdot\left[\rho_1^{(n_1+n_{11})}(t)\right]\cdot\left[\rho_2^{(n_2+n_{22})}(t)\right]}{(n_0+n_{01}+n_{02})!\,(n_1+n_{11})!\,(n_2+n_{22})!}\ \ \forall\ \ \mathbf{n}\in\Omega_s \tag{6.39}$$

where

$$\mathcal{K} = \sum_{\mathbf{n}\in\Omega_s}\frac{\left[\rho^{(n+n_{01}+n_{02})}(t)\right]\cdot\left[\rho_1^{(n_1+n_{11})}(t)\right]\cdot\left[\rho_2^{(n_2+n_{22})}(t)\right]}{(n_0+n_{01}+n_{02})!\,(n_1+n_{11})!\,(n_2+n_{22})!}. \tag{6.40}$$

The blocking probability formula for the ith operator can be given by

$$P_{b_i}(t) = \sum_{\mathbf{n}\in S_R}P(\mathbf{n},t) = \frac{\displaystyle\sum_{\mathbf{n}\in S_R}\frac{\left[\rho^{(n+n_{01}+n_{02})}(t)\right]\cdot\left[\rho_1^{(n_1+n_{11})}(t)\right]\cdot\left[\rho_2^{(n_2+n_{22})}(t)\right]}{(n_0+n_{01}+n_{02})!\,(n_1+n_{11})!\,(n_2+n_{22})!}}{\displaystyle\sum_{\mathbf{n}\in\Omega_s}\frac{\left[\rho^{(n+n_{01}+n_{02})}(t)\right]\cdot\left[\rho_1^{(n_1+n_{11})}(t)\right]\cdot\left[\rho_2^{(n_2+n_{22})}(t)\right]}{(n_0+n_{01}+n_{02})!\,(n_1+n_{11})!\,(n_2+n_{22})!}}\ \ \forall\ \ \mathbf{n}\in\Omega_s \tag{6.41}$$

where the set S_R is again the restricted state space, and varies for the SNO and PNOs. For the SNO, it is defined as

$$S_R = \left\{\mathbf{n}\in\Omega_s\,|\,(n_0 = c_0\ \cap\ n_{01}+n_{11} = c_1'\ \cap\ n_{02}+n_{22} = c_2')\right\}, \tag{6.42}$$

and for the ith PNO, S_R can be replaced by S_i and defined as

$$S_i = \left\{\mathbf{n}\in\Omega_s\,|\,(n_i = c_i\cap n_{0i}+n_{ii} = c_i')\right\},\quad i=1,2. \tag{6.43}$$

6.3.8.3 Case 3: SNO is sharing with one PNO

Under the sharing agreement when only the primary operator 1 is sharing with the secondary operator the equation (6.29) takes the following form

$$P(\mathbf{n},t) = \mathcal{K}^{-1}\frac{\left[\rho^{(n_0+n_{01})}(t)\right]\cdot\left[\rho_1^{(n_1+n_{11})}(t)\right]}{(n_0+n_{01})!\,(n_1+n_{11})!} \;\;\forall\;\; \mathbf{n}\in\Omega_s \tag{6.44}$$

where

$$\mathcal{K} = \sum_{\mathbf{n}\in\Omega_s}\frac{\left[\rho^{(n_0+n_{01})}(t)\right]\cdot\left[\rho_1^{(n_1+n_{11})}(t)\right]}{(n_0+n_{01})!\,(n_1+n_{11})!}. \tag{6.45}$$

The blocking probability formula for the ith operator is given by

$$P_{b_i}(t) = \sum_{\mathbf{n}\in S_R} P(\mathbf{n},t) = \frac{\displaystyle\sum_{\mathbf{n}\in S_R}\frac{\left[\rho^{(n+n_{01})}(t)\right]\cdot\left[\rho_1^{(n_1+n_{11})}(t)\right]}{(n_0+n_{01})!\,(n_1+n_{11})!}}{\displaystyle\sum_{\mathbf{n}\in\Omega_s}\frac{\left[\rho^{(n+n_{01})}(t)\right]\cdot\left[\rho_1^{(n_1+n_{11})}(t)\right]}{(n_0+n_{01})!\,(n_1+n_{11})!}} \;\;\forall\;\; \mathbf{n}\in\Omega_s \tag{6.46}$$

where the set S_R is again the restricted state space, and varies for the SNO and PNOs. For the SNO, it is defined as

$$S_R = \left\{\mathbf{n}\in\Omega_s \,|\, (n_0 = c_0 \cap n_{01}+n_{11} = c_1')\right\}, \tag{6.47}$$

and for the ith PNO, S_R can be replaced by S_1 and defined as

$$S_1 = \left\{\mathbf{n}\in\Omega_s \,|\, (n_1 = c_1 \cap n_{01}+n_{11} = c_1')\right\}. \tag{6.48}$$

6.4 Analysis and results

In this section, we show the analysis of optimal borrowing solutions by Algorithms 6.1 and 6.3 corresponding to the cost minimisation and profit maximisation with restricted budget scenarios, respectively. To explore the advantages of the proposed formulations, we compare the results from Algorithm 6.1 and 6.3 with a heuristic spectrum selection formulation by Algorithm 6.2 and 6.4, respectively. We simulate the functionalities of the network management, which are necessary to generate the optimal solution and to compare with the heuristic spectrum selection algorithms. We consider one SNO and four PNOs ($N = 4$) to simulate the dynamics of the *merchant mode* resource sharing mechanism.

Selecting different number of PNOs would have an effect on the cost of borrowing as well as the profit made by the SNO. It is pertinent to note that, as we increase the number of PNOs, the difference in gain between our proposed method and the heuristic becomes more conspicuous, with the advantage being greater for our proposed solution. On the other hand, if a small number of PNOs (e.g., $N < 3$) is selected, the performance of the two solutions would match with higher probability. For simplicity and clarity we only pick $N = 4$ for analysis. However, our proposed model can be configured with any number of PNOs and SNOs.

Some parameters are determined randomly by the algorithms with specific distribution (e.g., λ_i, μ_i, w_i) and other parameters are preset (e.g., L, p_{i_j}). We have varied the parameters in each cell of the network to see how they affect the cost of the borrowing and the amount of profit made. The algorithms are tested for different scenarios subject to those network parameters.

6.4.1 Cost analysis under target performance (Problem 1)

In the simulation, we consider the PNOs spectral usage for all cells L, where four base stations of primary network operators in each cell are deployed (collocated

topology), e.g., the case in densely populated cities. The demand of service for each provider (primary or secondary) varies over time and location. We assume the spectral utilisation of secondary provider at time interval t is high whereas the primary operators are underloaded in the same time interval and at the same location. The number of idle spectrum resources of PNOs and the level of spectrum demand of the SNO vary over time and location.

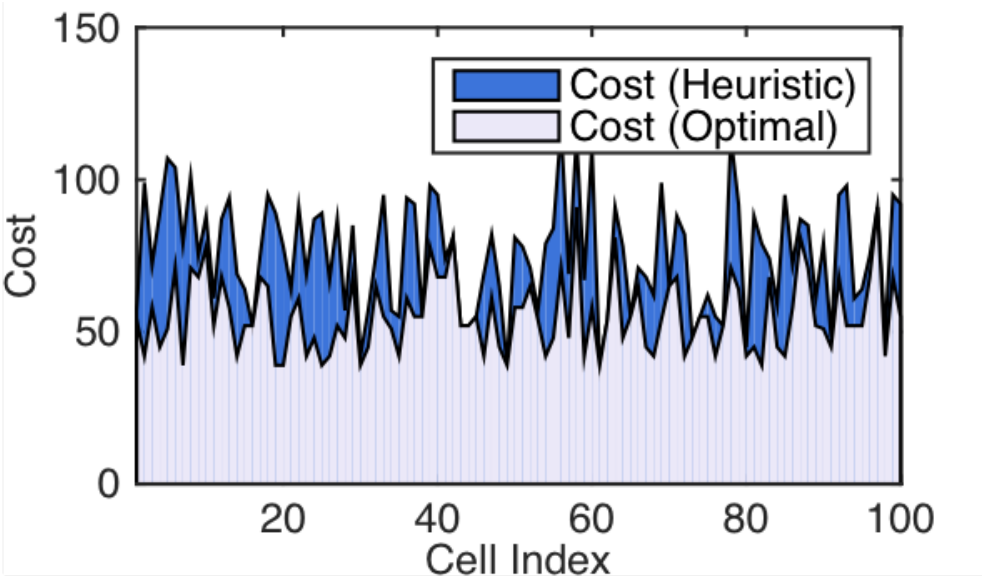

FIGURE 6.2: Cost of optimal and heuristic algorithms per cell

The PNOs charge the SNO at variable rates. The charges may be assessed by the market on the basis of the current supply-demand balance for each individual operator at each cell and possibly other factors [127]. However, we set limits to the price of unit bandwidth as maximum $X_{(max)}$ and minimum price $X_{(min)}$ to

TABLE 6.1: Simulation parameters.

Parameter	L	M	N	p_{i_j}	λ_{i_j}	μ_{i_j}	w_{i_j}	$c_{i_j k}$	$a_{i_j k}$	b_{i_j}
Values for *problem 1*	100	1	4	0.01	10	1	1	$(3, 9)$	$(5, 10)$	$--$
Values for *problem 2*	100	1	4	0.01	$(40, 120)$	$(1, 5)$	$(1, 5)$	$(10, 13)$	$(30, 40)$	50

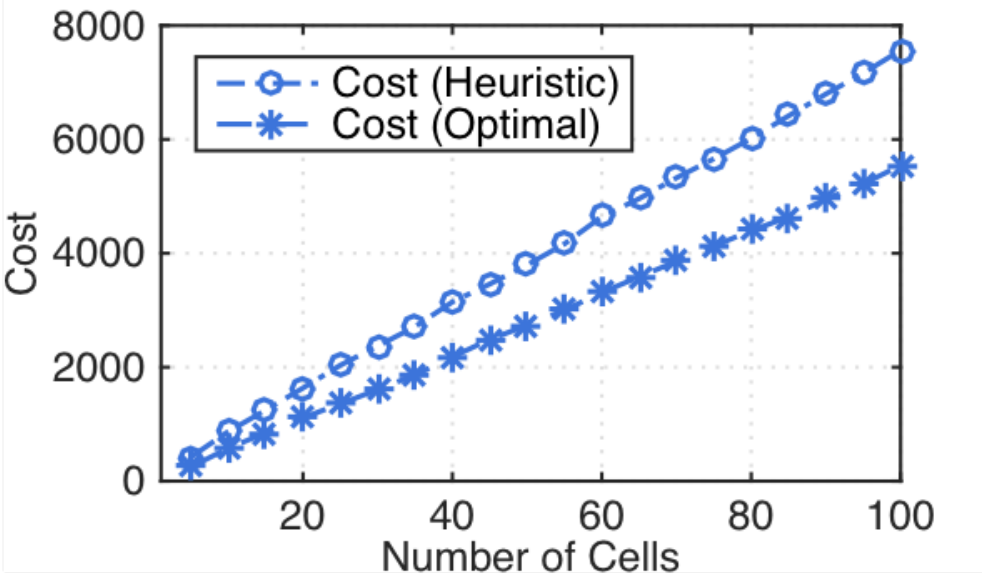

FIGURE 6.3: Cost of optimal and heuristic algorithms for varying number of cells.

structure the problem space. For the purpose of analysis, we parametrise the borrowing cost as

$$c_{i_jk}(t) = \left\{ c_{i_jk}(t) \mid X_{(min)} \leq c_{i_jk}(t) \leq X_{(max)} \right\}, \tag{6.49}$$

where $c_{i_jk}(t)$ follows a uniform distribution from $[X_{(min)} = 3,\ X_{(max)} = 9]$. We keep the difference between $X_{(max)}$ and $X_{(min)}$ relatively small at all cells. This assumption captures the highly competitive nature of the market economic environment. We determine the admission cost per unit bandwidth based on a discrete uniform random variables. In our mathematical model all possible variations of the available bandwidth values $a_{i_jk}(t)$ to provide the SNO demand are considered. This assumption provides realistic scenarios where PNOs could have different values of leasable spectrum resources. More details about the simulation parameters are given in Table 6.1.

At time t and in each cell i, the SNO has a particular blocking probability target p_{i_j}. By considering the SNO's expected traffic load λ_{i_j} in the next time interval,

the available capacity w_{i_j} and service rate μ_{i_j}, each cell determines its required number of channels $r_{i_j}(t)$.

For comparisons, we simulate the interactions between the network providers and we solve the resource allocation problem by the optimal and the heuristic allocation as described in Algorithms 6.1 and 6.2, respectively. For the simulation of the heuristic allocation, each cell i makes heuristic selection of aggregated channels for dynamic access from the set $\{a_{i_jk}\}$ which are collocated in the same cell. The selection of aggregated channels is performed regardless of the admission cost associated with the choice of selected channels. Algorithm 6.2 is allowed to perform spectrum borrowing until the demand is satisfied, assuming $\sum_{k=1}^{N_{i_j}} a_{i_jk}(t) \geq r_{i_j}(t)$. If $\sum_{k=1}^{N_{i_j}} a_{i_jk}(t) < r_{i_j}(t)$ then the algorithm takes all available bandwidths, however, the target blocking probability will not be satisfied, such that, $P_{(b_{new})}(t) < p_{i_j}(t)$.

For the Algorithm 6.1, the cells of SNO select the combination $\{x_{i_jk}\}$ with the lowest admission cost from the set $\{a_{i_jk}(t)\}$, $\forall k, i$, to achieve the optimal channel borrowing admission costs. It is possible that there may be multiple solutions for the allocation problem which provide the same required bandwidth to the SNO with different costs.

The main observation here is that the optimal model achieves lower costs compared to the heuristic algorithm, except for cells with $\sum_{k=1}^{N_{i_j}} a_{i_jk}(t) < r_{i_j}(t)$, see Figure 6.2. It is also observed that the total borrowing cost of both the heuristic and optimal configuration varies in every cell due to the stochastic nature of the costs and number of available channels.

If we consider the admission cost for large number of cells, as we can see from Figure 6.3, we notice that as the number of cells increases, the difference in cost between the heuristic and the optimal selection algorithm becomes larger, which implies substantial savings for operators with large territories when the optimal algorithm is used.

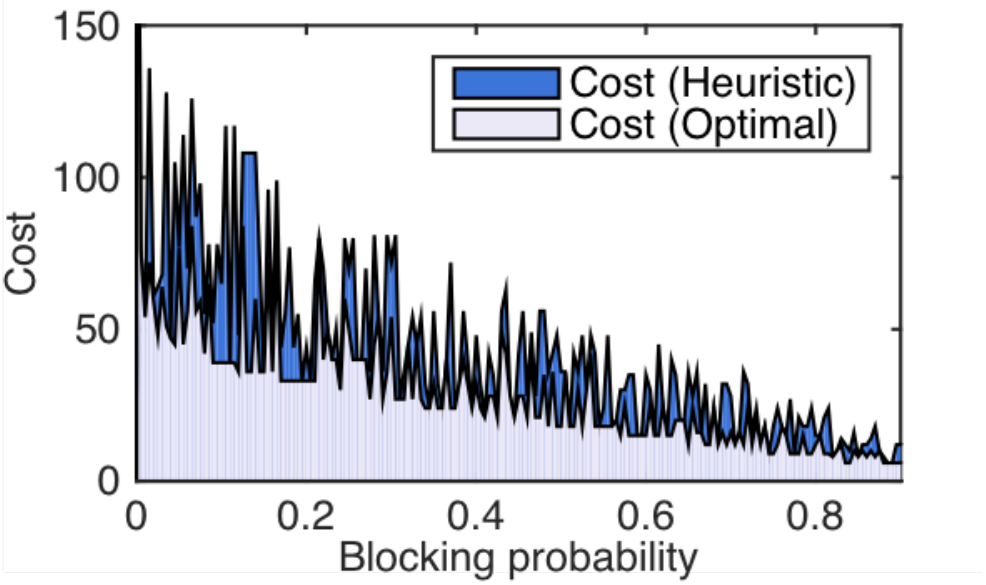

FIGURE 6.4: Effect of varying target blocking probability on cost for optimal and heuristic algorithms.

We also investigate the effect of target blocking probability on the admission cost. In Figure 6.4 we show the results for different target blocking probabilities ranging from $0 - 0.9$ for a single cell. We clearly see that as $p_{i_j} \to 0$, the admission cost increases for both algorithms. However, the optimal algorithm (Algorithm 1) provides lower borrowing cost for most of the points.

The total number of aggregated channels which are acquired through borrowing by using Algorithms 6.1 and 6.2 is equal, see Figure 6.5. This is because both algorithms allow channels to be acquired until a certain grade of service is reached or until all channels from the available bandwidths of primary operators $\{a_{i_j k}\}$ are consumed. This also implies that $P^{rand}_{(b_{new})}(t) = P^{opt}_{(b_{new})}(t)$, where $P^{rand}_{(b_{new})}(t)$ results from using the heuristic algorithm 6.1 and $P^{rand}_{(b_{new})}(t)$ results from using Algorithm 6.2.

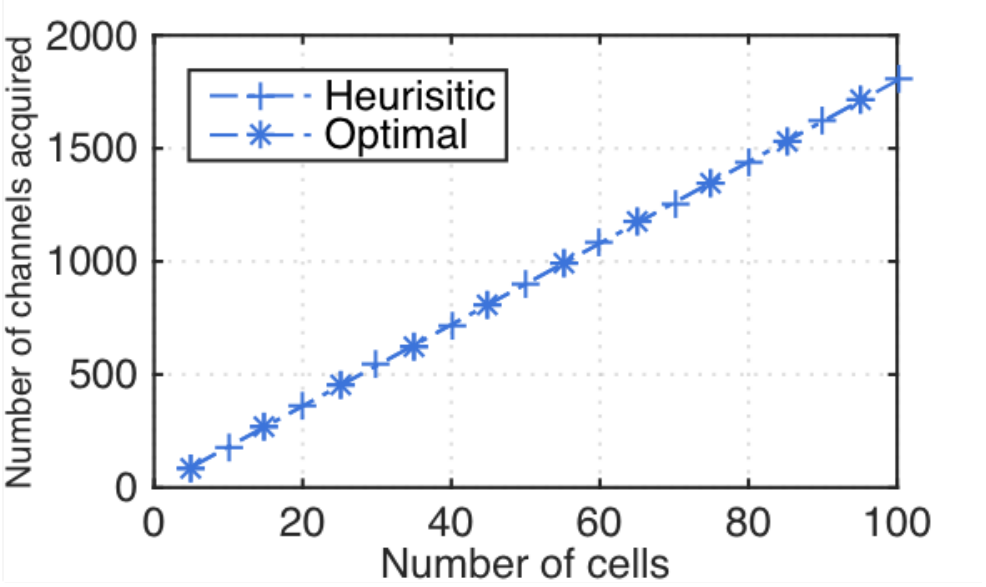

FIGURE 6.5: Effect of borrowing on bandwidth acquisition for the optimal and heuristic algorithms.

6.4.2 Expected profit under budget constraints analysis (Problem 2)

The objective of the SNO can be described from both economic and system performance perspective. Firstly, the SNO aims to lower the blocking probability for its subscribers. Secondly, the SNO attempts to maximise its profit by leasing additional spectrum from the PNOs in terms of cost and intrinsic quality. However, since network operators often operate with limited budget e.g., SNO can only spend $b_{i_j}(t)$ amount of resources/money at a cell i and time interval t. This is imposed by the government and regulatory bodies to keep the fairness of spectrum leasing among network operators.

To demonstrate the gain of the optimal algorithm, detailed investigation has been made and the results are compared with the heuristic allocation algorithm (see Figure 6.6). The figure shows the optimal algorithm achieves a substantial gain in comparison to the heuristic allocation approach. However, both algorithms

provide acceptable efficiency in terms of GoS. We also notice that as the number of cells increases the profit of the SNO gets larger, see Figure 6.7.

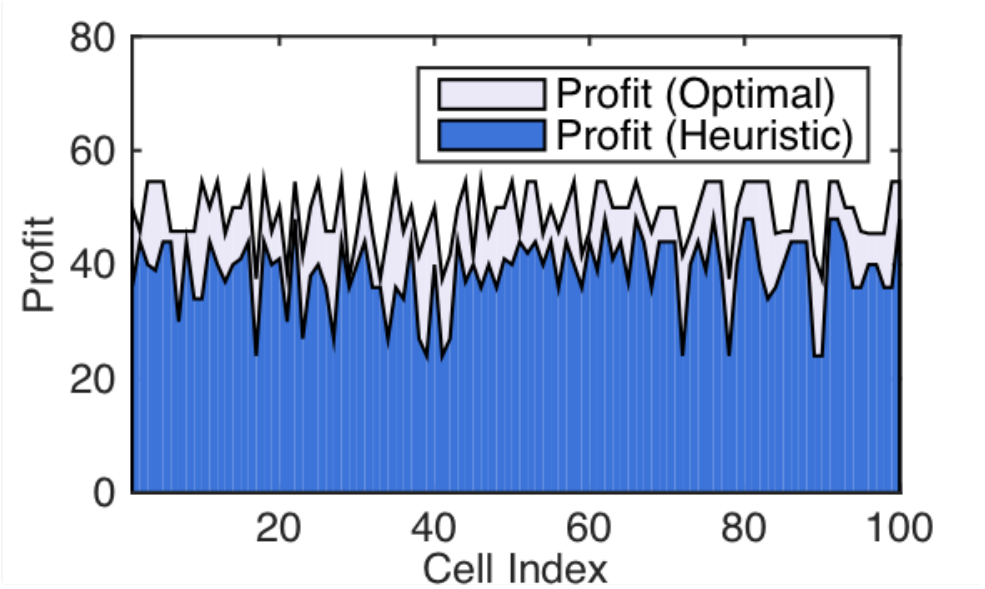

FIGURE 6.6: Profit using the optimal and heuristic algorithms per cell.

Figure 6.8 shows the effect of budget and target blocking probability on achievable profit with varying budget expenditure between $0 - 250$ and target blocking probability between $0 - 0.8$ for a single cell. It is clear that as we increase the

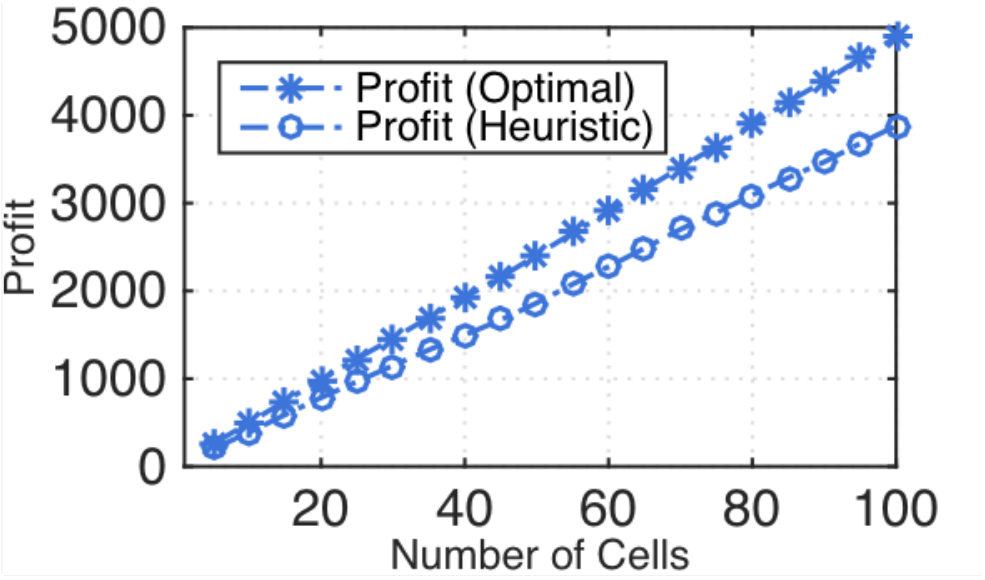

FIGURE 6.7: Profit using the optimal and heuristic algorithms for varying number of cells.

budget further $b_{i_j} \to 250$, the profit increases with respect to the increase of budget and demand. However, as the budget reaches a certain value, the profit does not increase because the budget is larger than required.

We also study how the optimal allocation based on profit maximisation affects the amount of acquired bandwidths. With number of cells between $1 - 100$, we compare the two algorithms presented in problem 2, see Figure 6.9. We find that, the optimal algorithm can achieve higher number of aggregated channels due to the higher efficiency in spectrum borrowing under the restricted budget.

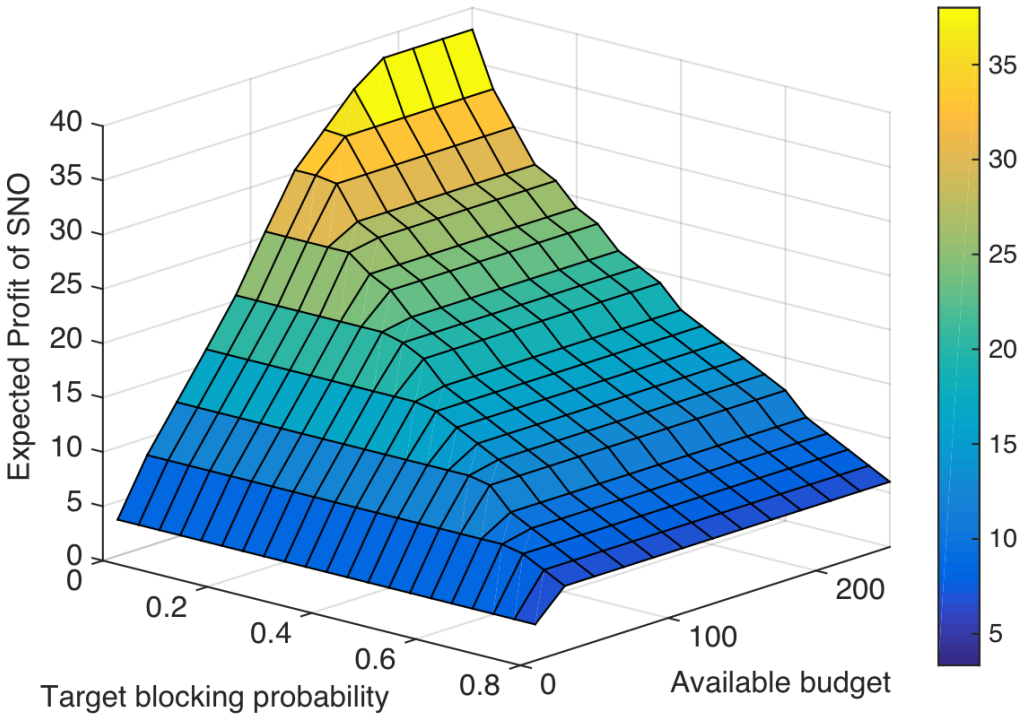

FIGURE 6.8: Expected profit of the SNO for spectrum borrowing with target blocking probability = 0 to 0.8 and budget = 0 to 250.

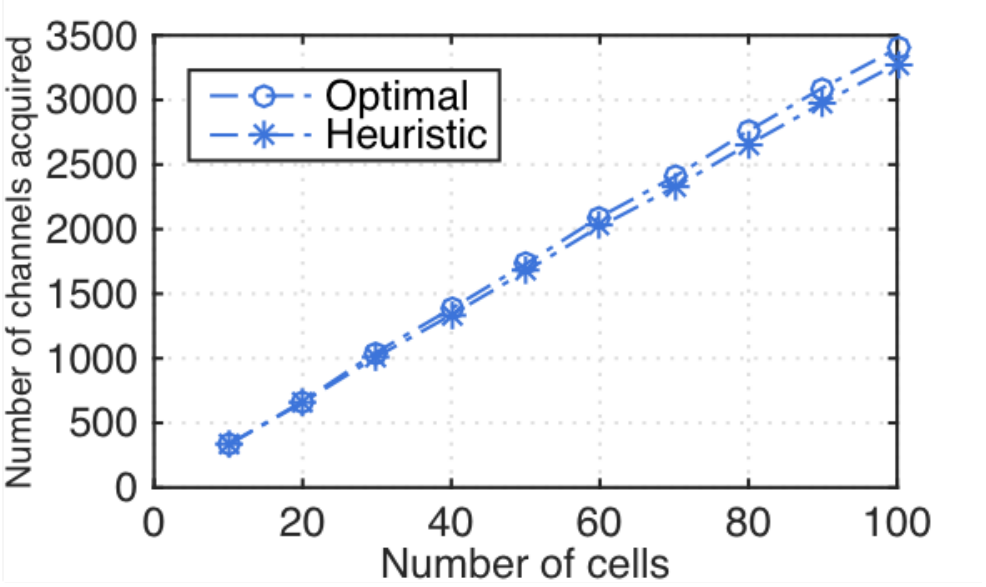

FIGURE 6.9: Bandwidth acquisition of the SNO for spectrum borrowing by the optimal and heuristic algorithms.

6.4.3 Expected profit under budget constraints with multiple types of services (Problem 2)

In the above analysis, we considered only one type of spectrum band ($M = 1$), which is provided to users at all cells (e.g., 900 MHz). In a more general model, different types of bands (e.g., 900 MHz, 2.3-2.4 GHz and 2.40-2.4835 GHz) can be operated by one network operator. Different bands provide different quality in the mobile broadband services [36]. The measures of quality include data rate and coverage. Therefore, they cannot be treated equally. In the proposed algorithms, we added a functionality to allow the trading to be managed more effectively by assigning each cell with a particular band type. In order to quantify the impact of the proposed algorithms we simulated a network which could support three different bands, ($M = 3$). We also tested the algorithms with two different budgets. In the simulation of 10 cells and allocated budget of 50 and 500 for each cell, we observed a markedly increased profit in both cases, see Figure 6.10. We can also see from the figures (top and bottom figures) that in all types of bands, the optimal algorithm outperforms its heuristic counterpart.

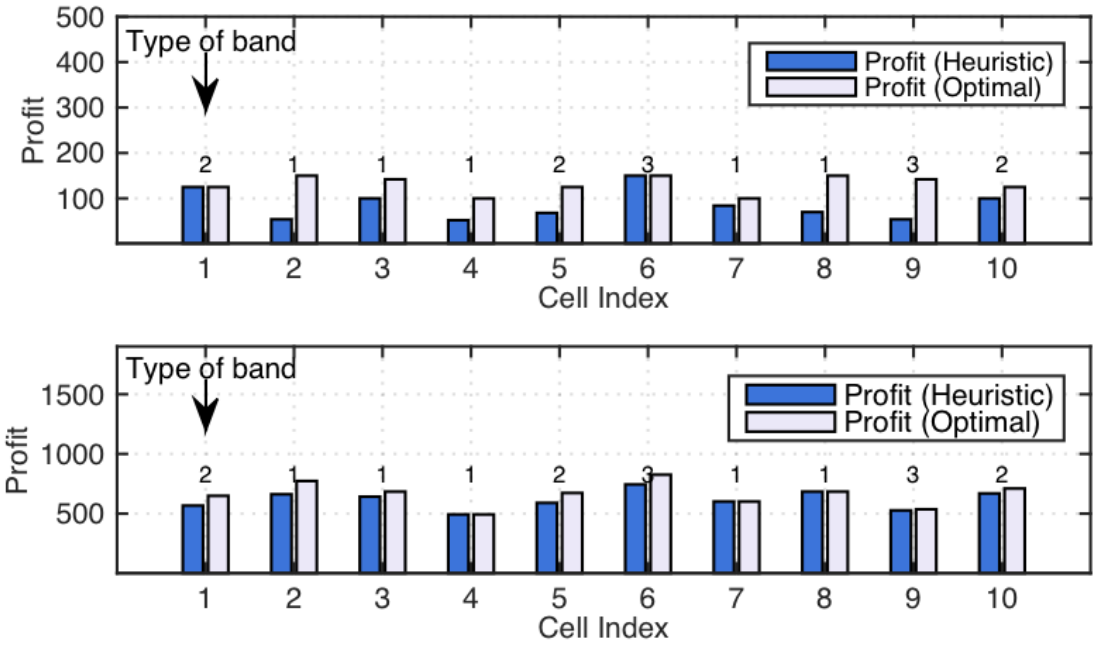

FIGURE 6.10: Effect of spectrum borrowing on profit with budget = 50 (top) and budget= 500 (bottom).

6.4.4 Impact on the performance of the operators

To analyze the impact of unilateral deviation strategy of the PNOs, we used the closed form formulae presented in Section 6.3.8 to compute the blocking probability of operators. The arrival processes involved in all operators are non-homogenous Poisson with rates $\lambda_{s_1}, \lambda_{s_2}, \lambda_1, \lambda_2$, and λ_3, respectively. The offered loads are λ_s/μ_s and λ_i/μ_i for the sth secondary and ith PNO, respectively. The number of aggregated channels and traffic intensities in each operator are independent as shown in table 6.2. The results show that the operators could obtain an actual blocking probability values to determine their benefits when they engage in spectrum trading.

In Figure 6.11, we observe the performance of the PNOs and the SNOs by varying the traffic load at the PNOs (from 1 to 5). If we fix a particular value of traffic intensity at the SNOs ($\rho_{s_1} = 1$ and $\rho_{s_2} = 5$) and change it for the PNOs, then the SNOs' blocking probability slightly increase due to the available capacity for

sharing (c'_1, c'_2 and c'_3) become overloaded by the PNOs' own traffic. We notice that the severity of traffic intensity change in the PNOs affects the performance of the SNO. To maintain the GoS, SNOs should be able to limit the resulting interference caused by each PNO, by increasing the frequency of trading windows. More specifically, the trading window is repeated more regularly to recompense the lost shared capacity caused by the deviation mechanism of the PNOs.

TABLE 6.2: Configurations used in Figure 6.11 and 6.12.

	Number of channels								Load (ρ)				
	SNO 1	SNO 2	PNO 1		PNO 2		PNO 3		SNO 1	SNO 2	PNO 1	PNO 2	PNO 3
	c_{s_1}	c_{s_1}	c_1	c'_1	c_2	c'_2	c_3	c'_3	ρ_{s_1}	ρ_{s_2}	ρ_1	ρ_2	ρ_3
Figure 6.11	2	2	5	2	5	2	5	2	1	5	(5, 1)	(7, 1)	(8, 1)
Figure 6.12	3	2	(7, 1)	(6, 1)	4	1	(7, 1)	(6, 1)	(5, 10)	(5, 10)	(5, 0)	2	(6, 1)

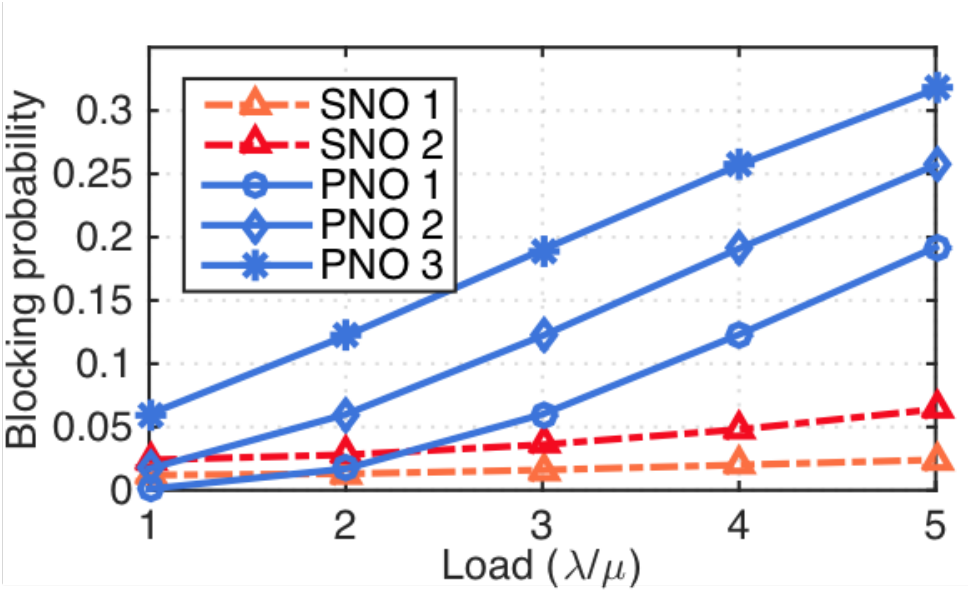

FIGURE 6.11: Blocking probability for each operator when configuration details are according to Table 6.2

In Figure 6.12, we analyse the impact of change in state of the PNOs from overloaded to underloaded. As the shared capacity becomes ample to meet the SNOs demand, we notice a significant reduction in blocking probability at the SNOs. We also notice that the blocking probability of PNO 2 is not affected by the changes in state of other primary and secondary operators since its shared capacity and traffic load remains constant for the duration. The results demonstrate that the

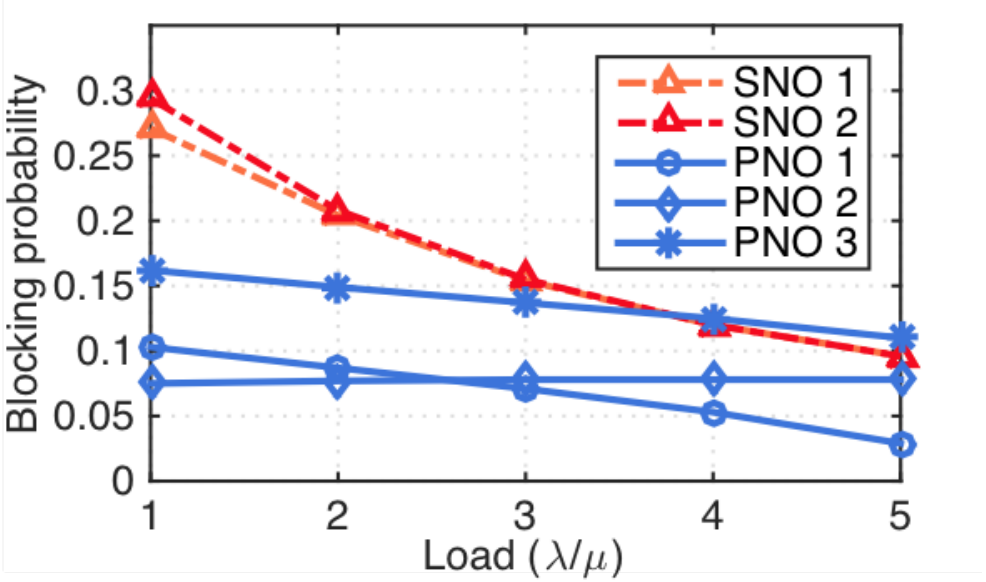

FIGURE 6.12: Blocking probability for each operator when configuration details are according to Table 6.2.

derived blocking probabilities can provide a crucial insight to the sharing strategies between operators.

6.5 Summary

In this chapter, we presented two finite horizon nonlinear optimisation algorithms to solve two optimisation problems for dynamic spectrum sharing. The efficiency of the proposed algorithms is compared with their corresponding heuristic algorithms. We also presented the post-optimisation performance analysis of the SNO and PNOs through blocking probability, which provides useful details about spectrum sharing strategy.

The optimisation problems investigated by considering a comprehensive process of delivering the secondary network operator's (SNO's) bandwidth demand and the solution algorithms ensured that either minimum cost of bandwidth borrowing or maximum profit under budget restrictions are achieved depending on the aim of

the SNO. In both cases the SNO aims to achieve a target performance by borrowing spectrum from other network operators (PNOs) on temporal and spatial basis. Results obtained from each model are then compared with results derived from algorithms in which spectrum borrowing were heuristic. Detailed comparisons are presented and they showed that the gain in the results obtained from our proposed stochastic-optimisation framework is markedly higher than heuristic borrowing algorithms. Our proposed approaches facilitate a dynamic purchasing (also called *automation of licensing*) scheme for such complex problems, which provide incentives to the network operators wishing to adopt dynamic spectrum sharing as well as substantial benefits for efficient use of spectrum. The proposed algorithms showed significant opportunities to increase spectrum utilisation while keeping GoS at a particular level and ensuring minimum cost. We also shown that our proposed optimisation solution not only reduces the total borrowing cost of the SNO, but also finds maximum spectrum access under any allocated budget.

A major challenge with the spectrum sharing optimisation models is to guarantee the operational grade of service (GoS) under different sharing protocols. Although a vast amount of literature addressed various spectrum sharing issues very little has discussed the post-optimisation results which are crucial for the operators to gain a detailed insight into the GoS. To study these issues and provide the final GoS, we derived the blocking probability behavior using a time-dependent continuous time Markov chain framework under various settings. Results showed that the final GoS is largely affected by the increase of traffic at the PNOs and the amount of shared resources.

Many researchers and academics have investigated dynamic spectrum sharing from various perspectives. However, dynamic spectrum management requires high level of cooperation between the involved network operators to guarantee interference-free transmission, which adds complexity the the network operations. This implication provides the reason to why dynamic spectrum sharing is difficult in practice.

In addition, if regulators allow dynamic spectrum sharing between operators, particularly in the enterprise space, the operators may have reservations over their participation. The complexity of the practical implementation associated with dynamic spectrum sharing motivates us to undertake more research, trials and tests.

Chapter 7

Conclusions and Future Work

7.1 Conclusions

Dynamic spectrum sharing (DSS) is considered as a promising solution to spectrum scarcity and inefficient static resource allocation. DSS exploits the unused spectrum by incumbent spectrum holders. Secondary operators with or without cognitive feature capabilities may access spectrum of primary networks without causing harmful interference to primary networks. Thus, DSS improves efficiency of spectrum utilisation. By applying the DSS approach, a number of spectrum sharing models were considered in this research. Due to the dynamic spectrum usage by primary networks, spectrum opportunity can be identified by spectrum sensing. While it is essential to reliably detect *spectrum holes*, the exploitation of cooperative spectrum sensing becomes a challenging task to implement efficient dynamic spectrum sharing. This thesis has contributed to this research by proposing spectrum sensing scheme considering location-awareness of nodes as well as a number of cooperative spectrum sharing models.

First, the thesis presents a comprehensive survey on cognitive radio networks and spectrum utilisation. The reason of spectrum sensing and mechanisms to overcome

erroneous detection and false alarm have been reviewed. A number of available spectrum sharing and dynamic overflow models are also assessed. In addition, literature on auction mode resource allocation for spectrum sharing has been surveyed.

In Chapter 3, we have studied the performance of cooperative cognitive spectrum sensing with energy detection in CR networks. Cooperative spectrum sensing with location-aware SUs have been investigated. The proposed scheme shows better radio operating characteristic, especially in highly shadowed regions, highlighting the requirements of location knowledge in cognitive radio networks. A major issue concerning the practical implementation of the proposed scheme is the availability of complete statistical information corresponding to source signal parameters, and particularly their variation with distance. However, lack of spectrum resources encourages the adoption of new ways of sharing including sharing of specific data related to the incumbent operators.

Considering overflow mechanisms in Chapter 4 we have proposed four different models: Non-Sharing Model, sharing model with uni-directional overflow (Model 1), sharing model with bi-directional overflow (Model 2) and sharing model with reserved capacity for one of the operators in the network and a bi-directional overflow between both operators (Model 3). The results show that the operators can achieve a notable reduction of blocking probability under the shared models compared with the Non-Sharing Model. The results highlight the importance of resource sharing for communication networks.

Extending the work in Chapter 4, we have presented three more models in Chapter 5 for dynamic spectrum sharing management in multi-operator cellular networks. Each model is defined by its own terms of sharing and interactions among the operators. The models represent the expected practical implementations of the next generation of cellular wireless networks. For each of the proposed models we

have derived the blocking probability of the individual operators and spectrum utilisation to quantify and analyse the benefits of the proposed models.

In Chapter 6, we presented two finite horizon nonlinear optimisation algorithms to solve two optimisation problems for dynamic spectrum sharing. The efficiency of the proposed algorithms is compared with their corresponding heuristic algorithms. We also presented the post-optimisation performance analysis of the secondary and primary network operator through blocking probability, which provides useful details about the spectrum sharing strategy. The proposed approaches facilitate a dynamic purchasing (also called *automation of licensing*) scheme for such complex problems, which provide incentives to the network operators wishing to adopt dynamic spectrum sharing as well as substantial benefits for efficient use of spectrum.

7.2 Future work

This research contributes to the topic of dynamic spectrum sharing by considering location-aware spectrum sensing and a number of overflow mechanisms including two optimisation algorithms. This section discusses possible directions for future research.

There are several natural directions suggested by the work in Chapter 3. The most obvious one is to utilise the eliminated CRs from the first step of the proposed cooperative sensing. For example, it would be interesting to develop more complex schemes of spectrum sensing, e.g., assign the eliminated CRs to sense different channels which are in LOS and/or in close proximity to the different source signal which could be used for secondary transmission. This could improve the efficiency of sensing not only by sensing more channels simultaneously but with high accuracy too.

In the case of Universal Mobile Telecommunications System (UMTS) the transmitting power is adapted to the propagation conditions. The transmitting power is always selected to be only as high as necessary for adequate connection quality. Moreover, each service supported by UMTS networks requires specific threshold values and the network behaviour and size changes with traffic. Data transmission adds yet another dimension of complexity. This makes detecting UMTS signals much more difficult than in the case of other technology e.g., Global System for Mobile Communications (GSM). Therefore, it would be useful to conduct a study that specifically addresses the UMTS networks.

In addition to the analysis presented in Chapter 4, we provide a preliminary method on how to set out the conditions and formulations of spectrum sharing agreement. A more thorough study on such formulations would improve the decision making of network operators when they engage in spectrum sharing trade deals.

In Chapter 6, the post-optimisation analysis of spectrum sharing among the operators is an emerging topic and requires further research that would cover other issues, for instance, different sharing strategies and configurations could be implemented and analysed.

In Chapter 6 although large number of cells are taken into account, the optimisation is performed for each cell individually. Optimisation which considers a cluster of cells or all cells together may be more desirable by operators in order to gain a better analysis of the network. Moreover, assuming one secondary operator in the optimisation problems presented in Chapter 6 was developed to highlight the possibility of such scenario that may exist in future network. However, when more secondary operators coexist in the network, the optimisation problem will require further attention due to likely competition that may arise between secondary operators.

Appendix A

Performance analysis under resource sharing between S SNOs and N PNOs

In this Appendix, we derive the blocking probability and state distribution under resource sharing between S SNOs and N PNOs (see Figure A.1).

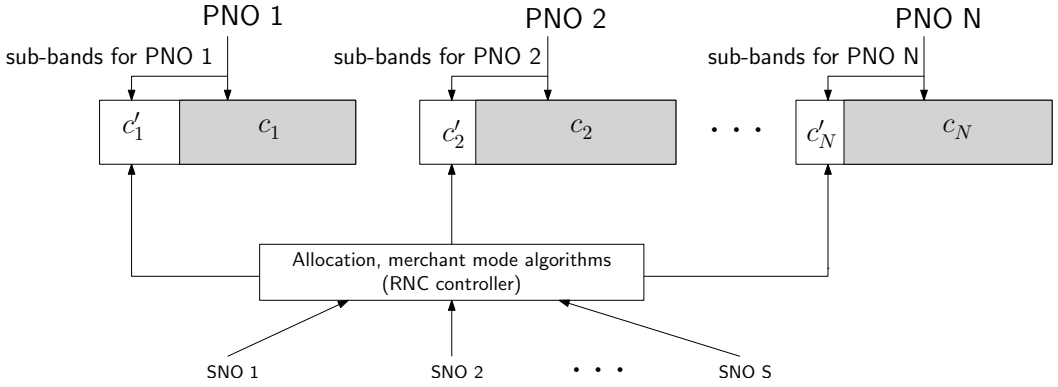

FIGURE A.1: Network model for cellular network with N PNOs and S SNOs

Consider a cell consisting of S SNOs with capacity $c_{s_1}, c_{s_2}, \ldots, c_{s_s}$ and N PNOs with capacity $c_1, c_2, \ldots, c_N$, respectively. Under a sharing agreement all N PNOs share part of their resources $c'_1, c'_2, \ldots, c'_N$, respectively with S SNOs determined

using the optimisation approach discussed in the previous sections. These resources may also be used by the corresponding PNO under mutual agreement. A state of the network is a vector of length $[S(1+N)+2N)]$ defined as

$$\mathbf{n} = \{(n_{s_1}, n_{s_2}, \ldots, n_{s_S}); ((n_{s_1 1}, n_{s_1 2}, \ldots, n_{s_1 N}), \ldots, (n_{s_S 1}, n_{s_S 2}, \ldots, n_{s_S N})); \\ (n_1, n_2, \ldots, n_N); (n_{11}, n_{22}, \ldots, n_{NN})\}$$

with the condition that $(n_{s_1 i}, n_{s_2 i}, \ldots, n_{s_S i}) + n_{ii} \leq c'_i \ \forall \ i = 1, 2, \ldots, N$, where n_{s_i} is the number of channel requests in progress in the ith SNO; $n_{s_i j}$ is the number of channel requests in the shared resources of the ith PNO from the s_ith SNO; n_j is the number of channel requests in progress in the jth PNO and n_{jj} is the number of request of the jth PNO on its own shared resources. The states $\mathbf{n}$ are restricted due to resource sharing constraints. The set of feasible states can be written as

$$\Omega_s = \{\mathbf{n} : \mathbf{An} \leq \mathbf{s}\} \tag{A.1}$$

where $\mathbf{A}$ is a $[S(1+N)+2N)]$ matrix and $\mathbf{s}$ is a d-vector, where d is the number of constraints. The network topology is reflected in the matrix $\mathbf{A}$ and the vector $\mathbf{s}$.

Let channel requests arrive to the ith secondary and jth primary operators according to a non-homogeneous Poisson process, with rates $\lambda_{s_i}(t)$ and $\lambda_j(t)$ at time t. These requests are admitted if $\mathbf{n} + \mathbf{e}_i \in \Omega_s$ (for a PNO) and $\mathbf{n} + \mathbf{e}_j \in \Omega_s$ (for a SNO), where $\mathbf{e}_i$ and $\mathbf{e}_j$ is the ith unit vector with 1 in place i and 0 elsewhere. When all c_{s_i} resources of the ith SNO is full then requests are diverted and admitted to the jth PNO if $\mathbf{n} + \mathbf{e}_{ij} \in \Omega_s$, where $\mathbf{e}_{ij}$ is the ith unit vector. Similarly, in the jth PNO if all c_j resources are occupied, the new channel requests are diverted to its shared resources c'_j for the jth primary network if $\mathbf{n} + \mathbf{e}_{jj} \in \Omega_s$, where $\mathbf{e}_{jj}$ is the jth unit vector. Assume that admitted requests in ith secondary and

jth primary operators have exponential holding times with rates $\mu_{s_i}(t)$ and $\mu_j(t)$ respectively at time t. Under these assumptions, the network can be modeled as a non-homogeneous continuous time Markov chain

$$\mathbf{X}(t) = (X_i(t), X_{ij}(t), X_{jj}(t), X_j(t);\ i = 1, 2, \ldots, S, j = 1, 2, \ldots, N,\ t \geq 0) \quad \text{(A.2)}$$

that records the number of channel requests in progress from all operators. The state space of the Markov chain is specified in (A.1), and its transition rates $\mathbf{Q}(t) = (q(\mathbf{n}, \mathbf{n}', t), \mathbf{n}, \mathbf{n}' \in \Omega_s)$ are given by

$$q(\mathbf{n}, \mathbf{n}', t) = \begin{cases} \lambda_{s_i}(t) & \mathbf{n}' = \mathbf{n} + \mathbf{e}_i \ \text{ or } \ \mathbf{n}' = \mathbf{n} + \mathbf{e}_{ij}, \text{ if } \ n_{s_i} = c_{s_i},\ i = 1, 2, \ldots, S \\ \lambda_j(t) & \mathbf{n}' = \mathbf{n} + \mathbf{e}_j \ \text{ or } \ \mathbf{n}' = \mathbf{n} + \mathbf{e}_{jj}, \text{ if } \ n_j = c_j,\ j = 1, 2, \ldots, N \\ n_{s_i}\mu_{s_i}(t) & \mathbf{n}' = \mathbf{n} - \mathbf{e}_i,\ i = 1, 2, \ldots, S \\ n_j\mu_j(t) & \mathbf{n}' = \mathbf{n} - \mathbf{e}_j,\ j = 1, 2, \ldots, N \\ n_{s_{ij}}\mu_{s_i}(t) & \mathbf{n}' = \mathbf{n} - \mathbf{e}_{ij},\ i = 1, 2, \ldots, S,\ j = 1, 2, \ldots, N \\ n_{jj}\mu_j(t) & \mathbf{n}' = \mathbf{n} - \mathbf{e}_{jj},\ j = 1, 2, \ldots, N \\ 0 & \text{otherwise.} \end{cases} \quad \text{(A.3)}$$

Theorem A.1. *The closed-form solution of* $\mathbf{n}$ *channel requests in progress at time* t *is given by equation (A.4).*

$$P(\mathbf{n}, t) = \mathcal{K}^{-1} \frac{\left[\rho_{s_1}^{(n_{s_1} + n_{s_1 1} + \cdots + n_{s_1 N})}(t)\right] \ \cdots \ \left[\rho_{s_S}^{(n_{s_S} + n_{s_S 1} + \cdots + n_{s_S N})}(t)\right]}{(n_{s_1} + n_{s_1 1} + \cdots + n_{s_1 N})! \ \cdots \ (n_{s_1} + n_{s_1 1} + \cdots + n_{s_1 N})!} \cdot \frac{\left[\rho_1^{(n_1 + n_{11})}(t)\right] \cdot \left[\rho_2^{(n_2 + n_{22})}(t)\right] \cdots \left[\rho_N^{(n_N + n_{NN})}(t)\right]}{(n_1 + n_{11})!\ (n_2 + n_{22})!\ \cdots\ (n_N + n_{NN})!} \ \ \forall \ \ \mathbf{n} \in \Omega_s \quad \text{(A.4)}$$

where $\rho_{s_i} = \lambda_{s_i}/\mu_{s_i}$ and $\rho_j = \lambda_j/\mu_j$ are traffic intensities of the s_ith SNO and jth PNO, respectively and $\mathcal{K}$ is the normalizing constant and given by

$$\mathcal{K} = \sum_{\mathbf{n}\in\Omega_s} \frac{\left[\rho_{s_1}^{(n_{s_1}+n_{s_11}+\cdots+n_{s_1N})}(t)\right] \cdots \left[\rho_{s_S}^{(n_{s_S}+n_{s_S1}+\cdots+n_{s_SN})}(t)\right]}{(n_{s_1}+n_{s_11}+\cdots+n_{s_1N})! \cdots (n_{s_1}+n_{s_11}+\cdots+n_{s_1N})!} \cdot \frac{\left[\rho_1^{(n_1+n_{11})}(t)\right] \cdot \left[\rho_2^{(n_2+n_{22})}(t)\right] \cdots \left[\rho_N^{(n_N+n_{NN})}(t)\right]}{(n_1+n_{11})!\,(n_2+n_{22})! \cdots (n_N+n_{NN})!} \quad \forall \ \mathbf{n} \in \Omega_s. \tag{A.5}$$

Proof. Define the state probabilities

$$P(\mathbf{n}, t) := Pr(X(t) = \mathbf{n}), \ \ \mathbf{n} \in \Omega_s, \ t \geq 0 \tag{A.6}$$

with initial condition $P_0(\mathbf{n}) = Pr(X(0) = \mathbf{n})$. Since the network has a finite state space, these probabilities are the unique solution of the Kolmogorov forward equations given in (A.7) for $\mathbf{n} \in \Omega_s, t > 0$.

The Kolmogorov forward equations can be defined as

$$\begin{aligned}
\frac{\mathrm{d}P(\mathbf{n},t)}{\mathrm{d}t} =& \left[\sum_{i=1}^{S} \lambda_{s_i}(t) \cdot (\mathbb{1}(n_{s_i} < c_{s_i}) + \mathbb{1}(n_{s_i} = c_{s_i} \cap \mathbf{n} + \mathbf{e}_{ij})) + \sum_{j=1}^{N} \lambda_j(t) \cdot \big(\mathbb{1}(n_j < c_j) \right. \\
&\left. + \mathbb{1}(n_j = c_j \cap \mathbf{n} - \mathbf{e}_{jj})\big)\right] \cdot P\left((\mathbf{n} - \mathbf{e}_i), t\right) + \sum_{i=1}^{S} (n_{s_i} + 1)\mu_{s_i}(t) P\left((\mathbf{n} + \mathbf{e}_i), t\right) \\
&+ \sum_{j=1}^{N} (n_j + 1)\mu_j(t) \cdot P((\mathbf{n} + \mathbf{e}_j), t) - \left[\sum_{i=1}^{S} \lambda_{s_i}(t) \cdot (\mathbb{1}(n_{s_i} < c_{s_i}) + \mathbb{1}(n_{s_i} = c_{s_i} \cap \mathbf{n} + \mathbf{e}_{ij}))\right. \\
&\left. + \sum_{j=1}^{N} \lambda_j(t) \cdot \big(\mathbb{1}(n_j < c_j) + \mathbb{1}(n_j = c_j \cap \mathbf{n} - \mathbf{e}_{jj}) + \sum_{i=1}^{S} n_{s_i}\mu_{s_i}(t) + \sum_{j=1}^{N} n_j\mu_j(t)\big)\right] P\left(\mathbf{n}, t\right)
\end{aligned} \tag{A.7}$$

where $\mathbb{1}(A)$ is the indicator function for an event A.

Equations in (A.7) can be written in the operator form as given by

$$\frac{\mathrm{d}\mathbf{P}(t)}{\mathrm{d}t} = \mathbf{P}(t)\,\mathbf{Q}(t), \quad \mathbf{P}(0) = \mathbf{P}_0,\, t > 0 \tag{A.8}$$

where $\mathbf{P}(t)$ is the vector of probabilities $\mathbf{P}(\mathbf{n}, t)$. The formal solution of the equation (A.8) is given by

$$\mathbf{P}(t) = \mathbf{P}_0\, E_Q(t), \quad t \geq 0 \tag{A.9}$$

where $E_Q(t)$ is the time-ordered exponential of the generator $\mathbf{Q}(t)$, that is the unique operator solution to the equation

$$\frac{\mathrm{d}E_Q(t)}{\mathrm{d}t} = E_Q(0)\,\mathbf{Q}(t), \quad t \geq 0 \tag{A.10}$$

where $E_Q(0) = \mathbf{I}$, the identity operator. The unique solution of the Kolmogorov forward equations (A.7) is then given by the equation (A.4). □

The blocking probability formula can then be derived from the closed-form solution (A.4). The blocking probability for an operator i[7] (ith operator could be an SNO or a PNO), is then given by

$$\begin{aligned} P_b(t) &= \sum_{\mathbf{n}\in\mathcal{S}} P(\mathbf{n}, t) \\ &= \frac{\sum_{\mathbf{n}\in\mathcal{S}} \frac{\left[\rho_{s_1}^{(n_{s_1}+n_{s_1 1}+\cdots+n_{s_1 N})}(t)\right] \cdots \left[\rho_{s_S}^{(n_{s_S}+n_{s_S 1}+\cdots+n_{s_S N})}(t)\right] \cdot \left[\rho_1^{(n_1+n_{11})}(t)\right] \cdots \left[\rho_N^{(n_N+n_{NN})}(t)\right]}{(n_{s_1}+n_{s_1 1}+\cdots+n_{s_1 N})! \cdots (n_{s_1}+n_{s_1 1}+\cdots+n_{s_1 N})!(n_1+n_{11})! \cdots (n_N+n_{NN})!}}{\sum_{\mathbf{n}\in\Omega_s} \frac{\left[\rho_{s_1}^{(n_{s_1}+n_{s_1 1}+\cdots+n_{s_1 N})}(t)\right] \cdots \left[\rho_{s_S}^{(n_{s_S}+n_{s_S 1}+\cdots+n_{s_S N})}(t)\right] \cdot \left[\rho_1^{(n_1+n_{11})}(t)\right] \cdots \left[\rho_N^{(n_N+n_{NN})}(t)\right]}{(n_{s_1}+n_{s_1 1}+\cdots+n_{s_1 N})! \cdots (n_{s_1}+n_{s_1 1}+\cdots+n_{s_1 N})!(n_1+n_{11})! \cdots (n_N+n_{NN})!}} \end{aligned} \tag{A.11}$$

[7]The set $\mathcal{S}$ in equation (A.11) is further defined in equation (A.12) and (A.12) to count for all the operators in the network.

where the set $\mathcal{S}$ is the restricted state space, and varies for the SNOs and PNOs. For the sth SNO, it is defined as

$$\mathcal{S}_i = \big\{\mathbf{n} \in \Omega_s \,|\, (n_{s_i} = c_{s_i} \cap n_{s_i1} + n_{11} = c_1' \cap n_{s_i2} + n_{22} = c_2' \cap \cdots \cap n_{s_iN} + n_{NN} = c_N')\big\}, \\ i = 1, 2, \ldots, S. \quad \text{(A.12)}$$

and for the jth PNO, $\mathcal{S}_i$ can be replaced by $\mathcal{S}_j$ and defined as

$$\mathcal{S}_j = \big\{\mathbf{n} \in \Omega_s \,|\, (n_{s_i} = c_{s_i} \cap n_{s_ij} + n_{jj} = c_i')\big\}, \; j = 1, 2, \ldots, N. \quad \text{(A.13)}$$

References

[1] A. Palaios, J. Riihijarvi, P. Mahonen, V. Atanasovski, L. Gavrilovska, P. Van Wesemael, A. Dejonghe, and P. Scheele, "Two days of spectrum use in Europe," in *7th International Conference on Cognitive Radio Oriented Wireless Networks and Communications*, pp. 24–29, 2012.

[2] M. Hoyhtya, M. Matinmikko, X. Chen, J. Hallio, J. Auranen, R. Ekman, J. Roning, J. Engelberg, J. Kalliovaara, T. Taher, A. Riaz, and D. Roberson, "Measurements and analysis of spectrum occupancy in the 2.3-2.4 GHz band in Finland and Chicago," in *9th International Conference on Cognitive Radio Oriented Wireless Networks and Communications*, pp. 95–101, Jun. 2014.

[3] I. F. Akyildiz, W.-Y. Lee, M. C. Vuran, and S. Mohanty, "NeXt generation/dynamic spectrum access/cognitive radio wireless networks: A survey," *Computer Networks*, vol. 50, no. 13, pp. 2127–2159, 2006.

[4] I. Akyildiz, W.-Y. Lee, and K. Chowdhury, "Spectrum management in cognitive radio ad hoc networks," *IEEE Network*, vol. 23, no. 4, pp. 6–12, 2009.

[5] B. Wang and K. Liu, "Advances in cognitive radio networks: A survey," *IEEE Journal of Selected Topics in Signal Processing*, vol. 5, pp. 5–23, Feb. 2011.

[6] P. Kolodzy, "Spectrum policy task force," Tech. Rep. ET Docket No. 02-135, Federal Communications Commission, Nov. 2002.

[7] A. Wyglinski, M. Nekovee, and Y. Hou, *Cognitive radio communications and networks: principles and practice*. Academic Press, 2010.

[8] I. Akyildiz, W.-Y. Lee, M. C. Vuran, and S. Mohanty, "A survey on spectrum management in cognitive radio networks," *IEEE Communications Magazine*, vol. 46, pp. 40–48, Apr. 2008.

[9] Z. Ji and K. R. Liu, "Cognitive radios for dynamic spectrum access-dynamic spectrum sharing: A game theoretical overview," *IEEE Communications Magazine*, vol. 45, no. 5, pp. 88–94, 2007.

[10] M. M. Buddhikot and K. Ryan, "Spectrum management in coordinated dynamic spectrum access based cellular networks," in *1st IEEE International Symposium on New Frontiers in Dynamic Spectrum Access Networks, 2005*, pp. 299–307, IEEE, 2005.

[11] E. Perez, K.-J. Friederichs, I. Viering, and J. Diego Naranjo, "Optimization of authorised/licensed shared access resources," in *9th International Conference on Cognitive Radio Oriented Wireless Networks and Communications*, pp. 241–246, Jun. 2014.

[12] R. Etkin, A. Parekh, and D. Tse, "Spectrum sharing for unlicensed bands," *IEEE Journal on Selected Areas in Communications*, vol. 25, pp. 517–528, Apr. 2007.

[13] C. Xin, M. Song, L. Ma, S. Shetty, and C.-C. Shen, "Control-free dynamic spectrum access for cognitive radio networks," in *IEEE International Conference on Communications*, pp. 1–5, May 2010.

[14] W. Song, W. Zhuang, and Y. Cheng, "Load balancing for cellular/WLAN integrated networks," *IEEE Network*, vol. 21, pp. 27–33, Jan. 2007.

[15] C. Leong, W. Zhuang, Y. Cheng, and L. Wang, "Optimal resource allocation and adaptive call admission control for voice/data integrated cellular networks," *IEEE Transactions on Vehicular Technology*, vol. 55, pp. 654–669, Mar. 2006.

[16] M. Fidler and A. Rizk, "A guide to the stochastic network calculus," *IEEE Communications Surveys Tutorials*, vol. 17, no. 1, pp. 92–105, 2015.

[17] L. Luo and S. Roy, "Analysis of dynamic spectrum access with heterogeneous networks: Benefits of channel packing scheme," in *IEEE Global Telecommunications Conference*, pp. 1–7, Nov. 2009.

[18] S. Tang and B. Mark, "Modelling an opportunistic spectrum sharing system with a correlated arrival process," in *IEEE Wireless Communications and Networking Conference*, pp. 3297–3302, Mar. 2008.

[19] P. Zhu, J. Li, and X. Wang, "Scheduling model for cognitive radio," in *3rd International Conference on Cognitive Radio Oriented Wireless Networks and Communications*, pp. 1–6, May 2008.

[20] T. S. Rappaport *et al.*, *Wireless communications: principles and practice*. New Jersey: Prentice Hall, 1996.

[21] H. Zhang, C. Jiang, X. Mao, and H.-H. Chen, "Interference-limited resource optimization in cognitive femtocells with fairness and imperfect spectrum sensing," *IEEE Transactions on Vehicular Technology*, vol. 65, no. 3, pp. 1761–1771, 2016.

[22] A. Afana, V. Asghari, A. Ghrayeb, and S. Affes, "On the performance of cooperative relaying spectrum-sharing systems with collaborative distributed beamforming," *IEEE Transactions on Communications*, vol. 62, no. 3, pp. 857–871, 2014.

[23] L. Wei, R. Q. Hu, Y. Qian, and G. Wu, "Energy efficiency and spectrum efficiency of multihop device-to-device communications underlaying cellular networks," *IEEE Transactions on Vehicular Technology*, vol. 65, no. 1, pp. 367–380, 2016.

[24] Y. Xiao, Z. Han, C. Yuen, and L. A. DaSilva, "Carrier aggregation between operators in next generation cellular networks: A stable roommate market," *IEEE Transactions on Wireless Communications*, vol. 15, no. 1, pp. 633–650, 2016.

[25] A. M. Wyglinski, M. Nekovee, and Y. T. Hou, "Cognitive radio communications and networks," *Principles & Practice, Elsevier*, 2010.

[26] P. Luoto, M. Bennis, P. Pirinen, S. Samarakoon, and M. Latva-aho, "Enhanced co-primary spectrum sharing method for multi-operator networks," *IEEE Transactions on Mobile Computing*, 2017.

[27] Y. G. Q. M. Yuan Ma, Xingjian Zhang, "An efficient joint sub-Nyquist spectrum sensing scheme with geolocation database over TV white space," in *2017 IEEE International Conference on Communications (ICC)*, pp. 1–6, IEEE, 2017.

[28] O. Holland, N. Sastry, S. Ping, R. Knopp, F. Kaltenberger, D. Nussbaum, J. Hallio, M. Jakobsson, J. Auranen, R. Ekman, *et al.*, "A series of trials in the UK as part of the Ofcom TV white spaces pilot," in *Cognitive Cellular Systems (CCS), 2014 1st International Workshop on*, pp. 1–5, IEEE, 2014.

[29] X. Yu, J. Zhang, M. Haenggi, and K. B. Letaief, "Coverage analysis for millimeter wave networks: The impact of directional antenna arrays," *IEEE Journal on Selected Areas in Communications*, 2017.

[30] U. Madhow, "Networking at 60 GHz: The emergence of MultiGigabit wireless," in *Second International Conference on Communication Systems and Networks (COMSNETS)*, pp. 1–6, IEEE, 2010.

[31] J. Du and R. A. Valenzuela, "How much spectrum is too much in millimeter wave wireless access," *IEEE Journal on Selected Areas in Communications*, 2017.

[32] J. G. Andrews, T. Bai, M. N. Kulkarni, A. Alkhateeb, A. K. Gupta, and R. W. Heath, "Modeling and analyzing millimeter wave cellular systems," *IEEE Transactions on Communications*, vol. 65, no. 1, pp. 403–430, 2017.

[33] B. Cho, K. Koufos, R. Jäntti, and S.-L. Kim, "Co-primary spectrum sharing for inter-operator device-to-device communication," *IEEE Journal on Selected Areas in Communications*, vol. 35, no. 1, pp. 91–105, 2017.

[34] R. H. Tehrani, S. Vahid, D. Triantafyllopoulou, H. Lee, and K. Moessner, "Licensed spectrum sharing schemes for mobile operators: A survey and outlook," *IEEE Communications Surveys & Tutorials*, vol. 18, no. 4, pp. 2591–2623, 2016.

[35] I. Sobron, W. A. Martins, M. L. de Campos, and M. Velez, "Incumbent and LSA licensee classification through distributed cognitive networks," *IEEE Transactions on Communications*, vol. 64, no. 1, pp. 94–103, 2016.

[36] M. Matinmikko, H. Okkonen, M. Palola, S. Yrjola, P. Ahokangas, and M. Mustonen, "Spectrum sharing using licensed shared access: The concept and its workflow for LTE-advanced networks," *IEEE Wireless Communications*, vol. 21, no. 2, pp. 72–79, 2014.

[37] O. Mehanna and N. D. Sidiropoulos, "Maximum likelihood passive and active sensing of wideband power spectra from few bits.," *IEEE Trans. Signal Processing*, vol. 63, no. 6, pp. 1391–1403, 2015.

[38] Pappas, N. and Kountouris, M., "Throughput of a cognitive radio network under congestion constraints: A network-level study," in *9th International Conference on Cognitive Radio Oriented Wireless Networks and Communications*, pp. 162–166, Jun. 2014.

[39] S. Haykin, "Cognitive radio: Brain-empowered wireless communications," *IEEE Journal on Selected Areas in Communications*, vol. 23, pp. 201–220, Feb. 2005.

[40] I. Mitola, J., "Cognitive radio for flexible mobile multimedia communications," in *IEEE International Workshop on Mobile Multimedia Communications*, pp. 3–10, 1999.

[41] A. De Domenico, E. Strinati, and M.-G. Di Benedetto, "A survey on MAC strategies for cognitive radio networks," *IEEE Communications Surveys Tutorials*, vol. 14, no. 1, pp. 21 –44, 2012.

[42] S. Atapattu, C. Tellambura, and H. Jiang, "Spectrum sensing via energy detector in low SNR," in *IEEE International Conference on Communications*, pp. 1–5, 2011.

[43] L. Wei and O. Tirkkonen, "Statistical test for multiple primary user spectrum sensing," in *Sixth International Conference on Cognitive Radio Oriented Wireless Networks and Communications*, pp. 41–45, 2011.

[44] A. Ghasemi and E. Sousa, "Spectrum sensing in cognitive radio networks: requirements, challenges and design trade-offs," *IEEE Communications Magazine*, vol. 46, no. 4, pp. 32–39, 2008.

[45] N. Kundargi and A. Tewfik, "Doubly sequential energy detection for distributed dynamic spectrum access," in *IEEE International Conference on Communications*, pp. 1–5, May 2010.

[46] N. Kundargi and A. Tewfik, "A performance study of novel sequential energy detection methods for spectrum sensing," in *IEEE International Conference on Acoustics Speech and Signal Processing*, pp. 3090–3093, Mar. 2010.

[47] H. Urkowitz, "Energy detection of unknown deterministic signals," *Proceedings of the IEEE*, vol. 55, pp. 523–531, Apr. 1967.

[48] F. Digham, M.-S. Alouini, and M. Simon, "On the energy detection of unknown signals over fading channels," in *IEEE International Conference on Communications*, vol. 5, pp. 3575–3579, May 2003.

[49] S. Atapattu, C. Tellambura, and H. Jiang, "Energy detection of primary signals over fading channels," in *International Conference on Industrial and Information Systems*, pp. 118–122, Dec. 2009.

[50] R. Blum, S. Kassam, and H. Poor, "Distributed detection with multiple sensors Part II. Advanced topics," *Proceedings of the IEEE*, vol. 85, no. 1, pp. 64–79, 1997.

[51] E. Axell, G. Leus, E. G. Larsson, and H. Poor, "Spectrum sensing for cognitive radio: State-of-the-art and recent advances," *IEEE Signal Processing Magazine*, vol. 29, no. 3, pp. 101–116, 2012.

[52] A. Ghasemi and E. Sousa, "Spectrum sensing in cognitive radio networks: requirements, challenges and design trade-offs," *IEEE Communications Magazine*, vol. 46, no. 4, pp. 32–39, 2008.

[53] S. Atapattu, C. Tellambura, and H. Jiang, "Performance of an energy detector over channels with both multipath fading and shadowing," *IEEE Transactions on Wireless Communications*, vol. 9, pp. 3662–3670, Dec. 2010.

[54] X. Liu, C. Zhang, and X. Tan, "Double-threshold cooperative detection for cognitive radio based on weighing," in *6th International ICST Conference on Communications and Networking in China (CHINACOM)*, pp. 205–209, 2011.

[55] S. K. Sharma, S. Chatzinotas, and B. Ottersten, "Spectrum sensing in dual polarized fading channels for cognitive SatComs," in *IEEE Globecom Conference*, Oct. 2012.

[56] T. Yucek and H. Arslan, "A survey of spectrum sensing algorithms for cognitive radio applications," *IEEE Communications Surveys & Tutorials*, vol. 11, no. 1, pp. 116 –130, 2009.

[57] J. Zhu, Z. Xu, F. Wang, B. Huang, and B. Zhang, "Double threshold energy detection of cooperative spectrum sensing in cognitive radio," in *3rd International Conference on Cognitive Radio Oriented Wireless Networks and Communications*, pp. 1–5, May 2008.

[58] X. Ling, B. Wu, H. Wen, P.-H. Ho, Z. Bao, and L. Pan, "Adaptive threshold control for energy detection based spectrum sensing in cognitive radios," *IEEE Wireless Communications Letters*, vol. 1, pp. 448 –451, Oct. 2012.

[59] Y. Wang, C. Feng, C. Guo, and F. Liu, "Optimization of parameters for spectrum sensing in cognitive radios," in *5th International Conference on Wireless Communications, Networking and Mobile Computing*, pp. 1–4, Sept. 2009.

[60] Z. Li, L. Liu, and C. Zhou, "Fast detection method in cooperative cognitive radio networks," *International Journal of Digital Multimedia Broadcasting*, Hindawi Publishing Corporation, 2010.

[61] A. Singh, M. Bhatnagar, and R. Mallik, "Cooperative spectrum sensing in multiple antenna based cognitive radio network using an improved energy detector," *IEEE Communications Letters*, vol. 16, pp. 64 –67, Jan. 2012.

[62] Y. Qi, H. Kobayashi, and H. Suda, "Analysis of wireless geolocation in a non-line-of-sight environment," *IEEE Transactions on Wireless Communications*, vol. 5, no. 3, pp. 672–681, 2006.

[63] A. F. Molisch, L. J. Greenstein, and M. Shafi, "Propagation issues for cognitive radio," *Proceedings of the IEEE*, vol. 97, no. 5, pp. 787–804, 2009.

[64] F. Chiti, R. Fantacci, F. Nizzi, L. Pierucci, and T. Pecorella, "A cooperative spectrum sensing protocol for IEEE 802.15. 4m wide-area WSNs," in

Communications (ICC), 2017 IEEE International Conference on, pp. 1–6, IEEE, 2017.

[65] I. F. Akyildiz, B. F. Lo, and R. Balakrishnan, "Cooperative spectrum sensing in cognitive radio networks: A survey," *Physical Communication*, vol. 4, no. 1, pp. 40–62, 2011.

[66] G. Ganesan and Y. Li, "Cooperative spectrum sensing in cognitive radio networks," in *1st IEEE International Symposium on New Frontiers in Dynamic Spectrum Access Networks, 2005*, pp. 137–143, IEEE, 2005.

[67] M. Di Renzo, F. Graziosi, and F. Santucci, "Cooperative spectrum sensing in cognitive radio networks over correlated log-normal shadowing," in *Vehicular Technology Conference, 2009. VTC Spring 2009. IEEE 69th*, pp. 1–5, IEEE, 2009.

[68] A. Ghasemi and E. S. Sousa, "Asymptotic performance of collaborative spectrum sensing under correlated log-normal shadowing," *IEEE Communications Letters*, vol. 11, no. 1, 2007.

[69] K. Ben Letaief and W. Zhang, "Cooperative communications for cognitive radio networks," *Proceedings of the IEEE*, vol. 97, pp. 878–893, May 2009.

[70] Q. Zou, S. Zheng, and A. Sayed, "Cooperative spectrum sensing via sequential detection for cognitive radio networks," in *IEEE 10th Workshop on Signal Processing Advances in Wireless Communications*, pp. 121–125, 2009.

[71] H. Mu and J. Tugnait, "Joint soft-decision cooperative spectrum sensing and power control in multiband cognitive radios," *IEEE Transactions on Signal Processing*, vol. 60, no. 10, pp. 5334–5346, 2012.

[72] Y. Tani and T. Saba, "Quantization scheme for energy detector of soft decision cooperative spectrum sensing in cognitive radio," in *IEEE GLOBECOM Workshops*, pp. 69–73, 2010.

[73] D. Bera, I. Chakrabarti, S. S. Pathak, and G. K. Karagiannidis, "Another look in the analysis of cooperative spectrum sensing over Nakagami-m fading channels," *IEEE Transactions on Wireless Communications*, vol. 16, no. 2, pp. 856–871, 2017.

[74] H. Li, X. Xing, J. Zhu, X. Cheng, K. Li, R. Bie, and T. Jing, "Utility-based cooperative spectrum sensing scheduling in cognitive radio networks," *IEEE Transactions on Vehicular Technology*, vol. 66, no. 1, pp. 645–655, 2017.

[75] M. Grissa, A. A. Yavuz, and B. Hamdaoui, "Preserving the location privacy of secondary users in cooperative spectrum sensing," *IEEE Transactions on Information Forensics and Security*, vol. 12, no. 2, pp. 418–431, 2017.

[76] B. Shen, L. Huang, C. Zhao, K. Kwak, and Z. Zhou, "Weighted cooperative spectrum sensing in cognitive radio networks," in *3rd International Conference on Convergence and Hybrid Information Technology*, vol. 1, pp. 1074–1079, 2008.

[77] X. Zhu, L. Shen, and T.-S. Yum, "Analysis of cognitive radio spectrum access with optimal channel reservation," *IEEE Communications Letters*, vol. 11, pp. 304–306, Apr. 2007.

[78] Q. Huang, K.-T. Ko, and V. Iversen, "Performance modeling for heterogeneous wireless networks with multiservice overflow traffic," in *Global Telecommunications Conference*, pp. 1–7, Nov. 2009.

[79] Q. Huang, Y.-C. Huang, K.-T. Ko, and V. Iversen, "Loss performance modeling for hierarchical heterogeneous wireless networks with speed-sensitive call admission control," *IEEE Transactions on Vehicular Technology*, vol. 60, pp. 2209–2223, Jun. 2011.

[80] W. Song and W. Zhuang, "Multi-service load sharing for resource management in the cellular/WLAN integrated network," *IEEE Transactions on Wireless Communications*, vol. 8, pp. 725–735, Feb. 2009.

[81] P. Fitzpatrick, C. S. Lee, and B. Warfield, "Teletraffic performance of mobile radio networks with hierarchical cells and overflow," *IEEE Journal on Selected Areas in Communications*, vol. 15, pp. 1549–1557, Oct. 1997.

[82] P. D. Mankar, B. R. Sahu, G. Das, and S. Pathak, "Evaluation of blocking probability for downlink in Poisson networks," *IEEE Wireless Communications Letters*, vol. 4, no. 6, pp. 625–628, 2015.

[83] O. Al-Khatib, W. Hardjawana, and B. Vucetic, "Wireless networks virtualisation: Traffic modeling and spectrum sharing," in *IEEE International Conference on Communications*, pp. 5859–5864, IEEE, 2015.

[84] N. Nathani, G. Manna, and S. Dorle, "Network architecture model of infrastructure based mobile cognitive radio system in licensed band with blocking probability assessment," in *Future Technologies Conference*, pp. 231–236, IEEE, 2016.

[85] D. T. C. Wong, A. T. Hoang, Y.-C. Liang, and F. P. S. Chin, "Complete sharing dynamic spectrum allocation for two cellular radio systems," in *19th International Symposium on Personal, Indoor and Mobile Radio Communications*, pp. 1–5, IEEE, 2008.

[86] Y. Fang and Y. Zhang, "Call admission control schemes and performance analysis in wireless mobile networks," *IEEE Transactions on Vehicular Technology*, vol. 51, no. 2, pp. 371–382, 2002.

[87] H. Elbadawy, "Modeling and analysis for heterogeneous wireless networks by using of multi-dimensional Markov models," in *International Conference on Computer and Communication Engineering*, pp. 1116–1120, IEEE, 2008.

[88] R. Abozariba, M. Asaduzzaman, and M. Patwary, "Radio resource sharing framework for cooperative multioperator networks with dynamic overflow modeling," *IEEE Transactions on Vehicular Technology*, vol. 66, no. 3, pp. 2433–2447, 2017.

[89] Y. Zhang, C. Lee, D. Niyato, and P. Wang, "Auction approaches for resource allocation in wireless systems: A survey," *IEEE Communications Surveys & Tutorials*, vol. 15, no. 3, pp. 1020–1041, 2013.

[90] C. A. Gizelis and D. D. Vergados, "A survey of pricing schemes in wireless networks," *IEEE Communications Surveys & Tutorials*, vol. 13, no. 1, pp. 126–145, 2011.

[91] X. Kang, R. Zhang, and M. Motani, "Price-based resource allocation for spectrum-sharing femtocell networks: A Stackelberg game approach," *IEEE Journal on Selected Areas in Communications*, vol. 30, no. 3, pp. 538–549, 2012.

[92] A.-H. Mohsenian-Rad, V. W. Wong, and V. Leung, "Two-fold pricing to guarantee individual profits and maximum social welfare in multi-hop wireless access networks," *IEEE Transactions on Wireless Communications*, vol. 8, no. 8, pp. 4110–4121, 2009.

[93] N. Tran, L. B. Le, S. Ren, Z. Han, and C. S. Hong, "Joint pricing and load balancing for cognitive spectrum access: Non-cooperation versus cooperation," *IEEE Journal on Selected Areas in Communications*, vol. 33, pp. 972–985, May 2015.

[94] S. Sengupta and M. Chatterjee, "An economic framework for dynamic spectrum access and service pricing," *IEEE/ACM Transactions on Networking*, vol. 17, no. 4, pp. 1200–1213, 2009.

[95] J. W. Mwangoka, P. Marques, and J. Rodriguez, "Broker based secondary spectrum trading," in *Sixth International Conference on Cognitive Radio Oriented Wireless Networks and Communications*, pp. 186–190, IEEE, 2011.

[96] D. S. Palguna, D. J. Love, and I. Pollak, "Secondary spectrum auctions for markets with communication constraints," *IEEE Transactions on Wireless Communications*, vol. 15, no. 1, pp. 116–130, 2016.

[97] M. Khaledi and A. A. Abouzeid, "Dynamic spectrum sharing auction with time-evolving channel qualities," *IEEE Transactions on Wireless Communications*, vol. 14, no. 11, pp. 5900–5912, 2015.

[98] Y. Wu, Q. Zhu, J. Huang, and D. H. Tsang, "Revenue sharing based resource allocation for dynamic spectrum access networks," *IEEE Journal on Selected Areas in Communications*, vol. 32, no. 11, pp. 2280–2296, 2014.

[99] S. Li, J. Huang, and S.-Y. R. Li, "Dynamic profit maximization of cognitive mobile virtual network operator," *IEEE Transactions on Mobile Computing*, vol. 13, no. 3, pp. 526–540, 2014.

[100] I. Sugathapala, I. Kovacevic, B. Lorenzo, S. Glisic, *et al.*, "Quantifying benefits in a business portfolio for multi-operator spectrum sharing," *IEEE Transactions on Wireless Communications*, vol. 14, no. 12, pp. 6635–6649, 2015.

[101] Y. Song, C. Zhang, Y. Fang, and P. Lin, "Revenue maximization in time-varying multi-hop wireless networks: A dynamic pricing approach," *IEEE Journal on Selected Areas in Communications*, vol. 30, no. 7, pp. 1237–1245, 2012.

[102] L. Gao, J. Huang, Y.-J. Chen, and B. Shou, "An integrated contract and auction design for secondary spectrum trading," *IEEE Journal on Selected Areas in Communications*, vol. 31, no. 3, pp. 581–592, 2013.

[103] G. Ganesan, Y. G. Li, B. Bing, and S. Li, "Spatiotemporal sensing in cognitive radio networks," *IEEE Journal on selected areas in communications*, vol. 26, no. 1, 2008.

[104] K. Jagannathan, E. Modiano, and L. Zheng, "Effective resource allocation in a queue: How much control is necessary?," in *Communication, Control, and Computing, 2008 46th Annual Allerton Conference on*, pp. 508–515, IEEE, 2008.

[105] S. A. Alvi, M. S. Younis, M. Imran, *et al.*, "A weighted linear combining scheme for cooperative spectrum sensing," *Procedia Computer Science*, vol. 32, pp. 149–157, 2014.

[106] Y.-C. Liang, K.-C. Chen, G. Y. Li, and P. Mahonen, "Cognitive radio networking and communications: An overview," *IEEE transactions on vehicular technology*, vol. 60, no. 7, pp. 3386–3407, 2011.

[107] Y.-C. Liang, Y. Zeng, E. C. Peh, and A. T. Hoang, "Sensing-throughput tradeoff for cognitive radio networks," *IEEE transactions on Wireless Communications*, vol. 7, no. 4, pp. 1326–1337, 2008.

[108] S. Chaudhari, J. Lunden, V. Koivunen, and H. Poor, "Cooperative sensing with imperfect reporting channels: Hard decisions or soft decisions?," *IEEE Transactions on Signal Processing*, vol. 60, no. 1, pp. 18–28, 2012.

[109] S. A. Alvi, M. S. Younis, M. Imran, M. Guizani, *et al.*, "A near-optimal LLR based cooperative spectrum sensing scheme for CRAHNs," *IEEE Transactions on Wireless Communications*, vol. 14, no. 7, pp. 3877–3887, 2015.

[110] D. Hamza, S. Aïssa, and G. Aniba, "Equal gain combining for cooperative spectrum sensing in cognitive radio networks," *IEEE Transactions on Wireless Communications*, vol. 13, no. 8, pp. 4334–4345, 2014.

[111] X. Li, "RSS-based location estimation with unknown pathloss model," *IEEE Transactions on Wireless Communications*, vol. 5, no. 12, pp. 3626–3633, 2006.

[112] G. E. Athanasiadou, A. R. Nix, and J. P. McGeehan, "A microcellular ray-tracing propagation model and evaluation of its narrow-band and wide-band predictions," *IEEE Journal on Selected Areas in Communications*, vol. 18, no. 3, pp. 322–335, 2000.

[113] A. Medeisis and A. Kajackas, "On the use of the universal Okumura-Hata propagation prediction model in rural areas," in *Vehicular Technology Conference Proceedings, 2000. VTC 2000-Spring Tokyo. 2000 IEEE 51st*, vol. 3, pp. 1815–1818, IEEE, 2000.

[114] M. Coinchon, A.-P. Salovaara, and J.-F. Wagen, "The impact of radio propagation predictions on urban UMTS planning," in *International Zurich Seminar on Broadband Communications. Access, Transmission, Networking.*, pp. 32–32, IEEE, 2002.

[115] Y. Singh, "Comparison of Okumura, Hata and cost-231 models on the basis of path loss and signal strength," *International journal of computer applications*, vol. 59, no. 11, 2012.

[116] S. Atapattu, C. Tellambura, and H. Jiang, "Energy detection based cooperative spectrum sensing in cognitive radio networks," *IEEE Transactions on Wireless Communications*, vol. 10, pp. 1232–1241, Apr. 2011.

[117] P. Lin, J. Jia, Q. Zhang, and M. Hamdi, "Dynamic spectrum sharing with multiple primary and secondary users," *IEEE Transactions on Vehicular Technology*, vol. 60, pp. 1756–1765, May 2011.

[118] P. Si, H. Ji, F. Yu, and V. Leung, "Optimal cooperative internetwork spectrum sharing for cognitive radio systems with spectrum pooling," *IEEE Transactions on Vehicular Technology*, vol. 59, pp. 1760–1768, May 2010.

[119] V. Asghari and S. Aissa, "End-to-end performance of cooperative relaying in spectrum-sharing systems with quality of service requirements," *IEEE Transactions on Vehicular Technology*, vol. 60, pp. 2656–2668, Jul. 2011.

[120] T. Kwon and J. Cioffi, "Spatial spectrum sharing for heterogeneous SIMO networks," *IEEE Transactions on Vehicular Technology*, vol. 63, pp. 688–702, Feb. 2014.

[121] M. G. Kibria, G. P. Villardi, K. Nguyen, K. Ishizu, and F. Kojima, "Heterogeneous networks in shared spectrum access communications," *IEEE Journal on Selected Areas in Communications*, vol. 35, no. 1, pp. 145–158, 2017.

[122] R. Boutaba and A. Hafid, "A generic platform for scalable access to multimedia-on-demand systems," *IEEE Journal on Selected Areas in Communications*, vol. 17, no. 9, pp. 1599–1613, 1999.

[123] C. V. N. Index, "Global mobile data traffic forecast update, 2015–2020 white paper," *link: http://goo. gl/ylTuVx*, 2016.

[124] G. Giambene, *Queuing theory and telecommunications*. Springer, 2005.

[125] P. Ahokangas, K. Horneman, H. Posti, M. Matinmikko, T. Hanninen, S. Yrjola, and V. Goncalves, "Defining "co-primary spectrum sharing" – a new business opportunity for MNOs?," in *9th International Conference on Cognitive Radio Oriented Wireless Networks and Communications*, pp. 395–400, Jun. 2014.

[126] L. Duan, J. Huang, and B. Shou, "Duopoly competition in dynamic spectrum leasing and pricing," *IEEE Transactions on Mobile Computing*, vol. 11, no. 11, pp. 1706–1719, 2012.

[127] G. Kasbekar, S. Sarkar, K. Kar, P. Muthuswamy, and A. Gupta, "Dynamic contract trading in spectrum markets," *IEEE Transactions on Automatic Control*, vol. 59, no. 10, pp. 2856–2862, 2014.

[128] L. Gao, X. Wang, Y. Xu, and Q. Zhang, "Spectrum trading in cognitive radio networks: A contract-theoretic modeling approach," *IEEE Journal on Selected Areas in Communications*, vol. 29, no. 4, pp. 843–855, 2011.

[129] K. I. Aardal, S. P. Van Hoesel, A. M. Koster, C. Mannino, and A. Sassano, "Models and solution techniques for frequency assignment problems," *Quarterly Journal of the Belgian, French and Italian Operations Research Societies*, vol. 1, no. 4, pp. 261–317, 2003.

[130] M. M. Buddhikot, P. Kolodzy, S. Miller, K. Ryan, and J. Evans, "DIMSUMnet: new directions in wireless networking using coordinated dynamic spectrum," in *6th IEEE International Symposium on a World of Wireless Mobile and Multimedia Networks*, pp. 78–85, IEEE, 2005.

[131] OfCom, *Application of spectrum liberalisation and trading to the mobile sector – A further consultation.* Tech. Rep., The Office of Communications, 2009.

[132] M. J. Marcus, "Unlicensed cognitive sharing of TV spectrum: The controversy at the Federal Communications Commission," *IEEE Communications Magazine*, vol. 43, no. 5, pp. 24–25, 2005.

[133] D. Gross and C. M. Harris, *Fundamentals of queueing theory.* Wiley, 1998.

[134] M. M. Buddhikot, I. Kennedy, F. Mullany, and H. Viswanathan, "Ultra-broadband femtocells via opportunistic reuse of multi-operator and multi-service spectrum," *Bell Labs Technical Journal*, vol. 13, no. 4, pp. 129–143, 2009.

[135] V. Sridhar and R. Prasad, "Towards a new policy framework for spectrum management in India," *Telecommunications Policy*, vol. 35, no. 2, pp. 172–184, 2011.

[136] A. Bourdena, E. Pallis, G. Kormentzas, and G. Mastorakis, "A prototype cognitive radio architecture for TVWS exploitation under the real time secondary spectrum market policy," *Physical Communication*, vol. 10, pp. 159–168, 2014.

[137] J. Lunden, V. Koivunen, and H. V. Poor, "Spectrum exploration and exploitation for cognitive radio: Recent advances," *IEEE Signal Processing Magazine*, vol. 32, no. 3, pp. 123–140, 2015.

[138] F. Akhtar, M. H. Rehmani, and M. Reisslein, "White space: Definitional perspectives and their role in exploiting spectrum opportunities," *Telecommunications Policy*, vol. 40, no. 4, pp. 319–331, 2016.

[139] A. A. Khan, M. H. Rehmani, and M. Reisslein, "Cognitive radio for smart grids: Survey of architectures, spectrum sensing mechanisms, and networking protocols," *IEEE Communications Surveys & Tutorials*, vol. 18, no. 1, pp. 860–898, 2016.

[140] G. Ding, J. Wang, Q. Wu, Y.-D. Yao, F. Song, and T. A. Tsiftsis, "Cellular-base-station-assisted device-to-device communications in TV white space," *IEEE Journal on Selected Areas in Communications*, vol. 34, no. 1, pp. 107–121, 2016.

[141] C. Jiang, Y. Chen, K. R. Liu, and Y. Ren, "Optimal pricing strategy for operators in cognitive femtocell networks," *IEEE Transactions on Wireless Communications*, vol. 13, no. 9, pp. 5288–5301, 2014.

[142] V. Valenta, R. Maršálek, G. Baudoin, M. Villegas, M. Suarez, and F. Robert, "Survey on spectrum utilization in Europe: Measurements, analyses and observations," in *5th International Conference on Cognitive Radio Oriented Wireless Networks and Communications*, pp. 1–5, IEEE, 2010.

[143] D. Niyato and E. Hossain, "Competitive pricing for spectrum sharing in cognitive radio networks: Dynamic game, inefficiency of Nash equilibrium, and collusion," *IEEE Journal on Selected Areas in Communications*, vol. 26, no. 1, pp. 192–202, 2008.

[144] J. Acharya and R. D. Yates, "Dynamic spectrum allocation for uplink users with heterogeneous utilities," *IEEE Transactions on Wireless Communications*, vol. 8, no. 3, pp. 1405–1413, 2009.

[145] L. Gao, B. Shou, Y.-J. Chen, and J. Huang, "Combining spot and futures markets: A hybrid market approach to dynamic spectrum access," *Operations Research*, vol. 64, no. 4, pp. 794–821, 2016.